

METAL SALEN COMPLEXES IN ANION BINDING AND CATALYSIS

By

ERIC R. LIBRA

A DISSERTATION PRESENTED TO THE GRADUATE SCHOOL
OF THE UNIVERSITY OF FLORIDA IN PARTIAL FULFILLMENT
OF THE REQUIREMENTS FOR THE DEGREE OF
DOCTOR OF PHILOSOPHY

UNIVERSITY OF FLORIDA

2007

© 2007 Eric R. Libra

To Caroline and my parents and my entire family

ACKNOWLEDGMENTS

Although I am unaware of when I made the decision to become a chemist, I know my interest in science and discovery has been in place since an early age. As a young child I always had an interest in dinosaurs and astronomy, but the person who may just have steered me in the direction of chemistry was Mr. Wizard. Watching his program led me to want to perform experiments at home and also stoked my desire for my first chemistry set. There are many people who have helped me reach this point not only as a chemist but also as a person and I would like to thank them for all they have done.

I owe a dept of gratitude to my parents, Dennis and JoAnne Libra, who have been instrumental in my life. I would not be in the position I am in now if it was not for them. They always put their children and our educations first and whether it was driving us to soccer practice or piano lessons or making the financial sacrifices so that my brothers and I could attend the colleges of our choosing, they have been selfless through it all. I thank my younger brothers, Broc and Garrett, for the fun times growing up and for taking all the abuse a big brother dishes out, as well as not giving it back to me too much when you both outgrew me and I was the “little” brother. I thank my grandparents, John and Bertha Kowalczyk, who help raise me as well as my grandparents, Peter and Cecelia Libra for the Sunday afternoon spaghetti dinners.

Three professors have had a tremendous impact on my life and have guided me to where I am today. Dr. William Armstrong at Boston College was the first professor to give me the opportunity to work in a research environment, and this positive experience is what made me decide to attend graduate school. He was also instrumental in helping me pick a graduate school and I eventually realized that the University of Florida and the Scott Group was the place where I belonged. My two plus years working in the X-Ray lab at the University of Florida, were very rewarding and I have Dr. Khalil Abboud to thank for that. Khalil was always there to talk and to

give advice on chemistry and many other subjects. I thoroughly enjoyed my time working with him and it was nice to have a few hours a day to be able to concentrate on topics other than synthesis. Most importantly, I would like to thank my advisor Dr. Michael Scott. Mike was responsible for my being at UF, and I hope that I have proven that his decision to bring me here was the right one. Since my arrival in Gainesville he has been a great mentor and I think that my chemical knowledge and intuition has exponentially increased since my arrival. He always was able to make a helpful suggestion when I hit a wall, and I was always ecstatic when it worked. He is one of the rare professors that has found the perfect median between giving the students enough space to figure things out for themselves, yet involved enough so students have a direction and a goal.

Many other people made my time here more enjoyable. I would like to thank my lab mates Ivanna, Hue, Nella, Ranjan, Ozge, Candace, Melanie, Patrick, Nate, Gary, Nicolas, Dempsey and Anna, among many other short term visitors, from whom I have learned many practical aspects of chemistry including many tricks of the trade. I had the pleasure of working with a great undergraduate, Nate Strutt, and I hope I did not teach him too many bad habits these last two years. A special thanks goes out to my lab mate Candace and pseudo lab mate Justin for making inorganic chemistry fun, from classes, to cumes, to orals, to the years of research. They were always there together to talk sports or get a drink at Gator City to take out minds off the tasks at hand. I am sure my graduate experience would not have been as enjoyable without them. Another thanks goes to James and the entire Quarter Barrel Saturday crew. It was definitely the most enjoyable part of my last four years in Gainesville and even if it was only a few Saturday afternoons a year it was much needed in order to maintain our sanity.

Most importantly, I would like to thank my wife to be Caroline. I moved to Gainesville with many mixed feelings, as I knew it would be several years we would not be together. Being apart for so long has been tremendously difficult and I can not wait to be back together and share our lives once again. I could not have done this without her love, encouragement and especially her patience with me and our situation.

TABLE OF CONTENTS

	<u>page</u>
ACKNOWLEDGMENTS	4
LIST OF TABLES	10
LIST OF FIGURES	11
ABSTRACT	15
 CHAPTER	
1 INTRODUCTION	16
Anion Coordination Modes	17
Initial Studies of Anion Receptor Systems	18
Pyrrolic Macrocyclic Receptors	19
Biologically Relevant Receptors Incorporating the Guanidinium Group	20
Neutrally Charged Receptors	20
Anion Coordination Through Lewis Acidic Metals	21
Hydrogen Bonding Interactions Through Oxygen Donors	22
Research Objectives	23
2 METAL SALEN COMPLEXES INCORPORATING TRIPHENOXYMETHANES: EFFICIENT, SIZE SELECTIVE BINDING OF FLUORIDE WITH A VISUAL REPORT	28
Introduction	28
Results and Discussion	28
Advantages of the Salen Macrocyclic	29
Design of Receptor System	29
Anion Binding Properties	31
Binding Constants	33
Solid State Structure of [2-2-F] ¹⁻	34
Anion Binding Studies for 2-3	34
Conclusions	35
Experimental Methods	36
General Considerations	36
Synthesis of 2-1	36
Synthesis of <i>R,R</i> -2-1	37
Synthesis of <i>R,R</i> -2-2	37
Synthesis of 2-2	38
Synthesis of 2-3	38
Synthesis of [2-2-F](Bu ₄ N)	39
Determination of binding constants (LogK _s)	39

3	A SYNTHETIC MODEL OF THE CLC CHLORIDE ION CHANNEL; A STRUCTURAL AND ANION BINDING STUDY	52
	Introduction.....	52
	Results and Discussion	53
	Salens as Anion Receptors	53
	Synthesis of a Mixed Salen Receptor.....	54
	Anion Coordination and Binding Constants.....	56
	Solid State Structure.....	57
	Conclusions.....	57
	Experimental Methods.....	58
	General Considerations.....	58
	Determination of binding constants (LogK _s).....	58
	Synthesis of 3-1	58
	Synthesis of 3-2	59
	Synthesis 3-3	60
	Synthesis of 3-4	61
	Synthesis of 3-5	61
	Synthesis of 3-6	62
	Synthesis of 3-7	63
	Synthesis of 3-8	63
4	METAL SALEN UREA COMPLEXES AND THEIR HIGH AFFINITIES FOR THE HALIDES	69
	Introduction.....	69
	Results and Discussion	70
	Conclusions.....	79
	Experimental Methods.....	80
	General Considerations	80
	Synthesis of 4-2	81
	Synthesis of 4-3	81
	Synthesis of 4-6	82
	Synthesis of 4-7	82
	Synthesis of 4-8	82
5	DESIGNER LEWIS ACIDS; THE DEVELOPMENT OF EXREMELY BULKY AND RIGID DINUCLEAR CHIRAL CATALYSTS	99
	Introduction.....	99
	Jacobsen's Catalyst.....	99
	Lewis Acid Catalysts.....	100
	Zn Salens in Catalysis	100
	The Promotion of the Diels-Alder Reaction by a Lewis Acid	102
	General Approaches of Synthetic Design.....	102
	Results and Discussion	102
	Binap Ligand	103

Racemic Zn Catalyst.....	104
Chiral Zn Catalyst.....	107
Co Catalysts.....	107
Low Solubility Chiral Ligands.....	108
Initial Catalysis Studies.....	109
Conclusions.....	109
Experimental Methods.....	110
General Considerations.....	110
Synthesis of 5-2.....	110
Synthesis of 5-3.....	111
Synthesis of 5-4.....	111
Synthesis of 5-5.....	112
Synthesis of 5-6.....	112
Synthesis of 5-7.....	113
Synthesis of 5-8.....	113
Synthesis of 5-9.....	114
Synthesis of racemic 5-10.....	114
Synthesis of 5-11.....	115
Synthesis of 5-12.....	115
Synthesis of 5-13.....	116
Synthesis of 5-14.....	116
Synthesis of 5-15.....	117
Synthesis of 5-16.....	117
Synthesis of 5-17.....	117
LIST OF REFERENCES.....	133
BIOGRAPHICAL SKETCH.....	140

LIST OF TABLES

<u>Table</u>		<u>page</u>
2-1	X-ray data for the crystal structures of 2-1 and the complexes <i>R,R</i> -2-1, 2-3, and 2-2-F.	40
4-1	LogK _s values of the two salen urea complexes with fluoride, chloride and bromide in acetone.	84
4-2	X-ray data from crystal structures of 4-2, 4-3, 4-4, 4-6, 4-8.....	84

LIST OF FIGURES

<u>Figure</u>	<u>page</u>
1-1	Structure of Park and Simon's katapinate; the first example of an anion binder.24
1-2	Structure of azacryptand that is an ideal size match for fluoride.....24
1-3	Structure of zwitterionic neutral receptor.24
1-4	Structure of the pyrrolic macrocycle sapphyrin.25
1-5	Structure of two bicyclic guanidiniums attached by a urethane linker.....25
1-6	Structure of neutral anion receptor.26
1-7	Structures of amide based receptors by Bowman-James.....26
1-8	Structure of salen complex with uranyl used for Lewis acidic anion binding.....27
1-9	Structure of conjugated polymer that efficiently binds fluoride though phenols.27
1-10	Structure of triphenoxymethane platform.....27
2-1	Open conformation of ClC chloride channel.....40
2-2	Triphenoxymethane platform with the phenols in the "all up" position relative to the methine carbon hydrogen.....41
2-3	Procedure used for the synthesis of 2-1, macrocycle metalation to form 2-2, and 2-3 and fluoride binding.....41
2-4	Solid-state structure of 2-1.....42
2-5	Solid-state structure of 2-2.....43
2-6	Solid-state structures of 2-3.....44
2-7	¹ H NMR spectrum of 2-3 (top) and [2-3-F] ¹⁻ (bottom) taken in d ⁶ -DMSO with an inset of the ¹⁹ F NMR spectrum of [2-3-F] ¹⁻ in the region of bound fluoride.45
2-8	¹ H NMR spectrum of 2-2.....45
2-9	¹ H NMR spectrum of 2-2 with 0.5 equivalents of fluoride added.....46
2-10	¹ H NMR spectrum of 2-2 with one equivalent or more of fluoride.....46
2-11	UV-Vis titration of 2-2 with tetra-butylammonium fluoride in acetone.47

2-12	Job plot of the titration of 2-2 with tetrabutylammonium fluoride.....	47
2-12	Absorbance plotted versus concentration of fluoride for the titration of 2-2 at 450nm with tetrabutylammonium fluoride.....	48
2-14	Crystal structure of [2-2-F] ¹⁻ with fluoride bound in the phenolic pocket.....	49
2-15	UV-Vis titration of 2-3 salen with tetra-butylammonium fluoride in acetone..	50
2-16	Job plot from UV-Vis spectra titration data of 2-3 in acetone with tetrabutylammonium fluoride.....	50
2-17	Absorbance plotted versus concentration of fluoride for the titration of 2-3 complex at 450 nm with tetrabutylammonium fluoride	51
3-1	Open conformation of CIC chloride channel.....	64
3-2	Compound [2-2-F] ⁻ with a fluoride hydrogen bonding with the four phenols of the anion receptor.....	64
3-3	Structure of salen based anion receptor with amine groups at the periphery. The receptor coordinates both cations and anions	65
3-4	Synthetic scheme for Compound 3-5.....	65
3-5	Synthetic scheme for the synthesis of mixed phenolic-urea salen system (3-7), metalation at salen binding site and anion coordination (3-8).....	66
3-6	Titration plot of 3-7 with fluoride.....	67
3-7	Depiction of the solid-state structure of [3-8-Cl] ⁻	68
4-1	Proposed structure and binding mode of an early urea based anion receptor.....	85
4-2	Structure of an urea subunit where the anion binding cavity is regulated by metal coordination	85
4-3	Synthetic scheme for the formation of salen urea (4-1).....	86
4-4	Solid-state structure of 4-2.....	86
4-5	Solid-state structure of 4-3.....	87
4-6	UV-Vis titration of 4-2 with tetra-butylammonium fluoride in acetone.....	88
4-7	Binding constant data of 4-2 titrated with F ⁻ at 450nm	89
4-8	Solid-state structure of 4-4.....	90

4-9	Job plot of 4-2 for chloride	91
4-10	Solid-state structure of 4-5	92
4-10	UV-Vis titration of 4-2 with tetra-butylammonium chloride in acetone.	93
4-12	Binding constant data of 4-2 titrated with Cl ⁻ at 450nm Log K _s = 5.27.	94
4-13	Synthetic scheme for compound 4-6.	77
4-14	Depiction of the solid-state structure of 4-6	96
4-15	Synthesis of ligand 4-7 and C ₃ symmetric anion receptor 4-8.....	97
4-16	Depiction of the solid-state structure of 4-8	98
5-1	Structure of Jacobsen's catalyst used for the asymmetric epoxidation of olefins	119
5-2	Proposed mechanism for the epoxidation of olefins with Jacobsen's catalyst.	119
5-3	Structure of catalyst with chiral binaphthyl groups that influence the geometry of the substrate.	120
5-4	Reaction scheme for the ethyl addition to benzaldehyde.....	120
5-5	Structure of a bifunctional catalyst containing both a Lewis acid and Lewis base component.....	120
5-6	Enantioselective alkylation of ketones.....	121
5-7	Proposed transition state for the alkylation of ketones with a zinc salen catalyst	121
5-8	Diels-Alder reaction between cyclopentadiene and cinnamaldehyde promoted by a Lewis acid catalyst.....	121
5-9	Solid state structure of compound 2-2.	122
5-10	Depiction of 2,2-diamino-1,1-binaphthylene showing the large torsion angle between the two naphthyl planes.	122
5-11	Synthetic scheme for the synthesis of 5-2.....	123
5-12	Synthetic scheme for the formation of 5-4.	123
5-13	Solid state structure of compound 5-4	124
5-14	Solid state structure of 5-6	125
5-15	Solid state structure of compound 5-7.	126

5-16	Solid state structure of the dinuclear catalyst 5-8.	127
5-17	Space filling model of the solid state structure of 5-8.	128
5-18	¹ H NMR spectrum of the paramagnetic compound 5-9.	128
5-19	Solid state structure of the dinuclear compound 5-10	129
5-20	Schematic of triphenoxymethane aldehyde showing its possible positions for ligand modification.	129
5-21	Synthetic scheme for compounds 5-11 and 5-12.	130
5-22	Synthetic scheme for the synthesis of 5-13 and 5-14	130
5-23	Schematic diagram of the structures of 5-15, 5-16, and 5-17.	131
5-24	Crystal structure of 5-16; Co (II) is arranged in an octahedral geometry.	131
5-25	Catalytic reaction of the ethyl addition to benzaldehyde used as a standard to monitor the catalytic ability of the compounds	132

Abstract of Dissertation Presented to the Graduate School
of the University of Florida in Partial Fulfillment of the
Requirements for the Degree of Doctor of Philosophy

METAL SALEN COMPLEXES IN ANION BINDING AND CATALYSIS

By

Eric R. Libra

August 2007

Chair: Michael J. Scott

Major: Chemistry

Most forms of life require the recognition and transportation of anions. There have been numerous efforts to develop synthetic receptor systems that are both efficient and selective for the coordination of anions. Nature often employs the use of OH groups for anion coordination, yet this binding mode is one that has not been explored in the area of synthetic anion receptor design. A series of substituted metal salen compounds have been developed that show a high affinity for the coordination of anions. The rigid metal salen macrocycle can orientate four phenol groups into a tetrahedral array that tightly and selectively binds fluoride through four strong OH-F hydrogen bonding interactions. The size of the anion binding cavity can be regulated by the incorporation of different metal centers, enabling the properties of the system to be modified. Metals also offer convenient pathways to report the binding event via spectral changes from the strong metal to ligand charge transfer transitions, making these receptors anion sensors. Not only can the metal salen system organize groups for anion binding, they can also be used as chiral catalysts. The synthesis of a rigid and sterically bulky metal salen complex has been undertaken for the use as an asymmetric catalyst to promote organic transformations.

CHAPTER 1 INTRODUCTION

Anions are ubiquitous in a variety of chemical and biological systems.¹ For complex forms of life to exist, many biochemical processes require the recognition and transportation of anions.² A number of enzyme substrate interactions rely on anions and it is reported that anions exist in about 70% of all enzymatic sites where they play a key role in enzyme substrate interactions, as well as having important structural roles in proteins.² The malfunction of channels that facilitate anions across cell membranes, especially chloride,³ is considered the primary cause of many diseases including cystic fibrosis,⁴ Bartter's syndrome,⁵ Dent's disease,⁶ Pendred's syndrome,⁷ and osteopetrosis.⁸

Over the last 25 years there have been numerous efforts to create systems for anion coordination.⁹ The development of selective anion receptors is difficult compared to those designed for selective cation complexation, as anions are typically larger than their isoelectronic cationic counterparts and thus typically have a more diffuse charge. Solvent and pH concerns also play major roles in anion complexation and the nature of coordinating solvents often regulates anion binding and selectivity. Cations are able to form covalent or dative bonds readily to receptor systems while anions must rely on weaker electrostatic forces such as hydrogen bonding or Lewis acidic interactions.¹⁰

There are many examples of anion recognition by host molecules containing various structural and binding modes.¹¹ Some of these systems are able to signal the binding event, which is often done by incorporating various substituents that have the ability to "report" the anion coordination process.¹² Some sensors display a change in color or fluorescence upon interaction with anions, and the ability to readily detect the binding event has recently become an important aspect of anion receptor design.^{13,14} The ability to determine on the macroscopic level

what is happening at the molecular level, such as the coordination of an anion guest into a host molecule may lead to the qualitative and/or qualitative sensing of certain guest molecules.¹ Although there has been much work done in the field of anion binding; the area of anion sensing is far less explored.

Anion Coordination Modes

The creation of molecules that coordinate anions is considered to be in the realm of supramolecular chemistry.¹⁵ The interactions involved in these systems are between molecular or ionic molecules and a guest anion which exist without the formation of covalent bonds. Most of the effort to design anion receptors has focused on the use of Lewis acidic metals¹⁶ or organic ligands that employ hydrogen bonding or electrostatic interactions.¹⁷ Hydrogen bonding has shown to be the binding motif that best induces selectivity of a specific anion,¹⁸ as it is difficult to regulate the direction of Lewis acids, while hydrogen bond donor groups can easily be arranged in a multitude of geometries. There are many potential applications of anion sensors as they can selectively recognize a large variety of anions ranging from fluoride to DNA.^{1,9, 17}

Hydrogen bonds are common in chemical systems as they often have an effect on molecular structure and mechanistic properties¹⁹ and are among the most well utilized means of anion coordination. A hydrogen bond is an attractive interaction between a hydrogen atom and an electronegative atom when the hydrogen is covalently bound to an electronegative donor such as oxygen or nitrogen²⁰ and the strength and length of the hydrogen bond is influenced by the nature of both the donor and receptor atoms.²¹

For the design of anion receptors one must select the proper donor, its orientation within the molecule and also regulate the size and geometry of the binding cavity. To provide hydrogen bond donors in a particular system, groups such as amides, amines, pyrroles, and ureas are normally used.²² N-H groups are relatively easy to preorganize and the majority of the current

examples of anion binding systems have employed this moiety to achieve this goal. Herein, this review will briefly examine the history and progress in the field of synthetic anion receptors.

Initial Studies of Anion Receptor Systems

Selective anion binding has been a topic of interest for almost 40 years since the first anion binding receptor was reported in 1968 by Park and Simon, who showed that bicyclic diaza katapinands (Figure 1-1) could coordinate to halide ions.²³ Park and Simon correctly predicted that hydrogen bonding and not the positive charge of the system was the main mode for halide complexation. Although the binding constants were modest with a $\log K_s$ value of 2, it set the stage for an entire field of research including that of macrocyclic ammonium based receptors.

This research area began to grow in the 1970's when Lehn began coordinating anions with polyammonium macrocycles.²⁴ Lehn's work demonstrated that anions could be selectively coordinate based on size and the design of certain receptors and binding cavities led to stronger interactions with certain anions. For example, a receptor that was an ideal size match for chloride was developed and had a $\log K_s$ value of 4 while iodide was too large to coordinate within the binding cavity and thus had a much lower binding constant.

Lehn and coworkers also noted that particular receptors showed a wide range of stability constants for different anions not only of different sizes, but also geometries. An elliptical shaped receptor was designed that was selective for the linear shaped azide, while it had a low binding constant for chloride.²⁵ The accommodation of chloride into the cavity had no geometric constraints, but it did not have the ideal fit that azide did. Due to these observations new synthetic cavities were developed with the intention of accommodating certain anions by incorporating geometric and spatial constraints. The structure seen in figure 1-2 has shown to be a superb size compliment to fluoride as determined by its solid state structure,²⁶ and this size compatibility has led to an extremely high binding constant of $\log K_s = 11.2$, which is 10^7 times

larger than its binding constant for chloride.²⁷ The strategy of creating a size and geometrically selective cavity for anion coordination became extremely prevalent and is now a basic requirement for the design of any receptor system.

Various quaternary ammonium based anion binders were developed that did not employ hydrogen bonding interactions, but rather arranged ammoniums into a cavity. By adjusting the length of the carbon linkers between the ammoniums, the cavity size could be altered and selectivity could be affected.²⁸ Receptors with a positive charge must contain counter ions which are in direct competition for the anion binding sites. Schmidtchen and coworkers were able to develop a zwitterionic receptor that has an overall neutral charge and avoids the problems incurred by the counter ions.²⁹ The creation of a size selective, neutral receptor that does not employ hydrogen bonding interactions is in contrast to most other systems, yet there has been little work in this area due to synthetic challenges.

Pyrrolic Macrocyclic Receptors

After this seminal work was introduced, the field of receptor chemistry exploded with activity. Pyrrolic macrocycles have been among the most versatile and useful molecules for anion binding, as pyrroles do not contain groups that may induce self association.¹ The ease to which they can be functionalized and ability to make cyclic variations greatly increases the opportunities to tune the system and this has led to the design of pyrrolic systems of many different sizes, shapes, structures, and electronic properties.

Sapphyrins are a common pyrrolic macrocyclic system for anion coordination³⁰ and was first seen as an anion binder in the work of Sessler and co-workers, who reported a crystal structure of a diprotonated sapphyrin with a fluoride bound in the core.³¹ The initial structure with a fluoride ion coordinated was obtained accidentally, but after this observation other anions were tested and modifications to the sapphyrin were made to tune the properties of the system.

Based on the examination of the solid state structure of the complex, chloride was found to be too large to fit inside the center core of the receptor. Instead, two chloride ions were positioned and coordinated above the plane of the receptor.³² Sapphyrins are highly colored and anion coordination leads to changes in the absorption and admission spectra of the molecule, making it an anion sensor. The measurement of these spectroscopic changes leads to high binding constants for fluoride, chloride, and bromide with $\log K_s$ values of 8.0, 7.2, and 6.1 respectively.³²

Biologically Relevant Receptors Incorporating the Guanidinium Group

While pyrrolic macrocycles are effective anion receptors, there are many other systems that incorporate N-H groups for anion coordination. The guanidinium ion has been extensively studied because of its prevalence in nature. Guanidiniums are present in arginine residues and are responsible for many hydrogen bonding interactions in biology. This group contains two N-H hydrogen bond donors as well as a delocalized positive charge that contribute to its strong interactions with the guest species. Guanidinium has a pKa of 13.5 which results in protonation of this moiety over a wide pH range where it will retain both its positive charge and hydrogen bond donor properties.³³ Many synthetic systems incorporating the guanidinium group, such as the molecule in Figure 1-5, have been successful anionic binders since it forms both electrostatic and hydrogen bonding interactions with anionic molecules.

Neutrally Charged Receptors

The presence of positive charges on a receptor system may be helpful for anion coordination, but it also leads to several problems in efficiency and selectivity. In a charged species, it is difficult to regulate the nondirectional electrostatic forces, so adjustments to a particular system become more complicated. The existence of counter ions also causes problems as they are in direct competition for binding sites which affects the selectivity and efficiency of the receptor.¹ The synthesis of neutral species eliminates many of these issues and they have proven to be

amongst the best selective receptors. Reinhoudt and coworkers were one of the first groups to use very simple neutral host molecules as anion hosts. Figure 1-6 depicts an example of a structure that incorporates N-H hydrogen bond donors to coordinate H_2PO_4^- selectively over HSO_4^- and Cl^- with a $\log K_s$ of 4.1.³⁵

The use of N-H donors exists in numerous examples of simple acyclic receptor systems and small modifications have shown to effect anion binding ability and selectivity.³⁶ The creation of cyclic or cage-like molecules however, has rigidified the molecules by placing less flexible spatial constraints on the anion. Recently Bowman-James and co-workers have developed a polyamide cryptand that has shown to bind anions.³⁷

Linking two sets of amides together as outlined in figure 1-7 will create a cavity with multiple N-H groups directed towards the center. Receptor A has shown to bind strongly with phosphate and sulfate and it is believed that the strong interactions are a result of the high correspondence of geometry and size between the guest and host. Amines can deprotonate the anion causing even stronger binding interactions. The tren based bicyclic aza cryptands (Figure 1-7, B) are neutrally charged and have shown to bind fluoride with a high efficiency. Crystal structures of the cryptand with both fluoride and chloride show the halides coordinated within the central cavity and there has also been a noted affinity for other halides as well as for H_2PO_4^- .

Anion Coordination Through Lewis Acidic Metals

Although hydrogen bonding and electrostatic interactions are the common modes of anion complexation, they are not the only available methods. Receptors containing Lewis acidic metals are capable of providing an anion binding site and typically incorporate centers such as boron, silicon, mercury and tin.³⁸ Since many anions are coordinatively saturated the donation of electrons to a Lewis acidic metal forms a strong interaction between the two.

Reinholdt and co-workers have incorporated a uranyl into the backbone of a salen macrocycle (Figure 1-8) and is able to coordinate anions through this Lewis acidic site.³⁹ The coordination of H_2PO_4^- occurs through both the Lewis acidic uranyl as well as a stabilizing force from the acetoamido groups.⁴⁰ Salens can also act as receptors for Ni (II) and Cu (II) sulfate when amine groups are bound at the periphery of the macrocycle.⁴¹ This receptor is able to coordinate an anion and a cation into the same complex. There is great potential in the further exploration of anion receptor systems with the salen macrocycle as they provide an excellent building block for the incorporation of a variety of binding groups.

The synthesis of the salen based ligands is relatively easy and a wide range of donor groups can be readily attached to the system. The incorporation of a metal center into the macrocyclic rings rigidifies the structure can also make these molecules suitable for anion sensing since metal salen compounds normally exhibit strong MLCT transitions in the visible region. The binding event can often be followed by monitoring the position of this intense absorption band. The size of the binding cavity can also be regulated by the incorporation of metals of different radii affecting the binding constants for different anions.

Hydrogen Bonding Interactions Through Oxygen Donors

The use of O-H donor groups interacting with anions in biological systems is extensive. For example, some protein recognition processes rely on an interaction between hydroxyl groups on a carbohydrate and an anionic protein.⁴² In spite of the utility of hydroxyl groups in nature; almost all synthetic receptor systems use some combination of N-H groups. There have been only a handful of examples of complexes that bind anions with an O-H group and none of them are particularly well defined systems. The O-H group can form strong hydrogen bonding interactions but the deficiency of O-H donor examples may be due to the synthetic difficulty in preorganizing such groups. Simple, off the shelf, phenols such as catechol can coordinate

anions, although not surprisingly with rather low binding constants.⁴³ Since then only a handful of other systems incorporating O-H donors have been developed including the work by Wang and coworkers who have created a conjugated polymer system that shows selectivity for fluoride and phosphate.^{43, 44}

The extremely limited body of work for O-H donors in synthetic anion receptor systems, while surprising, offers the opportunity to make important contribution to this field. Presumably, most receptors employ N-H donors opposed to O-H groups as they are relatively easy to organize. Creation of a binding cavity utilizing O-H groups has proven synthetically challenging. In previous work with the pre-organization of phenols, our group has developed the triphenoxymethane molecule (Figure 1-10) and noted that it prefers an “all up” configuration, where all three phenols are pointed in the same direction with respect to the central methine carbon.⁴⁵ This molecule is readily modified and its properties can easily be tuned.

Research Objectives

Our objective is to incorporate the triphenoxymethane molecule into the backbone of a salen macrocycle for the use of selective anion sensing. We envisioned creating a cavity of phenolic donors offering four O-H groups available for anion coordination. This type of molecule would be the first example of a well defined receptor system that employs purely hydroxyl groups. As described above, the salen system was chosen for its ability to provide a visual report, allowing the binding event to be monitored by UV-Vis spectroscopy. The choice of metal also plays an important role in structurally regulating the cavity size. Herein, we report the design, synthesis and study of metal salen complexes and their anion binding properties.

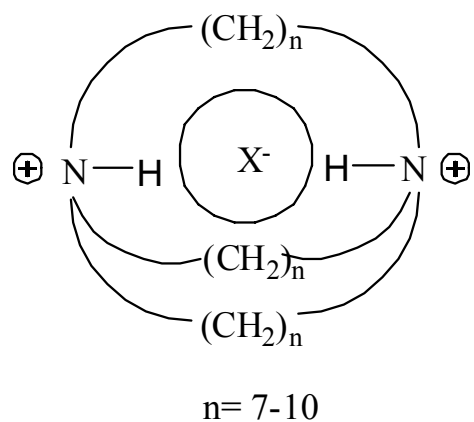


Figure 1-1. Structure of Park and Simon's katapinate; the first example of an anion binder.

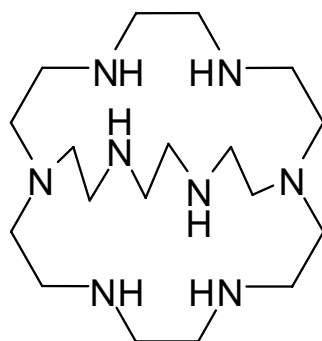


Figure 1-2. Structure of azacryptand that is an ideal size match for fluoride and shows an extremely high binding constant for fluoride ($\log K_s = 11.2$)

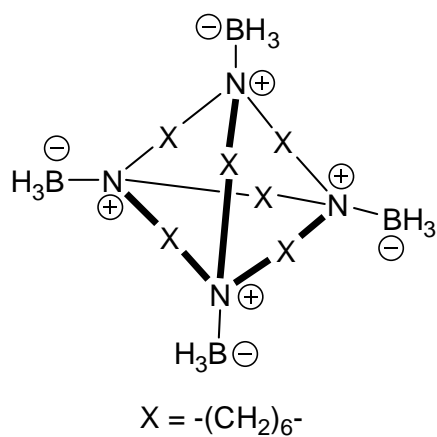


Figure 1-3. Structure of zwitterionic neutral receptor. Anion coordination is done through electrostatic interactions only.

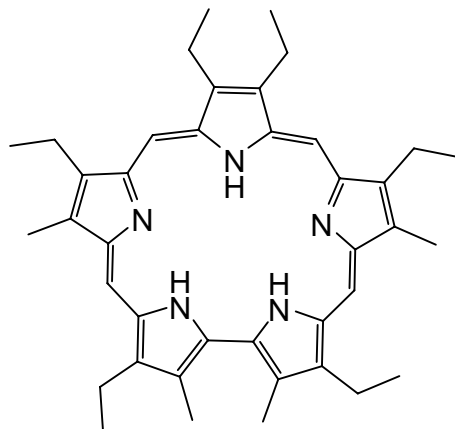


Figure 1-4. Structure of the pyrrolic macrocycle sapphyrin. Upon protonation there are five N-H's donors that form hydrogen bonds to anions.

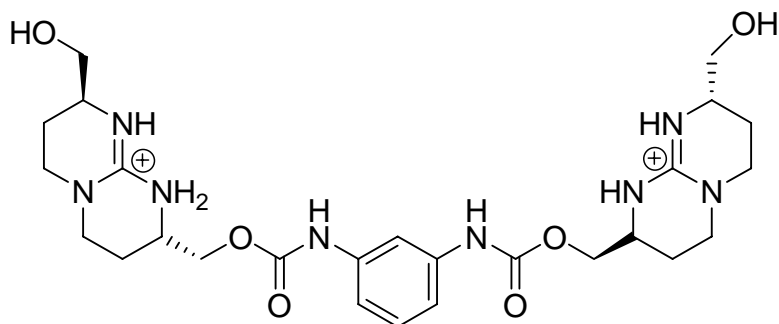


Figure 1-5. Structure of two bicyclic guanidiniums attached by a urethane linker.

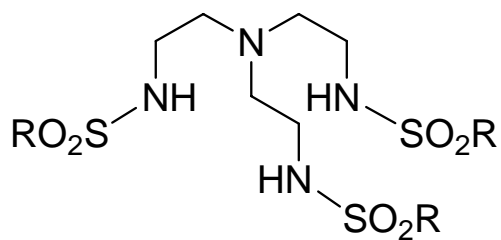


Figure 1-6. Structure of neutral anion receptor.

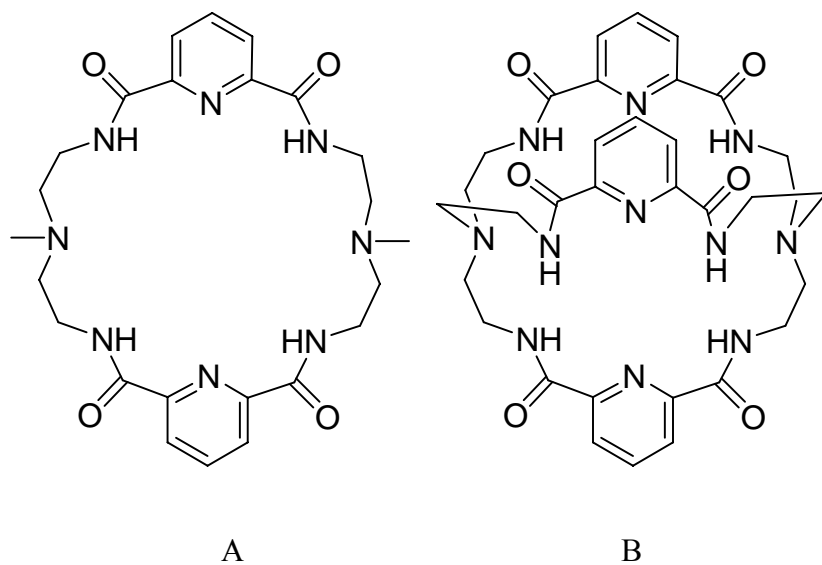


Figure 1-7. Structures of amide based receptors by Bowman-James

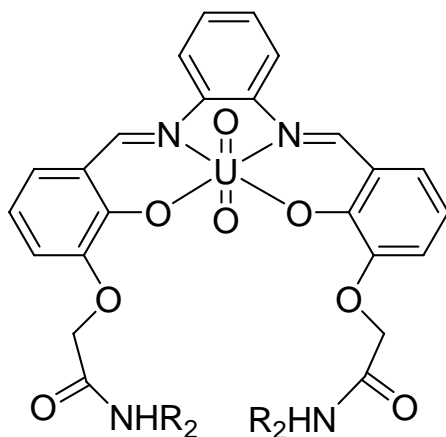


Figure 1-8. Structure of salen complex with uranyl used for Lewis acidic anion binding

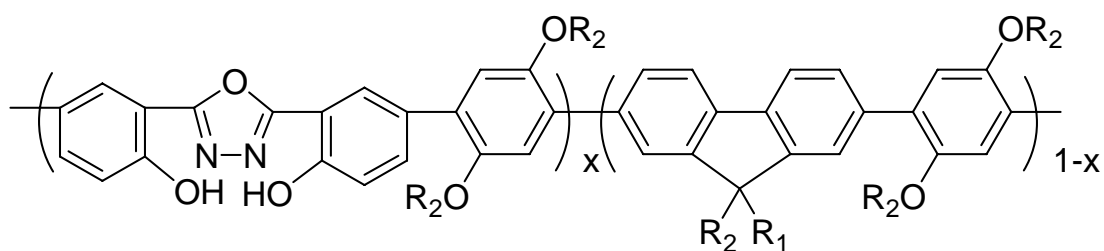


Figure 1-9. Structure of conjugated polymer that efficiently binds fluoride through phenols.

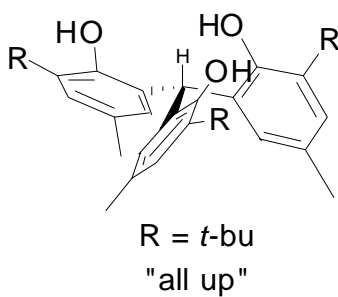


Figure 1-10. Structure of triphenoxymethane platform with three phenols aligned with respect to each other.

CHAPTER 2
METAL SALEN COMPLEXES INCORPORATING TRIPHENOXYMETHANES:
EFFICIENT, SIZE SELECTIVE BINDING OF FLUORIDE WITH A VISUAL REPORT

Introduction

For the design of anion receptors, Lewis acidic metals¹⁶ or organic ligands that employ hydrogen bonding and/or electrostatic interactions are often used.¹⁰ In the case of hydrogen bond donors, virtually all of the attention has focused on ligands incorporating N-H groups such as amides, amines, pyrroles, and ureas,²² and in some instances, metals help orient these groups.⁴⁶ Surprisingly, despite the wide participation of serine and tyrosine hydroxides in anion binding sites in biological systems including ClC chloride channels⁴⁷ and Bacteriorhodopsin⁴⁸ among numerous others,⁴⁹ the use of O-H donors in the design of anion receptors has been limited to only a handful of examples that are not particularly well defined systems.⁵⁰

To provide hydrogen bond donors to coordinate anions, N-H as well as O-H donor groups can be used. A hydrogen bonding interaction can take place between a hydrogen covalently bound to an electronegative donor and an electronegative acceptor (D-H...A). The limited work in the area of O-H based anion receptors may be due to the difficulties in pre-organizing O-H groups compared to N-H groups. The phenolic proton is quite acidic (pKa ~10) compared to that of amines (~26) and amides (~20) and thus O-H groups should form stronger hydrogen bonds than those formed by N-H groups.

Results and Discussion

The presence of O-H groups can increase the affinity of N-H containing ligands for anions,⁵¹ but we envisioned that a tetrahedral pocket of phenolic donors templated by a metal could provide an ideal environment for the selective binding of anions, particularly since the size of the cavity could be modulated by the choice of metal. Metals also offer convenient pathways to report the binding event via spectral changes. Salens have been engineered to orient two sets

of N-H donors by several groups,⁵² and herein, we report the synthesis and attributes of an anion receptor incorporating four phenols at the periphery of salen.

Advantages of the Salen Macrocycle

In previous work with triphenoxymethanes⁴⁴ (Figure 2-2), a profound preference has been noted for the molecule to adopt an “all-up” orientation wherein all three phenolic oxygens align with respect to the central methine hydrogen. A derivative incorporating an aldehyde group on a single phenol can be readily isolated.⁵³ The molecule reacts with 1,2-diamino cyclohexane to form 2-1 as outlined in Figure 2-3.

A range of metals including Mn (II), Ni (II), Zn (II), and Pd (II) can be incorporated into the salen binding sites without affecting the four remaining phenols. The six triphenoxymethane phenols still prefer to remain aligned, and since the metal coordinates to two of them, a pocket is created which is lined by four hydrogen bond donor groups in a pseudo tetrahedral arrangement. Initial work on the development of an anion sensor has focused on the diamagnetic, square planar Ni (II) and Pd (II) metals since their radii differ by approximately ~ 0.15 Å, providing the opportunity to adjust the size of the binding cavity. Salen complexes with these metals also exhibit intense MLCT absorptions ($\epsilon \sim 7400$) in the visible region.⁵⁴ The relative synthetic ease of the system and the possibility to tune the receptor’s properties by complexation of different metals offers many advantages and the synthesis of the receptor is seen in Figure 2-3.

Design of Receptor System

Compound 2-1 has been structurally characterized (Figure 2-4) and in the solid-state, the two sets of triphenoxymethanes align themselves on opposite sides of the 1,2-diaminocyclohexane linker. The phenols remain aligned in the same direction with respect to

each other. The incorporation of a metal center into the ligand aligns and rigidifies the molecule positioning the four remaining phenols into tetrahedral environment.

For the development of an anion sensor, focus has been placed on the diamagnetic, square planar Ni (II) and Pd (II), providing the opportunity to adjust significantly the size of the binding cavity. Ni (II) and Pd (II) are also d^8 and prefer a square planer geometry which makes them diamagnetic and enables us to follow the synthesis and anion binding by NMR spectroscopy. Salen complexes with these metals also exhibit intense MLCT absorptions ($\epsilon \sim 7400$) in the visible region⁵⁴ and the compounds have shown significant color change upon addition of fluoride.

Both Ni (II) (2-2) and Pd (II) (2-3) metal complexes with 2-1 were structurally characterized, and in each, two symmetry independent molecules crystallized in the asymmetric unit. In both cases, the molecules were nearly indistinguishable, but the orientation of the unbound phenols with respect to the chiral centers on the cyclohexyl rings differed. The chiral *R,R*-cyclohexyl backbone was used to isolate single crystals of 2-2 and the structure of one of the two symmetry independent molecules is presented in Figure 2-5. The chiral *R,R*-1,2-diaminocyclohexane backbone as well as the racemic version was used to isolate the Ni (II) complex. There were significant differences in solubilities between the two molecules yet they showed identical UV-Vis and NMR spectra. While the racemic complex had a limited solubility the chiral receptor was soluble in solvents with a wide range of polarities.

As expected, the average distance of the four Ni-oxygen bonds in the two complexes (1.842(8) Å) are typical for a Ni (II) salen complex⁵⁵ but significantly shorter than the corresponding average Pd-oxygen distances (2.009(4) Å). The subtle size difference between the two metals produces a profound increase in the separation between the two sets of phenolic

donors attached to the salen backbone. The distance between the two methine carbons, C (15) and C (46), increases from 5.28 Å in 1-Ni (II) complex to 6.03 Å in the 1-Pd (II), and this increase manifests other changes. In both symmetry independent Ni (II) complexes, a phenolic group from each side of the cavity maintains short hydrogen bonding interactions with the salen phenolates (O-O separations vary from 2.677(7) Å to 2.885(9) Å) and the two remaining phenolic oxygens are situated 2.762(7) Å or 2.784(8) Å from each other, creating a cavity held together by several intramolecular hydrogen bonds. In contrast, only a single phenol hydrogen bonds to the salen phenolate in the cavity formed in 2-3 with a O-O separation of 2.824(4) Å, and this oxygen also maintains a close contact of 2.804(4) Å with a phenol oxygen on the opposite side of the cavity. The remaining two phenols are more than 3.989 Å from the nearest oxygen. These intramolecular hydrogen bonding interactions not only play a structural role, but may also have an effect on the colorimetric properties of this system.

Anion Binding Properties

Anion binding properties of the two metal complexes were tested with *n*-Bu₄N⁺ halide salts in a variety of solvents including chloroform, acetone, and DMSO, and both 2-2 and 2-3 complexes only reacted with fluoride at low anion concentrations. The binding cavity appears to be too small to accommodate the larger anions and even after the addition of a large excess of Cl⁻, Br⁻, I⁻, NO₃⁻, ClO₄⁻, or HSO₄⁻ no changes could be detected in the ¹H NMR or UV/Vis spectra. . Treatment of 2-2 and 2-3 with one equivalent of more basic anions such as H₂PO₄⁻ and OAc⁻ produced no discernable change in the UV/Vis or ¹H NMR spectrum other than the disappearance of the OH resonances in the ¹H NMR spectrum, but at very high concentrations (> 30 eq), the anions induced precipitation in the NMR experiment and a small (<8 nm) shift of the absorption maxima in the UV/Vis spectra of the complexes.

In contrast, the addition of fluoride to 2-2 induced a dramatic change in the ^1H NMR spectrum, and with any amount less than a full equivalent of fluoride, the spectrum was quite broad, suggesting a rapid equilibrium of fluoride between open binding sites since the complex remains diamagnetic. Unfortunately, cooling of the sample initiated crystallization and variable temperature NMR experiments could not be performed. Addition of fluoride to 2-3 produced a less dramatic effect on the ^1H NMR spectrum of the complex (Figure 2-7), and the only significant change involved the two resonances associated with the phenolic protons that shift from 6.83 and 6.44 ppm in $\text{d}^6\text{-DMSO}$ and appear as a doublet at 9.93 ppm ($J_{\text{HF}} = 46$ Hz).

Similar magnitudes for H-F coupling constants have been noted in halide receptors incorporating amides⁵⁶ and pyrroles.⁵⁷ The phenolic resonances for $[\text{2-2-F}]^{1-}$ also occur as a doublet downfield at 9.69 ppm ($J_{\text{HF}} = 42$ Hz) in $\text{d}^6\text{-DMSO}$, but in solvents such as CDCl_3 and $(\text{CD}_3)_2\text{CO}$, the resonances for the phenolic protons on both 2-2 and 2-3 are absent, presumably due to deuterium exchange with solvent. Fluoride is known to facilitate deuterium exchange on amides in halide receptors.⁵⁸ In the ^{19}F NMR spectrum, a quintet resonance ($J_{\text{HF}} = 46$ Hz) slowly grows in at -117.2 ppm (referenced against trifluorotoluene at -63.7 ppm) as fluoride is added to a $\text{d}^6\text{-DMSO}$ solution of 2-3, intimating that the four phenolic O-H...F interactions are equivalent and produce the $2nI + 1$ quintet resonance.

After addition of more than a one equivalent of anion, a new resonance arises at -145.7 ppm, the normal position of the resonance of free fluoride ion. The ^{19}F NMR spectrum of 2-2 after addition of fluoride exhibited a broad resonance at -116.2 ppm, and the value for the H-F coupling constant could not be accurately determined. Once again, solvents such as chloroform and acetone favor deuterium exchange, and all H-F coupling in the ^{19}F NMR disappear in these solvents.

Addition of fluoride to 2-2 and 2-3 disrupts the hydrogen bonds to the salen phenolates and induces a red shift in the MLCT absorption with two distinct isobestic points (Figure 2-11), intimating a single species forms in solution. In the case of 2-2, the absorption shifts from 411 nm to 431 nm with a small decrease in the molar absorptivity while the 2-3 exhibits a slightly larger shift from 407 nm to 440 nm. The color change is abrupt and can easily be seen by the naked eye.

The determination of the binding mode of the anion and the ratio of bound anion to receptor requires the production of Job plots. Both ¹H NMR and UV-Vis spectral data are commonly used to derive Job plots, but due to the complicated nature of ¹H NMR spectrum and the clarity of the absorption data for 2-2, UV-Vis spectra were used to determine the guest-host stoichiometry. The location of the apex of the plot indicates the ratio of fluoride bound to each 2-2 molecule. A Job plot for the spectral data of 2-2 shows a maximum at 0.5 indicating a single equivalent of fluoride binds in the phenolic cavity (Figure 2-12).

Binding Constants

The binding constants (K_s) were determined from the data obtained by UV-Vis spectroscopy fluoride titrations. The measured absorbance were plotted as a function of fluoride ion concentration of the solution at 450nm and a non-linear least squares regression was used to determine binding constants with the equation:⁵⁹ $X = X_0 + [(X_{lim} - X_0) / 2c_0] \cdot [c_0 + c_m + 1/K_s - [(c_0 + c_m + 1/K_s)^2 - 4c_0c_m]^{1/2}]$. In this equation, X is the measured absorbance, X_0 is the initial absorbance, X_{lim} is the limiting absorbance, c_0 is concentration of anion in solution, c_m is the concentration of the receptor, and K_s is the binding constant. A program to perform a non-linear least squares regression on the data⁶⁰ which minimizes the error of each data point to fit the standard equation by altering K_s was written in excel. The value of K_s that leads to the lowest sum of errors is the binding constant for the system. The $\log K_s$ values (errors $\pm 10\%$) were

determined to be 5.6 for 2-2 and 5.8 for 2-3 in acetone ($\log K_s = 5.8$ for both complexes in DMSO).

Solid State Structure of [2-2-F]¹⁻

Single crystals of the 2-2 with a fluoride ion were obtained, and in the solid state (Figure 2-14), the fluoride is held in the phenolic cavity by three short and one long hydrogen bond to form [2-2-F]¹⁻ (fluorine oxygen separations of 2.539(2) Å, 2.509(2) Å, 2.573(2) Å, and 3.098(3) Å). Although the resonances are a bit broader than the data presented in Figure 3 for [2-3-F]¹⁻, the solution NMR spectra for [2-2-F]¹⁻ suggest the fluoride is held in a symmetric environment by the four phenols, and the lone, long OH...F interaction may be an artifact of crystal packing.

In order to fit the anion, the phenolic pocket has had to open up, and the separation between the methine carbons, C(15) and C(46), has increased by almost 0.5 Å to 5.73 Å in comparison to 2-2. Ni (II) appears to be resisting the increase in size of the cavity, and the metal distorts from planarity with an angle of 15.8° between the two N-Ni-O planes in the salen. The cavity created by the Pd(II) center should be able to accommodate the fluoride anion with much less distortion, since the separation between C(15) and C(46) is already 6.03 Å in 2-3 which may lead to the larger K_s ($\log K_s = 5.81$) compared to that of 2-2. The clarity of the ¹H NMR spectrum of 2-3 during the titration experiment suggests structural distortions are less pronounced than in 2-2.

Anion Binding Studies for 2-3

Binding studies of compound 2-3 were tested with the various anions and the increase in cavity size for 2-3 between the methine carbons to 6.03 Å compared to 5.23 Å in the Ni complex was quite dramatic and the ability to bind larger anions was a possibility. As with 2-2, 2-3 had a profound affinity for fluoride while showing no interaction with other anions. Titration experiments with tetrabutylammonium salts in acetone, and once again showed there was no

change in the NMR spectra or UV-Vis spectra from Cl^- , Br^- , I^- , NO_3^- , ClO_4^- , or PO_4^{3-} . Titration of 2-3 with fluoride led to a large red shift in the absorbance spectra, where the main absorption shifts from 407 nm to 440 nm. There were also two isobestic points for this titration implying only a single product is formed. The job plot for 2-3 shows that fluoride binds to the Pd complex in a 1:1 ratio (Figure 2-16).

Even though the cavity of 2-3 is considerably larger than 2-2 it is still size selective for fluoride and can not accommodate other large anions. The ionic radius of fluoride is considerably smaller than that of most other anions at 1.36Å, such as chloride (1.81Å), and phosphate (2.38Å).

The larger cavity does have an effect on the binding ability of fluoride and influences several of the properties of 2-3. The ^1H NMR spectrum of 2-2 with less than one equivalent of fluoride is very complicated possibly due to a fast exchange of fluoride between open binding sites. However, compound 2-3 has only minor changes in the spectrum other than the disappearance of the peaks representing the two different phenols in the structure. Due to the increased cavity size there is potentially a lack of strain places on 2-3 upon binding fluoride eliminating the exchange that is seen with 2-2. Another consequence is the slightly higher binding constant of 2-3 which has a $\log K_s$ of 5.81 compared to 2-2 which has a $\log K_s$ of 5.64.

Conclusions

In conclusion, a salen ligand, 2-1, has been designed with a pair of phenolic donors tethered to the *ortho*-position of each of the salen phenols. Complexation of square planar metal centers into the macrocyclic binding pocket forces the four remaining phenolic groups to form a tetrahedral array, and this pocket tightly binds fluoride. The ion is bound by three short and one long O-H...F interactions, representing a rare example of efficient anion binding by purely OH hydrogen bonding in a well-defined sensor. The binding event induces a red-shift in the intense

MLCT transition, offering a distinct visual report of the binding event. Efforts to increase the size and the number of phenolic donors that create the cavity by using different metal centers and amine linkers are currently underway.

Experimental Methods

General Considerations

^1H and ^{13}C NMR spectra were recorded on a Varian Mercury 300 MHz spectrometer at 299.95 and 75.47 MHz for the proton and carbon channels. UV-Vis spectra were recorded on a Varian Cary 50 spectrometer. Elemental analyses were performed at either the in-house facility of the Department of Chemistry at the University of Florida or by Complete Analysis Laboratories Inc., Parsippany, NJ. All solvents were ACS or HPLC grade and used as purchased. For the metalation reactions, the solvents were dried with a Meyer Solvent Purification system.

Synthesis of 2-1

A portion of 0.63 g (5.52mmol) of 1,2-diaminocyclohexane was dissolved in 50 mL absolute ethanol. To this solution a slurry of 5.00 g (11.05 mmol) of 3-(2,2'-Methylenebis (4-methyl-6-*tert*-butylphenol)-5-methyl-2-hydroxybenzaldehyde)⁵³ in 300 mL ethanol was added. The reaction was refluxed open to the air for 12 hours. The solution was cooled to room temperature and water was added to the solution resulting in the precipitation of a bright yellow solid. The solid was filtered and dried to afford the product in 83% yield (4.73 g). ^1H NMR: δ 8.12 (s, 2H); 7.04 (s, 4H); 6.93 (s, 2H); 6.77 (s, 2H); 6.66 (s, 4H); 5.94 (s, 2H); 5.62 (s, 2H); 5.40 (s, 2H); 3.30 (d, 2H); 2.20 (s, 6H); 2.17 (s, 6H); 2.10 (s, 6H); 2.00-1.85 (m.); 1.38 (s, 36H). ^{13}C NMR δ 165.4; 157.7; 151.4; 137.7; 134.5; 131.2; 129.2; 128.3; 127.9; 127.7; 127.5; 117.9; 72.0; 39.2; 34.9; 33.2; 30.0; 24.33; 21.3; 20.7. HR-FABMS: calcd for $\text{C}_{68}\text{H}_{87}\text{O}_6\text{N}_2$ 1027.6564; found 1027.6568 [MH^+]. IR: ν [cm^{-1}] 3495 (OH); 1625 (C=N).

Synthesis of *R,R*-2-1

Using a modified literature procedure,⁶¹ a portion of 2.00 g (7.57 mmol) of (*R,R*)-(-)-1,2-diaminocyclohexane mono-L-(+)-tartrate was mixed with 2.09 g (15.14 mmol) of potassium carbonate and dissolved in 15 mL water. To this solution, 60 mL of absolute ethanol was added and the solution was brought to a reflux. A slurry of 6.85 g (15.14 mmol) 3-(2,2'-Methylenebis(4-methyl-6-*tert*-butylphenol))-5-methyl-2-hydroxy-benzaldehyde in approximately 150 mL of ethanol was slowly added to the amine with an addition funnel. The solution was then refluxed for three hours. 20 mL of water was added and it was cooled in the refrigerator for 12 hours. The bright yellow solid was filtered and then dissolved in methylene chloride. It was washed three times with water in a separatory funnel, dried with magnesium sulfate and the solvent was removed to afford the pure product in 78% yield (6.05 g). ¹H NMR: δ 8.12 (s, 2H); 7.04 (s, 4H); 6.93 (s, 2H); 6.77 (s, 2H); 6.66 (s, 4H); 5.94 (s, 2H); 5.62 (s, 2H); 5.40 (s, 2H); 3.30 (d, 2H); 2.20 (s, 6H); 2.17 (s, 6H); 2.10 (s, 6H); 2.00-1.85 (m); 1.38 (s, 36H). ¹³C NMR δ 165.4; 157.7; 151.4; 137.7; 134.5; 131.2; 129.2; 128.3; 127.9; 127.7; 127.5; 117.9; 72.0; 39.2; 34.9; 33.2; 30.0; 24.33; 21.3; 20.7.

Synthesis of *R,R*-2-2

A portion of 1.0 g (0.974 mmol) *R,R*-1-H₂ was dissolved in dry THF. To this solution 0.27 g (10.30 mmol) of nickel acetate was added and it was refluxed under nitrogen for 12 hours. The solution was cooled, filtered and the solvent removed. The remaining solid was then dissolved in pentane, filtered and a dark red solid was obtained in an 87% yield (0.92 g). Crystals suitable for X-ray diffraction were grown by slow evaporation from a concentrated acetonitrile solution. ¹H NMR: δ 7.45 (s, 2H); 7.17 (d, 2H); 6.87 (s, 4H); 6.83 (s, 2H); 6.76 (s, 4H); 6.57 (s, 2H); 6.38 (s, 2H); 6.25 (s, 2H); 3.20-3.15 (m, 2H); 2.55-2.45 (m, 2H); 2.17 (s, 6H); 2.14 (s, 12H); 2.00-1.9 (m, 2H); 1.12 (s, 18H); 1.11 (s, 18H). ¹³C NMR δ 158.2; 152.0; 151.8;

137.5; 137.3; 137.2; 132.2; 130.6; 128.9; 128.6; 127.4; 127.3; 126.6; 126.8; 119.6; 70.3; 36.4; 34.6; 29.5; 28.7; 24.4; 21.0; 20.4. Anal. Calc. for $C_{68}H_{84}N_2O_6Ni$ CH_3CN : C, 74.72; H, 7.79; N, 3.73. Found C, 74.24; H, 7.84; N, 3.44.

Synthesis of 2-2

A portion of 1.0 g (0.974 mmol) of 1- H_2 was dissolved in dry THF. To this solution 0.27 g (1.07 mmol) of nickel acetate was added and it was refluxed under nitrogen for 12 hours. The solution was cooled, filtered and the solvent removed. The solid was then washed with pentane and filtered producing a red solid product in 91% yield (0.96 g). 1H NMR: δ 7.45 (s, 2H); 7.17 (d, 2H); 6.87 (s, 4H); 6.83 (s, 2H); 6.76 (s, 4H); 6.57 (s, 2H); 6.38 (s, 2H); 6.25 (s, 2H); 3.20-3.15 (m, 2H); 2.55-2.45 (m, 2H); 2.17 (s, 6H); 2.14 (s, 12H); 2.00-1.9 (m, 2H); 1.12 (s, 18H); 1.11 (s, 18H). ^{13}C NMR δ 158.2; 152.0; 151.8; 137.5; 137.3; 137.2; 132.2; 130.6; 128.9; 128.6; 127.4; 127.3; 126.6; 126.8; 119.6; 70.3; 36.4; 34.6; 29.5; 28.7; 24.4; 21.0; 20.4.

Synthesis of 2-3

Using a modified literature procedure,⁶² a portion of 1.00 g (0.974 mmol) of 1- H_2 was dissolved in dry ether. To this solution 0.092 g (2.14 mmol) sodium methoxide was added along with 0.240 g (1.07 mmol) of palladium acetate. The solution was refluxed for three hours under nitrogen during which time a green precipitate formed. The solution was cooled and the precipitate was filtered. The product was redissolved in methylene chloride, filtered and then solvent was removed leaving a yellow solid in a 62% yield (0.68 g). Crystals suitable for X-ray diffraction were grown by a chloroform / pentane diffusion. 1H NMR: δ 7.57 (s, 2H); 7.10 (d, 2H); 6.98 (s, 4H); 6.95 (s, 2H); 6.91 (s, 2H); 6.88 (s, 2H); 6.60 (s, 2H); 6.58 (s, 2H); 6.28 (s, 2H); 5.81 (s, 2H); 3.50-3.40 (m, 2H); 2.41 (d, 2H); 2.16 (s, 6H); 2.14 (s, 6H); 2.09 (s, 6H); 1.71 (d, 2H); 1.28 (s, 18H); 1.18 (s, 18H). ^{13}C NMR δ 160.49; 156.44; 151.26; 138.74; 137.58; 136.90; 134.04; 132.91; 130.16; 129.61; 128.60; 128.41; 128.06; 125.91; 125.08; 120.64;

72.62; 38.86; 34.89; 30.05; 28.99; 24.47; 21.47; 20.23. Anal. Calc. for C₆₈H₈₄N₂O₆Pd: C, 72.16; H, 7.48; N, 2.48. Found C, 72.03; H, 7.65; N, 2.51.

Synthesis of [2-2-F](Bu₄N)

A portion of 0.050 g (0.046 mmol) of 1-Ni along with 0.029 g (0.092 mmol) tetrabutylammonium fluoride trihydrate was dissolved in 1 mL toluene. Crystals suitable for X-ray diffraction were grown by a slow diffusion of pentane into toluene solution. ¹H NMR: δ 7.44 (s, 2H); 7.16 (d, 2H); 6.86 (s, 4H); 6.83 (s, 2H); 6.75 (s, 4H); 6.37 (s, 2H); 3.37 (m, 8H); 3.14 (s, 2H); 2.46 (m, 2H); 2.17 (m, 6H); 2.13 (s, 12H); 1.92 (m, 2H); 1.68 (m, 8H); 1.46 (q, 8H); 1.30 (m, 2H); 1.12 (s, 18H); 1.10 (s, 18H); 1.02 (t, 12H). Anal. Calc. for C₈₄H₁₂₀N₃O₆NiF: C, 74.98; H, 8.99; N, 3.12. Found C, 74.24; H, 8.91; N, 2.64.

Determination of binding constants (LogK_s)

A 4.61 x 10⁻⁵M solution of 2-2 in acetone was titrated with 23 μL aliquots of a tetrabutylammonium fluoride solution. Absorbance was plotted versus fluoride concentration at 450 nm and a non-linear least squares regression was then run on the data using the following equation:⁵⁹ $X = X_0 + [(X_{lim} - X_0) / 2c_0] \cdot [c_0 + c_m + 1/K_s - [(c_0 + c_m + 1/K_s)^2 - 4c_0c_m]^{1/2}]$. By solving this equation for K_s we were able to obtain logK_s of 5.64 for 1-Ni(II) and 5.81 for 2-3.

Table 2-1. X-ray data for the crystal structures of 2-1 and the complexes *R,R*-2-1, 2-3, and 2-2-F.

	2-1·CH ₃ CN	<i>R,R</i> -2-2·CH ₃ CN	2-3·Et ₂ O	2-2-F·Et ₂ O
total reflections	16607	18198	40023	29805
unique reflections	10576	14424	26428	19898
Θ_{\max}°	25	28	28	28
empirical formula	C ₇₀ H ₈₉ N ₃ O ₆	C ₇₂ H ₉₀ N ₄ O ₆ Ni	C ₇₀ H ₈₉ N ₂ O ₇ Pd	C ₈₈ H ₁₃₀ F N ₃ O ₇ Ni
M_r	1068.44	1166.19	1176.86	1419.66
crystal system	triclinic	triclinic	triclinic	triclinic
space group	P-1	P1	P-1	P-1
<i>a</i> (Å)	13.8245(12)	13.1800(9)	16.6011(11)	13.7248(9)
<i>b</i> (Å)	14.1393(12)	13.7606(10)	21.7001(15)	17.0299(11)
<i>c</i> (Å)	17.9268(15)	20.2871(14)	23.4994(16)	22.1543(14)
α (°)	70.554(2)	83.2670(10)	71.3800(10)	71.4080(10)
β (°)	89.380(2)	77.1700(10)	86.2890(10)	89.0850(10)
γ (°)	71.177(2)	66.1000(10)	71.1520(10)	72.8510(10)
V_c (Å ³)	3109.2(5)	3278.4(4)	7585.3(9)	4672.3(5)
D_c (g cm ⁻³)	1.141	1.181	1.031	1.009
<i>Z</i>	2	2	4	2
$\mu(\text{Mo-}K\alpha)$ (mm ⁻¹)	0.072	0.349	0.289	0.257
R_1 [$I \geq 2\sigma(I)$ data] ^b	0.0907	0.0506	0.0584	0.0608
wR_2 (all data) ^c	0.1629	0.1179	0.1230	0.1687
GoF	0.946	1.019	0.821	0.968

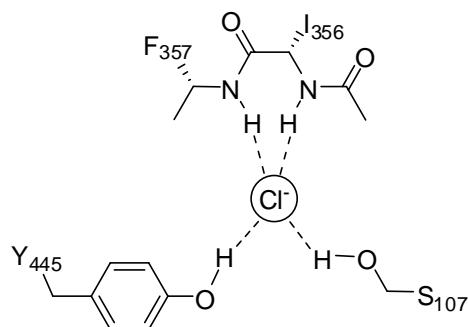


Figure 2-1. Schematic diagram of the open conformation of ClC chloride channel. Chloride is held in place by two OH-Cl hydrogen bonds from Y445 and S107.

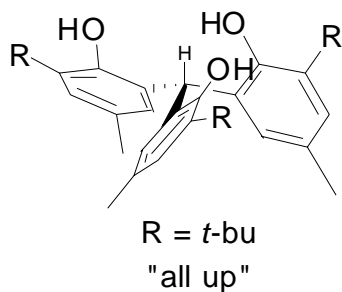


Figure 2-2. Triphenoxymethane platform with the phenols in the “all up” position relative to the methine carbon hydrogen.

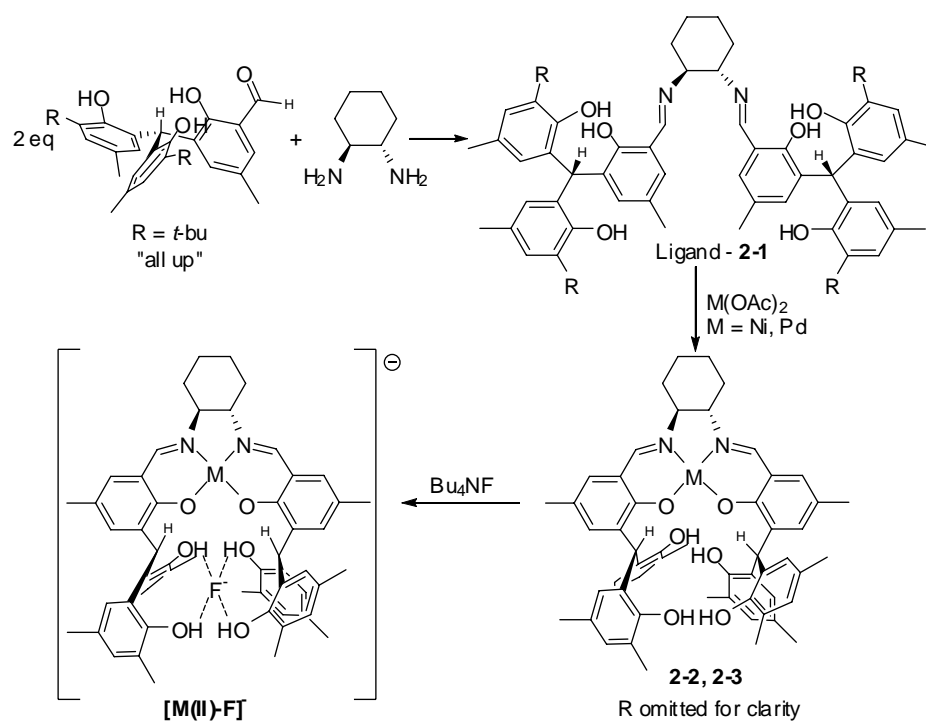


Figure 2-3. Procedure used for the synthesis of 2-1, macrocycle metalation to form 2-2, and 2-3 and fluoride binding.

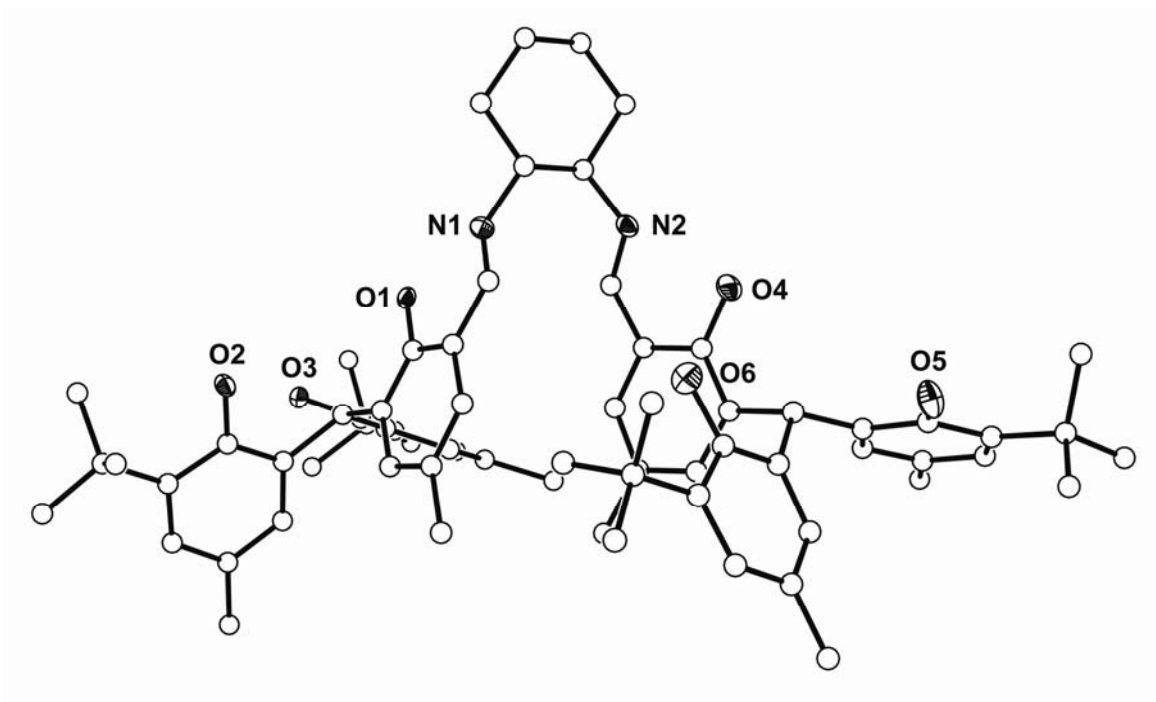


Figure 2-4. Depiction of the solid-state structure of 2-1 (30% probability ellipsoids for nitrogen and oxygen, carbons drawn with arbitrary radii)

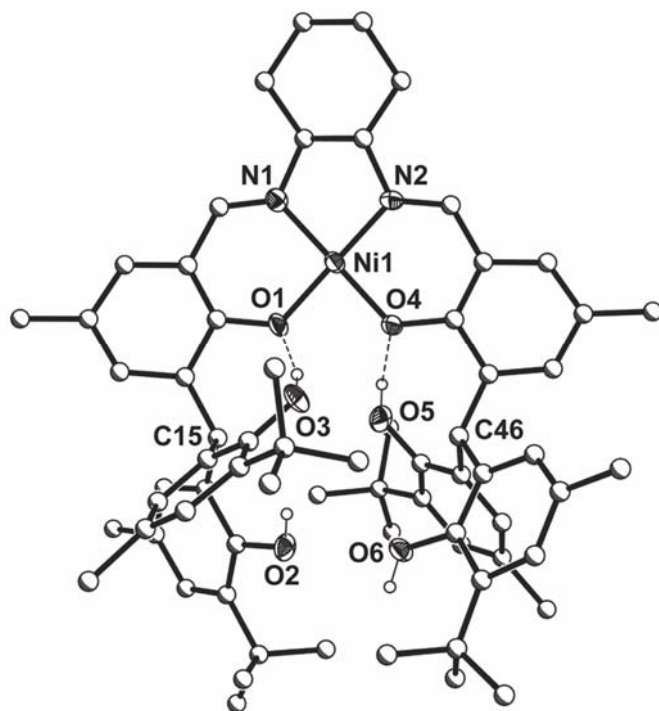


Figure 2-5. Depiction of the solid-state structure of 2-2 (30% probability ellipsoids for nitrogen, oxygen and nickel, carbons drawn with arbitrary radii)

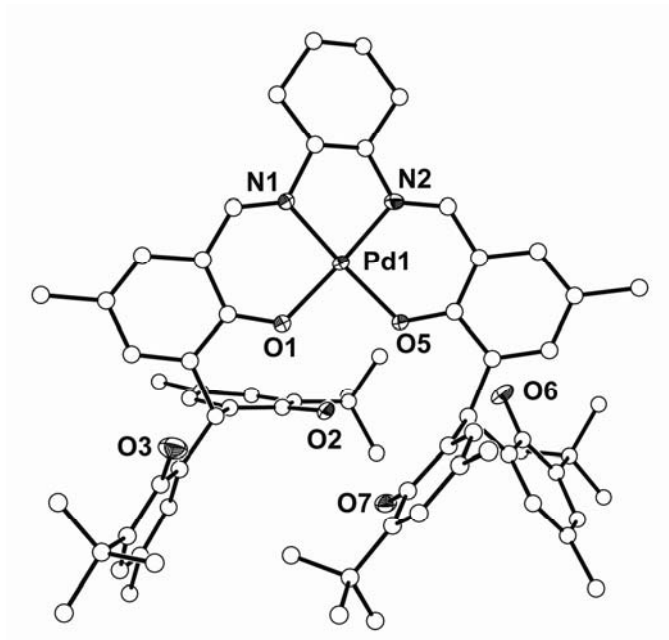


Figure 2-6. Depiction of the solid-state structures of 2-3 (30% probability ellipsoids for nitrogen, oxygen and palladium, carbons drawn with arbitrary radii)

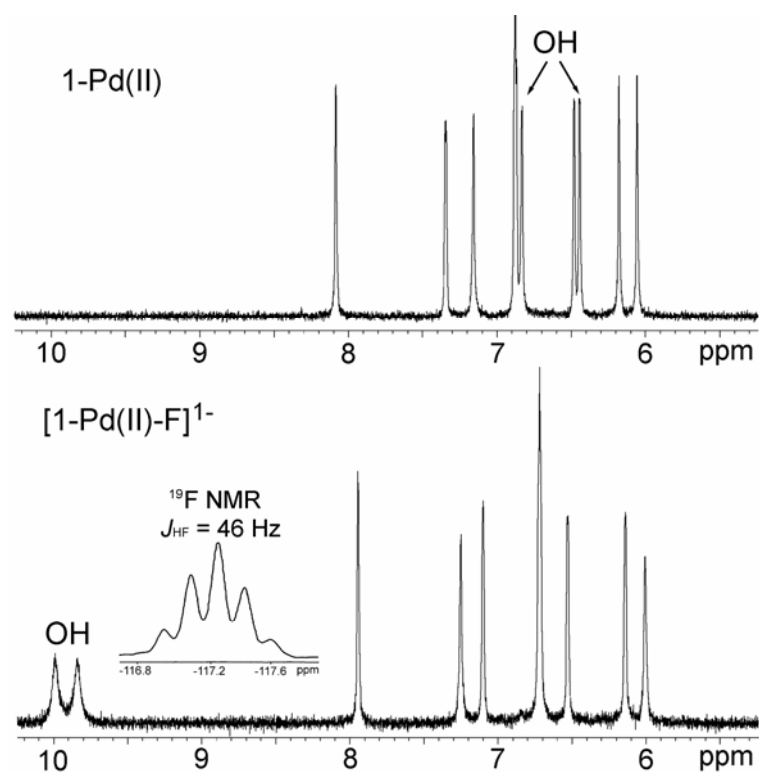


Figure 2-7. ¹H NMR spectrum of 2-3 (top) and [2-3-F]¹⁻ (bottom) taken in d⁶-DMSO with an inset of the ¹⁹F NMR spectrum of [2-3-F]¹⁻ in the region of bound fluoride.

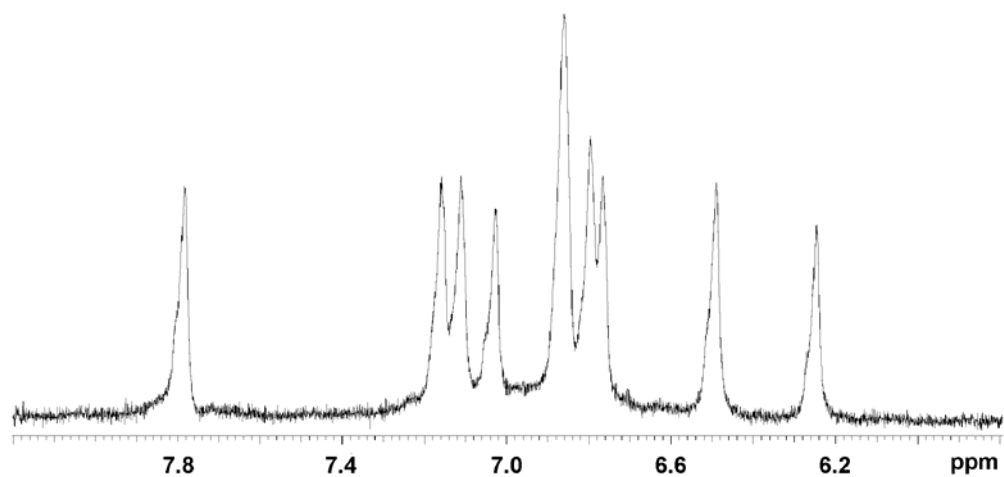


Figure 2-8. ¹H NMR spectrum of 2-2 with a sharp and well defined aromatic region.

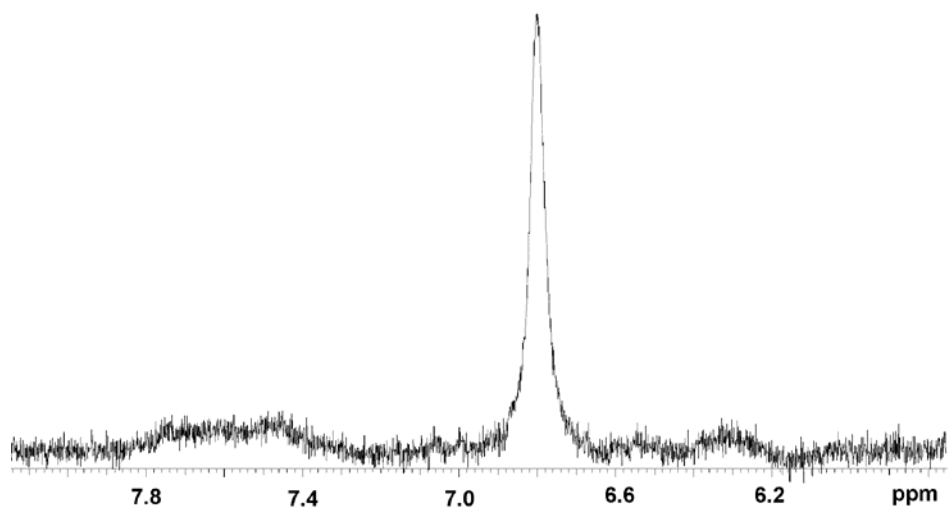


Figure 2-9. ^1H NMR spectrum of 2-2 with 0.5 equivalents of fluoride added.

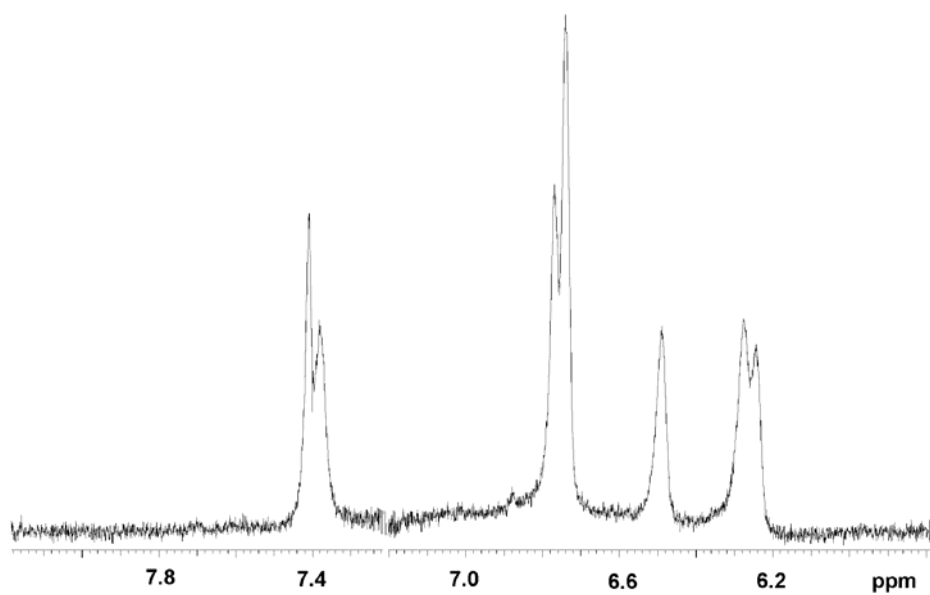


Figure 2-10. ^1H NMR spectrum of 2-2 with one equivalent or more of fluoride.

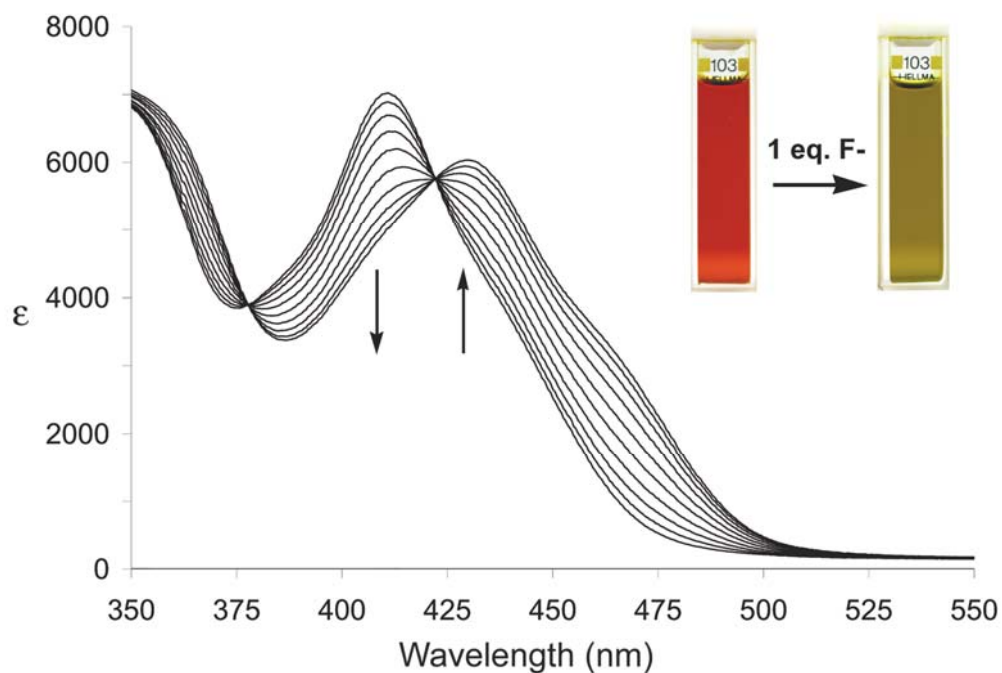


Figure 2-11. UV-Vis titration of 2-2 (4.61×10^{-5} M) with tetra-butylammonium fluoride in acetone. Titration was complete after the addition of a single equivalent of fluoride. Inset shows the change in color upon anion coordination from bright red to dark green.

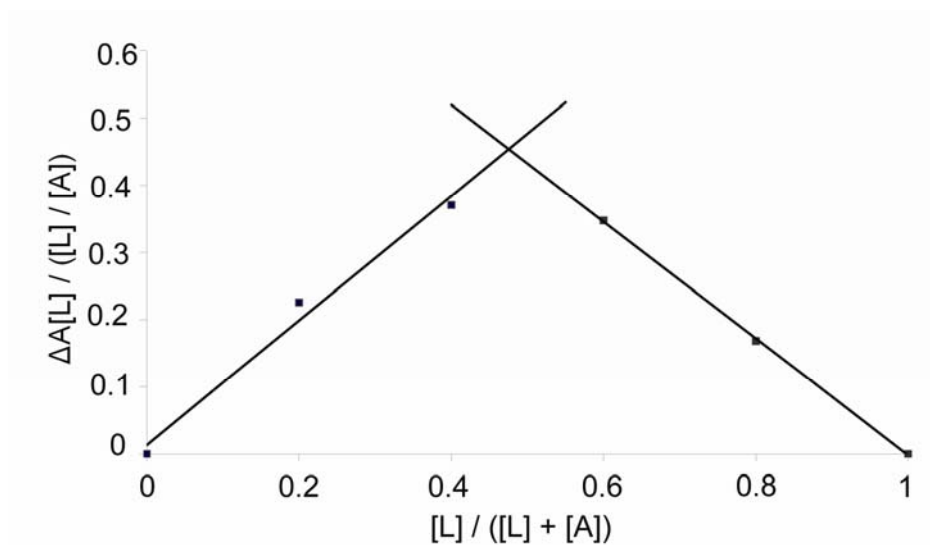


Figure 2-12. Job plot shows the titration of 2-2 with tetrabutylammonium fluoride. Apex at 0.5 indicates a 1:1 binding mode of anion to receptor. $[L]$ = concentration of receptor; $[A]$ = concentration of anion; A = absorbance.

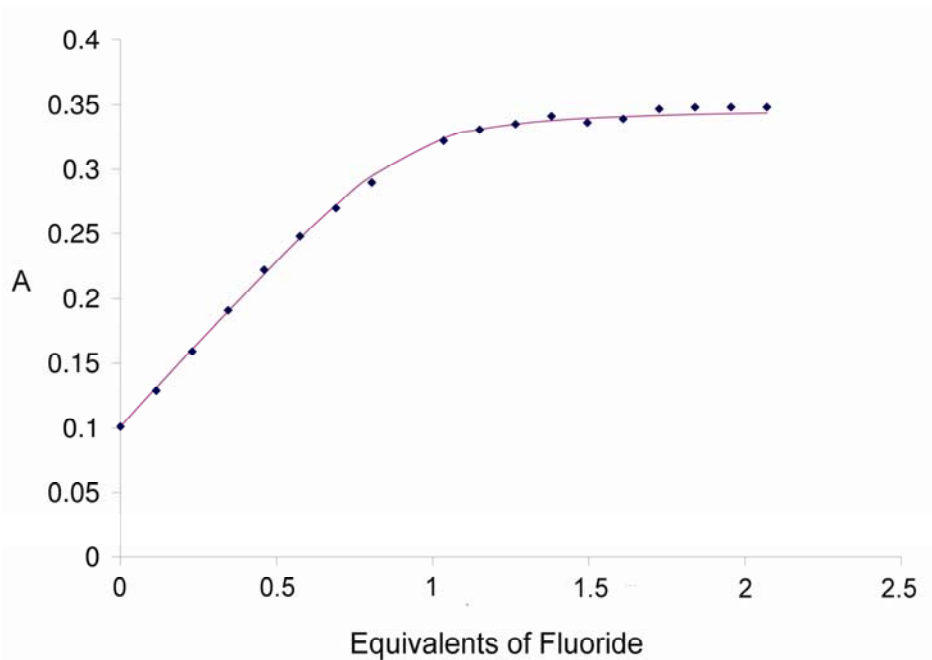


Figure 2-13. Absorbance plotted versus concentration of fluoride for the titration of 2-2 at 450nm with tetrabutylammonium fluoride. The data points represent experimental values and solid line represents the fit to the data.

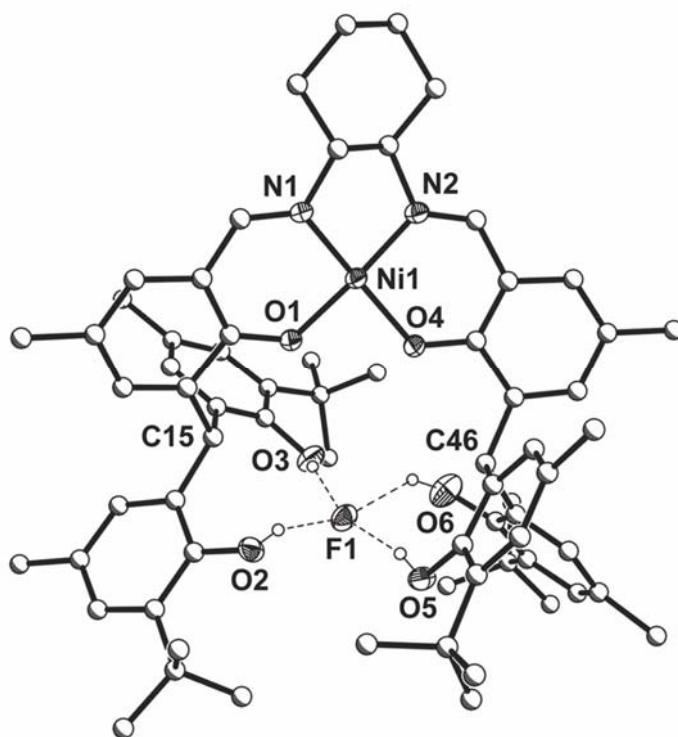


Figure 2-14 Crystal structure of $[2-2-F]^{1-}$ with fluoride bound in the phenolic pocket. The tetrabutylammonium cation, solvates, and hydrogens have been omitted for clarity. Selected distances: (a) $C(15)\cdots C(46)$ 5.28 Å; $O(1)\cdots O(3)$ 2.697(7) Å; $O(4)\cdots O(5)$ 2.784(8) Å (b) $C(15)\cdots C(46)$ 5.73 Å; $O(2)\cdots F(1)$ 2.539(2) Å; $O(3)\cdots F(1)$ 2.509(2) Å; $O(5)\cdots F(1)$ 3.098(3) Å; $O(6)\cdots F(1)$ 2.573(2) Å.

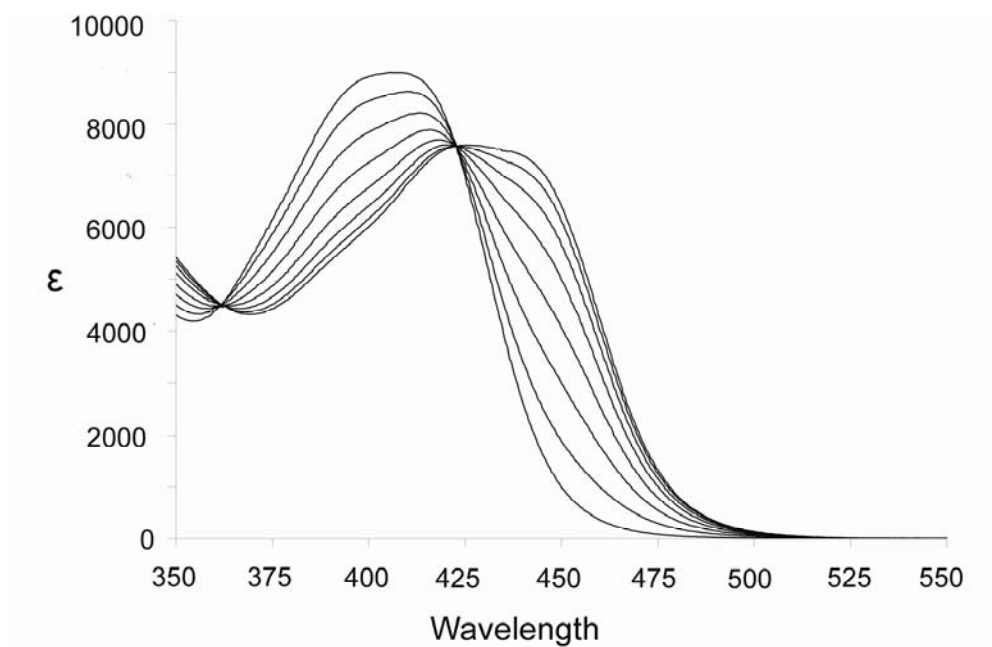


Figure 2-15. UV-Vis titration of 2-3 salen (4.61×10^{-5} M) with tetra-butylammonium fluoride in acetone. Titration was complete after the addition of a single equivalent of fluoride.

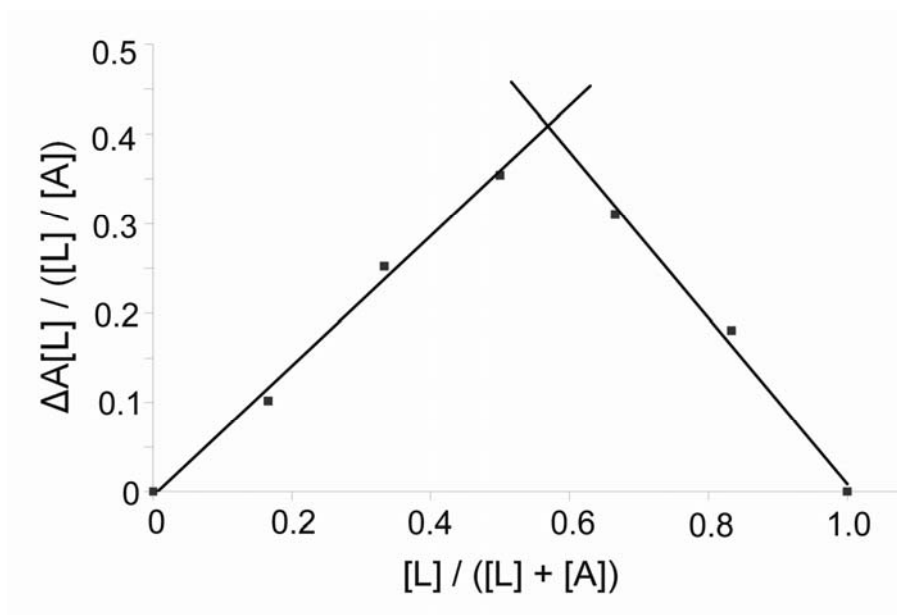


Figure 2-16. Job plot from UV-Vis spectra titration data of 2-3 in acetone with tetra-butylammonium fluoride

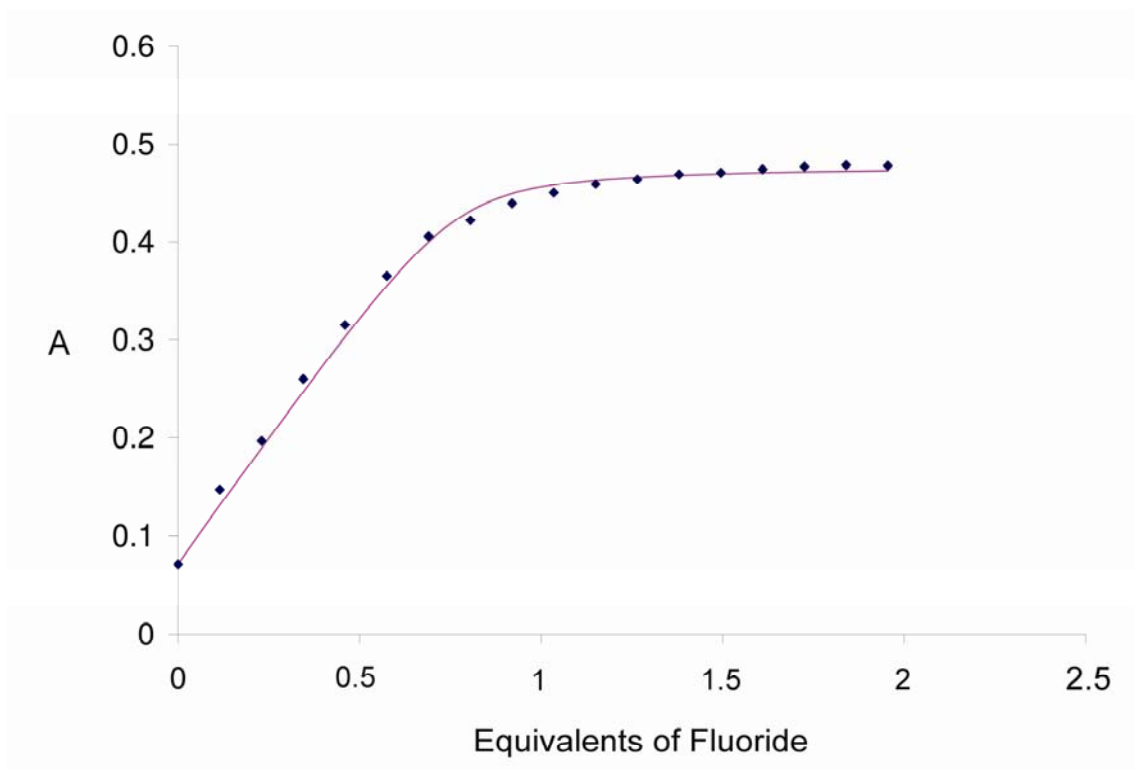


Figure 2-17. Absorbance plotted versus concentration of fluoride for the titration of 2-3 complex at 450 nm with tetrabutylammonium fluoride. The data points represent experimental values and solid line represents the calculated values.

CHAPTER 3
A SYNTHETIC MODEL OF THE CLC CHLORIDE ION CHANNEL; A STRUCTURAL
AND ANION BINDING STUDY

Introduction

In nature, the ClC chloride channel selectively transfers chloride ions across membranes, and with the recent elucidation of the structure by MacKinnon and coworkers, a clear picture of the halide binding site is now available.⁴⁷ At one point in the transfer process, chloride is held by hydrogen bonds to four amino acid residues. Amide nitrogens from Ile 356 and Phe 357 provide two hydrogen bonds while the hydroxide groups on Ser 107 and Tyr 445 provide the remaining stabilizing interactions. In this instance, nature employs a mixture of N-H and O-H donors for the transportation of halides, but surprisingly, the scientific community has primarily focused their efforts on the use of N-H groups such as amides, amines, pyrroles, and ureas to provide the hydrogen bonding interactions for artificial anion receptors.²² The utility of O-H groups in anion receptors has been quite limited with only a handful of examples reported in the literature.⁵⁰

Recently, we demonstrated that four phenols could be carefully positioned to produce a selective and efficient receptor for the fluoride anion.⁶³ In this system, the phenolic groups were tethered to a salen macrocycle, and metal complexation helps to orient the four groups into a pocket via hydrogen bonding and steric interactions. The metal macrocycle receptor offered other advantages such as the capacity to modulate the size of the halide binding pocket and the ability to monitor the binding event through spectral changes in the intense MLCT transitions.

In view of the proclivity for 2-1 to bind selectively fluoride and the mixed N-H and O-H binding site found in the ClC channel, we set out to prepare a structural model of the ClC channel with a mixture of two N-H and two O-H donors attached to the salen backbone. Herein,

we report the synthesis and study of a CIC channel model complex with a focus on its structural and anion binding properties.

Results and Discussion

For the design of artificial anion receptors, the salen macrocycle offers many advantages. The ligands are easily prepared via a simple Schiff base condensation of salicylaldehyde and a diamine, and a range of donor groups adept at binding to both cationic and anionic groups can be attached to the salicylaldehyde moiety with little synthetic effort. Incorporation of a metal center into the macrocyclic rings affords a rigid framework, and if the donor groups are properly placed in the periphery of the salicylaldehyde, a tight binding pocket can be produced at the cleft between the two sides of the macrocycle. The size of the binding site can be modulated by changing the identity and radii of the metal center within the macrocycle, and since metal salen compounds normally exhibit MLCT transitions in the visible region, the binding event can often be followed by monitoring the position of this intense absorption band.

Salens as Anion Receptors

Reinholdt and coworkers were the first to utilize metal salens for anion binding.³⁹ Their strategy focused on using acetoamido groups tethered to the salen phenoxide groups to act as hydrogen bond donors to a phosphate anion, while uranyl was incorporated into the macrocycle to provide hydrogen bonding acceptor site for the phosphate proton. Salens can also act as receptors for Ni(II) and Cu(II) sulfate when amine groups are bound at the periphery of the macrocycle.⁵²

We have recently demonstrated that four phenols tethered to a salen backbone in a pseudo tetrahedral arrangement creates an efficient and selective fluoride sensor. Initial work with 2-1 focused on the diamagnetic and square planar metals Ni(II) and Pd(II) which afforded the opportunity to monitor the receptor synthesis and the anion binding event by NMR spectroscopy.

Each molecule was structurally characterized and the difference in metal radii had an impact on the size of the binding cavity as well as an influence of the binding constants for fluoride.

Binding properties of these complexes were tested with *n*-Bu₄N⁺ halide salts in a variety of solvents. The intense MLCT absorptions ($\epsilon \sim 7400$) offered by both 2-2 and 2-3 offer a convenient way to monitor the fluoride binding event. Addition of fluoride to these receptors causes a dramatic red shift in the absorption spectrum with two distinct isobestic points indicating a single species forms in solution. The logK_s values were determined to be 5.6 for 2-2 and 5.8 for 2-3 in acetone and were 5.8 for both complexes in DMSO. Both 2-2 and 2-3 only reacted with fluoride. Steric constraints in the binding cavity precluded the binding ability of larger halides Cl⁻, Br⁻, and I⁻. Upon addition of large excesses of the larger anions no changes were detected in the ¹H NMR spectrum or the UV-Vis spectra.

Synthesis of a Mixed Salen Receptor

With the ability to incorporate O-H donors into an anion receptor system, we envisioned a synthetic mimic of the ClC chloride channel could be created, but this would also require two amide type N-H's to replicate the donors from Ser 107 and Tyr 445. The salen macrocycle can be used as a way to organize groups for anion binding, and mixed salen systems that involve two different moieties have been reported in high yields. However, to employ this method a molecule with N-H donor groups that could be incorporated into a salen system had to be developed.⁶⁴

In our group, Melanie Veige isolated a urea substituted salicylaldehyde and this group can be incorporated into a salen macrocycle (Figure 3-4). The resulting macrocycle would provide two N-H donors from the urea group.⁶⁵ Urea groups are a common motif in synthetic anion receptor systems and have shown the ability to coordinate a range of anions including the target chloride ion.⁶⁶ The two N-H groups from the urea are separated by a carbonyl creating an

environment that is similar to the backbone of the protein. Both N-H's are also aligned in the same direction which is critical to the receptor for anion coordination.

While mixed salen systems have previously been reported, they have included only simple salicylaldehydes,⁶⁴ so the incorporation of highly functionalized groups would require modified procedures to obtain the desired mixed salen products. With a combination of urea and the two phenolic groups onto a single platform, the molecule could serve as a model of the ClC channel with two O-H and two N-H donors available for anion coordination. In order to synthesize a mixed salen product, 1,2-diaminocyclohexane · HCl was prepared and the hydrochloride salt acts as a protecting group to prevent further reactions at one of the amine positions. A stepwise series of condensation reactions followed by metalation with Ni(II) (Figure 3-5) affords a product.

The choice of solvent, reaction time, temperature and purification methods are critically important to the synthesis of this system. The isolation of (3-6) is readily attainable, but the condensation of 3-6 and the urea compound 3-5 often leads to a mixture of products. The major product formed is 2-1 as the imine bond of 3-6 breaks and a rearrangement of the molecule is occurring. Rather than forming a compound with both the phenol group and urea groups, the major products of the reaction were the bis-phenol and bis-urea compounds. Initial attempts for the formation of 3-7 were performed in ethanol as most salens, including mixed salen systems,⁶⁴ are typically carried out in this solvent. However, the isolation of the desired product was never obtained in polar solvents. Compound 3-7 was synthesized by a reaction in methylene chloride at room temperature. The isolation of the pure product was never obtained, as column chromatography of salen molecules can lead to decomposition due to the high sensitivity of the imine bonds. Metal salen compounds are usually more stable than the uncoordinated ligand, and

upon the metalation of 3-7 with Ni (II) a more rigid compound (**3-8**) was easily purified with an overall yield of 20%.

Anion Coordination and Binding Constants

The anion binding properties of this system were tested by the addition of tetra-*butyl*-ammonium halide salts to solutions of the receptor. Compound 3-8 was able to bind fluoride and chloride while having no interaction with the larger bromide anion. A distinct red shift in the strong MLCT absorptions is detected upon anion complexation for both fluoride and chloride with the main absorption peaks of the spectrum shifting from 411 nm to 428 nm for fluoride and from 411 nm to 421 nm for chloride. The addition of a large excess of bromide to the solution causes no changes to either the UV-Vis or NMR spectra.

The binding constants (K_s) were determined from the data obtained by UV-Vis spectroscopy anion titrations. The measured absorbance were plotted as a function of fluoride ion concentration of the solution at 450nm and a non-linear least squares regression was used to determine binding constants with the equation:⁵⁹ $X = X_0 + [(X_{lim} - X_0) / 2c_0] \cdot [c_0 + c_m + 1/K_s - [(c_0 + c_m + 1/K_s)^2 - 4c_0c_m]^{1/2}]$. In this equation, X is the measured absorbance, X_0 is the initial absorbance, X_{lim} is the limiting absorbance, c_0 is concentration of anion in solution, c_m is the concentration of the receptor, and K_s is the binding constant. A program to perform a non-linear least squares regression on the data⁶⁰ which minimizes the error of each data point to fit the standard equation by altering K_s was written in excel. The value of K_s that leads to the lowest sum of errors is the binding constant for the system. Binding constants for 3-8 were determined to be $\text{Log } K_s = 8.3$ for fluoride and $\text{Log } K_s = 1.74$ for chloride. The coordination of fluoride occurs readily as seen by its extremely high binding constant. Although chloride does coordinate to the receptor, it is less favorable. The larger size of chloride as well as its lower charge density

led to the smaller interactions. Compound 3-8 fully coordinates fluoride upon addition of ~ 1 equivalent of anion while it takes ~ 30 equivalents of chloride to fully titrate the receptor.

Solid State Structure

Upon addition of excess chloride ion, 3-8 binds the anion and single crystals of the complex with chloride coordinated were obtained. In the solid state (Figure 3-7), chloride is held in the cavity by four rather strong hydrogen bonds (chloride oxygen distances of 3.158(3) Å and 3.108(4); chloride nitrogen distances of 3.512(4) Å and 3.183(4)). There is a slight distortion of the urea group and the phenols in order for the receptor to accommodate the chloride ion. These small structural changes to the receptor, which are caused by anion coordination, have also been observed for 2-1 upon binding fluoride.

Conclusions

A synthetic model of a CIC chloride channel has been designed and developed. The incorporation of phenolic and urea subunits onto a salen macrocycle platform has created a highly functionalized mixed salen system which is able to coordinate chloride in a similar manner as seen in receptors found in nature. A solid-state structure of 3-8 with a chloride anion bound has been obtained and it shows the binding mode with chloride interacting with all four hydrogen bond donors in the system. The structure is the first example of a synthetic chloride receptor that involves the same hydrogen bonding interactions as the CIC chloride ion channel. The positioning of the donor group to form a cavity of a specific size are important to the anion binding event as the receptor can easily accommodate fluoride and chloride while there are no interactions with larger anions such as bromide.

Binding constants for the receptor system have been obtained and follow the expected selectivity trend with a greater preference for the smaller anions. The metalated salen macrocycle serves multiple purposes, as a rigidifying structural component and also it enables

the binding constants to be monitored by UV-Vis spectroscopy due to strong MLCT transitions. The receptor has a high binding constant for fluoride of $\log K_s = 8.3$ and a much lower $\log K_s = 1.74$ for chloride. There is no evidence that the larger bromide anion interacts with the receptor.

Experimental Methods

General Considerations.

^1H and ^{13}C NMR spectra were recorded on a Varian Mercury 300 MHz spectrometer at 299.95 and 75.47 MHz for the proton and carbon channels. UV-Vis spectra were recorded on a Varian Cary 50 spectrometer. Elemental analyses were performed at either the in-house facility of the Department of Chemistry and the University of Florida. All solvents were ACS or HPLC grade and used as purchased except for metalation reactions where the solvents were dried with a Meyer distillation system prior to use. Melanie Veige was responsible for the synthesis of compounds 3-1 through 3-5.

Determination of binding constants ($\text{Log}K_s$)

A solution of receptor in acetone was titrated with aliquots of a tetra-butylammonium halide solution. Absorbance was plotted versus fluoride concentration at 450 nm and a non-linear least squares regression was then run on the data using the following equation:⁵⁹ $X = X_0 + [(X_{\text{lim}} - X_0) / 2c_0] \cdot [c_0 + c_m + 1/K_s - [(c_0 + c_m + 1/K_s)^2 - 4c_0c_m]^{1/2}]$. Solving this equation for K_s gives the binding constant. Job plots were obtained by measuring the absorbance of a series of solutions with different proportions of receptor and anion and indicate a 1:1 ratio.

Synthesis of 3-1

A solution of 5-tert-butyl-2-hydroxybenzaldehyde (60.0 g, 337 mmol) in glacial acetic acid (240 mL) was cooled in an ice bath. Fuming nitric acid (15.3 mL, 1 equiv., 337 mmol) was slowly added via addition funnel. After 15 min of stirring, the ice bath was removed and the solution was stirred at ambient temperature for 90 min. The ice bath was reapplied intermittently

to prevent the internal reaction temperature from exceeding ca. 45 °C. The reaction mixture was poured onto crushed ice (800 mL). The yellow precipitate thus formed was filtered and washed with water, then recrystallized from abs. EtOH/H₂O to give 3-1 as a yellow crystalline solid (68.7 g, 91%). The compound was used without further purification. An analytically pure sample was obtained by further purification by column chromatography (pentane-ether 3:1). ¹H NMR (DMSO-*d*₆): δ 11.34 (bs s, OH), 10.28 (s, CHO), 8.20 (d, *J*=2.4 Hz, Ar-H), 8.07 (d, *J*=2.4 Hz, Ar-H), 1.30 (s, 9H). ¹³C NMR (DMSO-*d*₆): δ 191.5, 151.8, 142.3, 137.6, 132.6, 127.7, 124.9, 34.2, 30.6. HRMS (EI): Theoretical 223.0845; Measured 223.0837. Anal. Calc. for C₁₁H₁₃NO₄; C, 59.46; H, 5.97; N, 6.22. Found C, 59.19; H, 5.87; N, 6.27.

Synthesis of 3-2

To a solution of 3-1 (53.3 g, 239 mmol) in CHCl₃ (350 mL) was added 1,3-propanedithiol (24 mL, 1 equiv.). The mixture was stirred at ambient temperature for 60 min. then was cooled in an ice bath. To the cold mixture was added BF₃OEt₂ (3 mL, 0.1 equiv., 23.9 mmol). The mixture was stirred 16 h with gradual warming to ambient temperature. The reaction mixture was transferred to a separatory funnel, diluted with CHCl₃ (250 mL), and washed successively with H₂O (3x100 mL) and brine (150 mL). The volatiles were removed *in vacuo* and EtOH (250 mL) was added to the residue. The slurry was stirred at ambient temperature for 1 h, then cooled in an ice bath for 30 min. The mixture was filtered and the collected solids were washed with cold EtOH. 3-2 was obtained as a bright yellow crystalline solid (65 g, 87 %). An analytically pure sample was obtained via further purification by column chromatography (pentane-ether 4:1). ¹H NMR (DMSO-*d*₆): δ 10.64 (br s, OH), 7.86 (d, *J*=2.4 Hz, Ar-H), 7.79 (d, *J*=2.4 Hz, Ar-H), 5.73 (s, dithiane-H), 3.19-3.11 (m, 2H), 2.94-2.29 (m, 2H), 2.21-2.15 (m, 1H), 1.82-1.69 (m, 1H), 1.27 (s, 9H). ¹³C NMR (DMSO-*d*₆): δ 146.8, 142.3, 135.7, 132.3, 130.0, 120.9, 42.3, 34.0,

31.2, 30.7, 24.6. HRMS (EI): Theoretical 313.0806, measured 313.0820. Anal. Calc. for $C_{14}H_{19}NO_3S_2$: C, 53.99; H, 6.24; N, 4.42. Found C, 53.65; H, 6.11; N, 4.47.

Synthesis 3-3

To a mixture of 3-2 (46.7 g, 149 mmol) in EtOH (475 mL) and AcOH (475 mL) was added Fe powder (33.3 g, 4 equiv., 597 mmol). The mixture was heated to reflux under a nitrogen atmosphere. The mixture gradually became a very dark solution, and after approximately 1 h copious solids precipitated. After 1 h at reflux TLC indicated completion of the reaction. The mixture was concentrated *in vacuo* and EtOAc (300 mL) and H₂O (300 mL) were added. Saturated K₂CO₃ was added to neutralize the aqueous layer. The aqueous layer was extracted with additional EtOAc (3x65 mL). The combined organic fractions were washed with brine, dried over MgSO₄ and filtered. The solution was transferred into a round-bottomed flask equipped with a stir bar. HCl in dioxane (4N, 75 mL, 300 mmol, 2 equiv.) was added slowly via addition funnel. The mixture was stirred at ambient temperature for 3 h, then transferred to a -20 °C freezer for 16 h. The mixture was filtered cold, and the collected solids washed with cold EtOAc to provide the HCl salt of 3-3 as a beige powder. The mother liquors were concentrated to approximately 200 mL and cooled to obtain a second crop of product. A total of 43.1 g (90%) of the HCl salt of 3-3 was obtained. Salt 3-3 (22.6 g, 70.8 mmol) was charged into a round-bottomed flask with CH₂Cl₂ (150 mL) and H₂O (150 mL) containing K₂CO₃ (20.0 g, 2 equiv., 142 mmol). The mixture was stirred at ambient temperature for 2 h. The organic phase was removed and the aqueous layer was extracted with additional CH₂Cl₂ (2x30 mL). The combined organics were washed with brine, dried over MgSO₄, filtered and concentrated to a small volume. Pentane was added slowly to precipitate the free amine 5 (17.3 g, 86% from the salt) as a beige solid. ¹H NMR (CDCl₃): δ 6.74 (d, *J*=2.4 Hz, Ar-H), 6.63 (d, *J*=2.4 Hz, Ar-H), 6.45 (br s, ArOH), 5.30 (s, dithiane-H), 3.74 (br s, ArNH₂), 3.11-3.01 (m, 2H), 2.95-2.88 (m, 2H), 2.24-

2.14 (m, 1H), 2.01-1.86 (m, 1H), 1.25 (s, 9H). ^{13}C NMR (CDCl_3): δ 143.9, 140.9, 135.7, 122.4, 115.6, 114.3, 48.2, 34.3, 31.7, 31.6, 25.1. HRMS (EI): Theoretical 283.1065, Measured 283.1083. Anal. Calc. for $\text{C}_{14}\text{H}_{21}\text{NOS}_2$: C, 59.55; H, 7.70; N, 4.97. Found C, 59.32; H, 7.47; N, 4.94.

Synthesis of 3-4

To a solution of amine 3-3 (12.64 g, 44.7 mmol) in CHCl_3 (125 mL) was added phenylisocyanate (4.85 mL, 1 equiv., 44.7 mmol). The solution was heated at reflux for 20 h, then cooled to ambient temperature. The solution was concentrated to approximately 1/3 the volume, and hexane was slowly added with stirring. The off-white precipitate 3-4 (17.0 g, 95%) was filtered and washed with hexane. ^1H NMR ($\text{DMSO}-d_6$): δ 9.26 and 9.24 (overlapping s, 2H), 8.34 (s, 1H), 7.80 (d, $J=2.4$ Hz, 1H), 7.45 (d, $J=8.7$ Hz, 2H), 7.28 (t, $J=7.8$ Hz, 2H), 7.09 (d, $J=2.4$ Hz, 1H), 6.99-6.95 (m, 1H), 5.70 (s, 1H), 3.12-3.04 (m, 2H), 2.90-2.86 (m, 2H), 2.15-2.10 (m, 1H), 1.80-1.69 (m, 1H), 1.23 (s, 9H). ^{13}C NMR ($\text{DMSO}-d_6$): 153.3, 142.4, 140.2, 139.6, 128.8, 128.4, 126.4, 121.9, 118.7, 118.2, 117.1, 44.1, 33.9, 31.5, 31.3, 24.8. Anal. Calc. for $\text{C}_{21}\text{H}_{26}\text{N}_2\text{O}_2\text{S}_2$: C, 62.25; H, 6.91; N, 6.66. Found C, 62.65; H, 6.51; N, 6.96.

Synthesis of 3-5

To a mixture of 3-4 (9.0 g, 22.4 mmol) in AcOH (400 mL) was added SeO_2 (12.4 g, 5 equiv., 112 mmol). The resulting mixture was stirred at ambient temperature for 90 min during which time 3-4 was fully dissolved and a byproduct precipitated. The mixture was filtered through a pad of Celite[®]. The filter cake was washed with AcOH, and the filtrate was concentrated *in vacuo* to a solid. To the solid was added EtOAc and H_2O , and the aqueous layer was basified with saturated K_2CO_3 . The biphasic mixture was filtered again through Celite[®] and the filtrate was transferred to a separatory funnel. The aqueous layer was extracted with EtOAc. The combined organics were washed with brine, dried (MgSO_4), filtered and concentrated to a

slurry. Hexane was added and the yellow-orange precipitate (6.5 g, 93%) was filtered and washed with hexanes. The solid could be recrystallized from MeOH/H₂O. An analytically pure sample was obtained by column chromatography (pentane-ether 4:1) however the urea was used without further purification. ¹H NMR (acetone-*d*₆): δ 11.34 (br s, OH), 9.98 (d, J=0.9 Hz, CHO), 8.77-8.74 (m, 2H), 7.93 (br s, 1H), 7.57-7.54 (m, 2H), 7.43-7.42 (m, 1H), 7.31-7.25 (m, 2H), 7.02-6.96 (m, 1H), 1.34 (s, 9H). ¹³C NMR (acetone-*d*₆): δ 198.6, 153.3, 148.5, 143.5, 140.6, 129.5, 129.1, 124.1, 123.0, 120.3, 119.3, 34.9, 31.5. HRMS (ESI-FT-ICR-MS) for [2M+Na]⁺ Theoretical 647.2840, Measured 647.2852; theoretical for [M+Na]⁺ 335.1366, measured 335.1372. Anal. calc. for C₁₈H₂₀N₂O₃: C, 68.84; H, 6.68; N, 8.71. Found C, 69.21; H, 6.45; N, 8.97.

Synthesis of 3-6

A portion of 1.0 g (6.66 mmol) 1,2-diaminocyclohexane · HCl was dissolved in 50 mL methanol. After dissolving 50 mL ethanol was added along with 3.0 g (6.33 mmol) of 3-(2,2'-Methylenebis (4-methyl-6-*tert*-butylphenol)-5-methyl-2-hydroxybenzaldehyde. The reaction mixture was stirred at room temperature overnight. The solvent was removed *in vacuo* and the solid was washed with water, filtered and dried. The solid was dissolved in dry ether and a pale yellow solid precipitated which was filtered and dried to afford the product in an 82% yield (3.1 g). ¹H NMR. δ 8.48 (s, 1H); 7.03 (s, 2H); 6.99 (s, 1H); 6.83 (s, 1H); 6.61 (s, 2H); 6.50 (s, 1H); 6.01 (s, 1H); 5.42 (bs, 2H); 5.09 (bs, 1H); 3.28 (m, 1H); 2.75 (m, 1H); 2.19 (s, 9H); 1.71(m, 4H); 1.38 (s, 9H); 1.35 (s, 9H). ¹³C NMR δ 167.6; 157.41; 151.12; 150.64; 137.42; 137.20; 133.78; 130.62; 128.61; 127.48; 126.95; 126.53; 118.45; 70.01; 55.76; 38.16; 34.86; 34.64; 33.00; 29.93; 28.47; 23.78; 23.27; 21.19; 20.83. HRMS: Theoretical 571.3894; Measured 571.3894 [M - Cl].

Synthesis of 3-7

A portion of 0.826 g (1.36 mmol) 3-6 was dissolved in 75 mL methylene chloride. To this solution was added 0.38 mL (2.72 mmol) of triethylamine and 0.425 g (1.36 mmol) of 3-5. The reaction mixture was stirred overnight at room temperature. The solution was poured into a separatory funnel and washed with a 1 M HCl solution and then with water. The solution was dried with sodium sulfate and the solvent was removed. No attempt at further purification was made and the resulting crude product was used as the starting material in the synthesis of 3-8. Purification was performed after metalation of the complex.

Synthesis of 3-8

A portion of 0.80 g 3-7 was dissolved in 100 mL of dry THF. To this solution was added 0.23 g nickel acetate and the reaction was stirred at room temperature for 2 hours. The solvent was removed under vacuum and the product was dissolved in pentane and filtered. The solvent was removed from the filtrate leaving a yellow / orange solid. The solid was then washed with an excess of methanol yielding 0.200g of pure product (24% for two steps). ^1H NMR: δ 8.62 (s, 1H); 8.33 (d, 1H); 7.03 (m, 12H); 6.90 (d, $J = 6.6$ Hz, 1H); 6.87 (s, 2H); 6.60 (s, 2H); 6.29 (s, 1H); 3.70 (bs, 1H); 3.29 (bs, 1H); 2.27 (s, 3H); 2.26 (s, 3H); 2.18 (s, 3H); 1.36 (s, 9H); 1.33 (s, 9H); 1.28 (s, 9H). ^{13}C NMR δ 158.13; 157.94; 157.26; 152.58; 151.30; 150.67; 150.57; 138.86; 138.76; 138.55; 138.25; 135.38; 131.91; 130.87; 130.75; 130.40; 130.33; 129.71; 129.11; 128.63; 127.22; 126.91; 126.52; 124.90; 122.25; 120.42; 119.94; 119.74; 119.08; 117.48; 70.79; 36.88; 34.82; 34.60; 34.19; 31.42; 30.02; 29.92; 29.45; 28.33; 28.14; 23.99; 21.29; 21.20. HRMS: Theoretical 921.4459; Measured 921.4487 [M + H⁺]. Anal. Calc. for C₅₅H₆₆N₄O₅Ni: C, 71.66; H, 7.22; N, 6.08. Found C, 71.44; H, 7.58; N, 5.79.

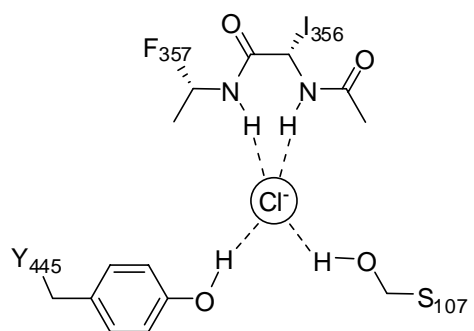


Figure 3-1. Schematic diagram of the open conformation of ClC chloride channel. Chloride is held in place by two OH-Cl hydrogen bonds from Y₄₄₅ and S₁₀₇.

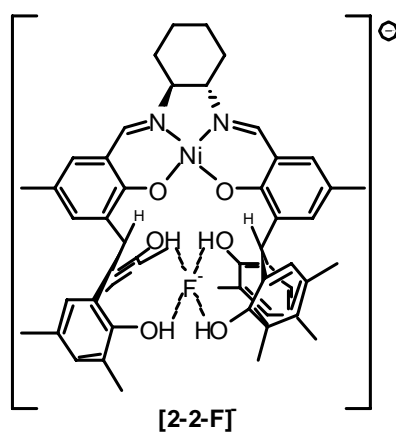


Figure 3-2. Schematic diagram of [2-2-F]⁻; a fluoride is hydrogen bonding with the four phenols of the anion receptor.

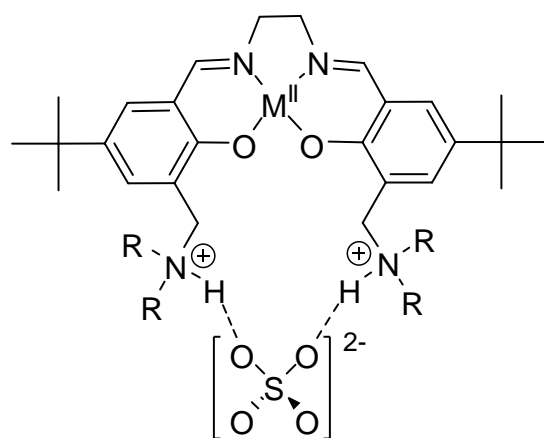


Figure 3-3. Structure of salen based anion receptor with amine groups at the periphery. The receptor coordinates both cations and anions

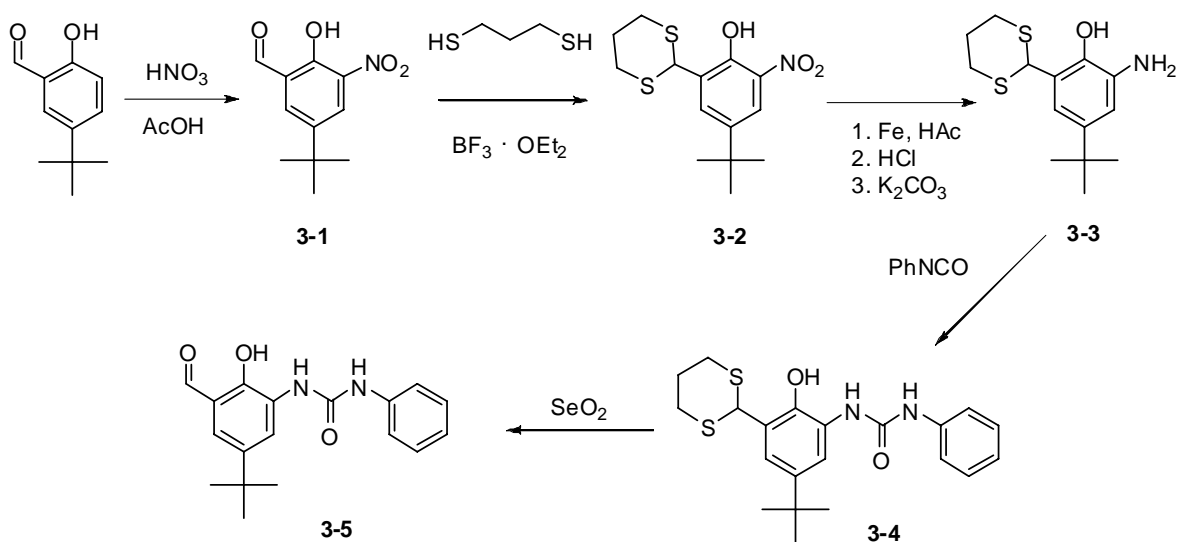


Figure 3-4. Synthetic scheme for compound 3-5.

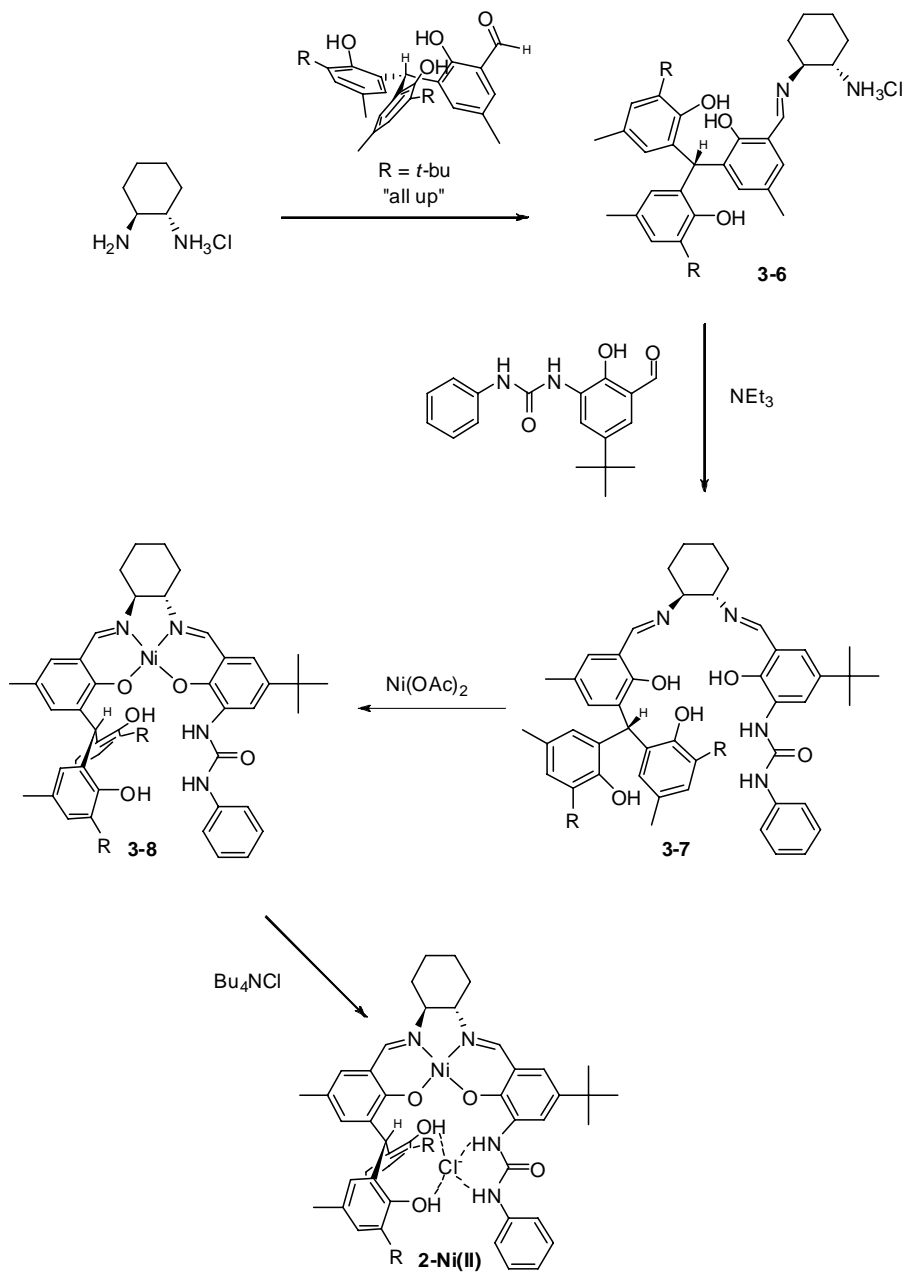


Figure 3-5. Synthetic scheme for the synthesis of mixed phenolic-urea salen system (3-7), metalation at salen binding site and anion coordination (3-8).

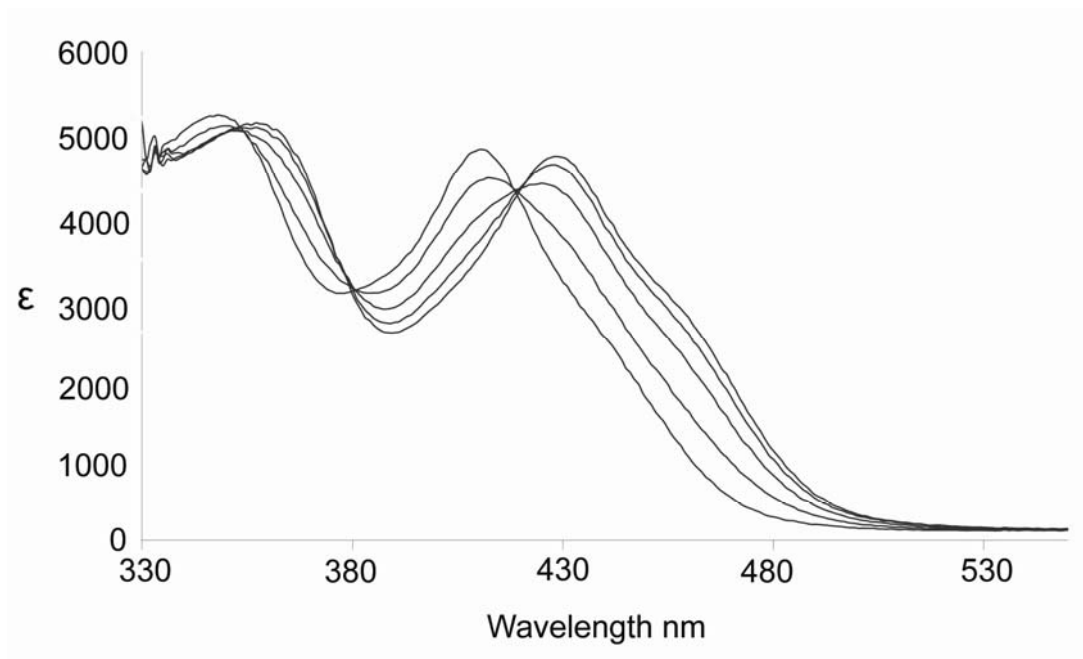


Figure 3-6. Titration plot of 3-7 with fluoride in acetone. There is a dramatic red shift in the absorption spectrum and also two well defined isobestic points.

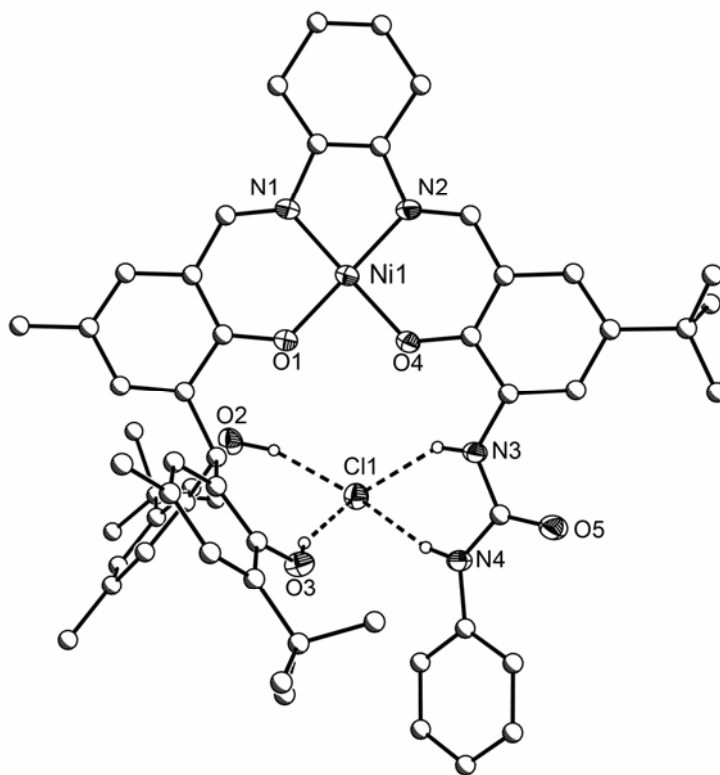


Figure 3-7. Depiction of the solid-state structure (30% probability ellipsoids, carbons drawn with arbitrary radii) of [3-8-Cl]⁻ with chloride hydrogen bound to two phenols and two N-H's from the urea. The tetrabutylammonium cation and carbon hydrogens have been omitted for clarity. Selected distances: O(2)•••Cl(1) 3.158 Å; O(3)•••Cl(1) 3.108 Å; N(3)•••Cl(1) 3.512 Å, N(4)•••Cl(1) 3.183

CHAPTER 4 METAL SALEN UREA COMPLEXES AND THEIR HIGH AFFINITIES FOR THE HALIDES

Introduction

The use of N-H groups as hydrogen bond donors is commonly employed in synthetic anion receptors¹¹ as virtually all reported receptors focus on ligands incorporating groups such as amides, amines, pyrroles, and ureas.²² The urea group is among the most popular binding motifs in synthetic anion receptors since it offers two hydrogen bond donor groups aligned in the same direction, which are also the appropriate distance from one other to have strong interactions with a variety of anions including fluoride, acetate, and phosphate among others.⁶⁷ The synthetic ease in which ureas can be prepared also accounts for much of their diversity in a multitude of receptor systems (figure 4-1)⁴⁸.

Anion Receptor Systems Incorporating Ureas. Urea groups have been incorporated into multiple macrocyclic systems where molecular flexibility and cycle size impacts the anion binding affinity.⁶⁹ Ureas have also been attached to various platforms in order to preorganize multiple urea groups.⁷⁰ Preorganization of multiple ureas can lead to stronger hydrogen bonding than a single moiety as well as a potential increase in selectivity. Since ureas have two donors aligned in the same direction, arranging multiple groups in a manner to create a cavity affords the opportunity to have a high number of possible hydrogen bonding sites. Ureas have also been seen to adopt different geometries depending on the anion that it binds, making them versatile.⁷¹

For the development of anion receptors, it would seem that thiourea groups would be a better candidate because it is more acidic (pKa of 21.1) than urea (pKa of 26.9).⁷² Thioureas also have the advantage that they do not self associate as is often seen with ureas.⁷³ Self association occurs when the N-H groups are hydrogen bonding to the carbonyl of another urea thus it is unavailable for anion coordination. Thioureas tend however, to deprotonate in the

presence of most anions preventing their use as an effective receptor.⁷⁴ In contrast ureas require a large excess of fluoride and using designed synthesis can prevent self associating from occurring.⁷⁵

Metals have been used as a way to assemble urea groups for hydrogen bonding.⁷⁶ The binding site can be regulated by the size and geometrical preferences of the metal as well as the nature of the hydrogen bond donor substituent. The coordination of two ligands seen in figure 4-2, coordinate around a Cu^{2+} ion which then sets the position of the urea groups. The four N-H's form a binding site that is the appropriate size for the coordination of chloride. Binding constants were determined by UV-Vis spectroscopy as the system offers strong absorption measurements due to the conjugation of the ligand as well as the presence of a metal.

The salen complexes discussed in chapters two and three have shown to be effective ways to induce anion coordination and the addition of metals into the systems modulates the size of the binding cavity as well as offers a convenient way to monitor the binding event. Ureas are among the best hydrogen bond donor groups and we envisioned creating a purely urea based cavity attached to a metal salen backbone. Compound 3-8 has shown that ureas in combination with phenols are selective for fluoride and chloride. The synthesis of a bis-urea receptor, its interactions with various anions as well as the effects of metal coordination and regulation of the size of the binding site are herein reported.

Results and Discussion

A simple Schiff base reaction with 1,2-diamino-cyclohexane and two equivalents of 3-5 affords compound 4-1. The two urea groups attached to the salen backbone have four N-H donors (Figure 4-3), which are arranged into an anion binding cavity upon metalation with the diamagnetic and square planar metals Ni (II) (4-2) and Pd (II) (4-3). Nickel and palladium behave similarly yet differ in radius by about 0.15 Å, affording the opportunity to regulate the

size of the binding cavity. The choice of metals allows the synthesis and the anion binding properties of the receptor to be monitored by NMR spectroscopy. Metalation of 4-1 occurs at the two salen imine nitrogens and the salen phenols but has no interaction with the urea N-H's.

Solid State Structures of Receptors. Both compound 4-2 and 4-3 were structurally characterized and studied. For the nickel complex 4-2, two symmetry independent molecules crystallized in the asymmetric unit and the structure is presented in figure 4-4. The average distance of the four Ni-oxygen bonds in the two complexes (1.835 Å) are typical for a Ni(II) salen complex¹⁴ but significantly shorter than the corresponding average Pd-oxygen distances (2.021 Å). The subtle size difference between the two metals produces a profound increase in the separation between the two urea groups which has many consequences for the structure and anion binding ability of the two receptors.

The relatively small size of square planar Ni(II) forces a significant distortion within the two arms. The phenyl rings on the urea, which would be expected to be coplanar due to the conjugated nature of the system, have an angle of 85° between them, which is likely caused by a steric clash between the phenyls. There is also a strong intramolecular hydrogen bond between an N-H (N3) on one urea and the carbonyl (O4) of the second urea of the system with a short N-H-O distance of 2.190 Å. The salen urea ligand system (4-1) is highly conjugated and thus highly planar. In order to break the planarity and conjugation of the system, there is a high energy cost to pay that will only occur under certain circumstances such as in compound 4-2 causing one of the urea arms to bend.

In contrast to compound 4-2, the Pd (II) compound 4-3 crystallizes with only one molecule in the asymmetric unit and the distortions of the urea arms are no longer observed (Figure 4-5). Since Pd (II) forms longer metal – oxygen bonds than Ni (II) with a concomitant increase in

separation between the two extended arms. The ureas are oriented at a distance where the phenyl rings are coplanar and the formation of an intramolecular hydrogen bond is less likely.

Compound 4-3 crystallized with a water molecule in the pocket which is hydrogen bound to all four urea nitrogens at distances of 3.062 Å, 3.155 Å, 3.063 Å, 3.248 Å. The small size of water allows it to lie within the plane of the urea molecule without causing distortions to the receptor

Anion binding properties of the two metal complexes were tested with $n\text{-Bu}_4\text{N}^+$ halide salts in a variety of solvents including acetone and DMSO, and both 4-2 and 4-3 show a high affinity for anions. As with compounds 2-2, 2-3 and 3-8 the binding constants of 4-2 and 4-3 for anions can be monitored by UV-Vis spectroscopy. The absorbance spectrum of 4-2 shows two strong MLCT transitions at 357 nm and 418 nm and the addition of fluoride to this solution induces a red shift in the spectrum with the main absorbance peaks shifting to 361 nm and 427 nm respectively (Figure 4-5). There is also three well defined isobestic point in the titration plot indicating a two state process.

There is a considerably smaller shift in the absorption spectra of 4-2 upon anion coordination than was seen with compounds such as 2-2 which contained phenolic substituents. The strongest absorbance of metal salen compounds is assigned to the MLCT transition.⁵⁴ The metal environments of compounds 2-2 and 2-3 are drastically altered by anion coordination. The most important being the change in geometry of the four phenols which much distort to accommodate the fluoride ion causing a distortion to the entire receptor including the salen backbone. In both 2-2 and 2-3, there were intramolecular hydrogen bonds between the phenols and the phenolates of the salen bound directly to the metal. The addition of fluoride to the receptor disrupts the intramolecular hydrogen bonds of the phenols in order to coordinate to the anion. The electronic environment of the metal is altered and this contributes to the shift in the

absorption spectrum. The colorimetric changes are less pronounced in 4-2 and 4-3 upon anion coordination; however, the binding event could be still be monitored, allowing the binding constant to be determined (Figure 4-6).

The data obtained from the titration of 4-2 with tetrabutylammonium fluoride affords the binding constant $\text{Log } K_s = 6.10$, which is high and indicative of the strong interactions between fluoride and the ureas. To determine this binding constant, the data from the titration was plotted as a function of the equation: $X = X_0 + [(X_{\text{lim}} - X_0) / 2c_0] \cdot [c_0 + c_m + 1/K_s - [(c_0 + c_M + 1/K_s)^2 - 4c_0c_M]^{1/2}]$ and a non-linear least squares regression was performed to find the K_s value that best fits the data (Figure 4-7).

While 4-2 has shown to have strong interactions with fluoride, the anion binding properties of the receptor were tested with other larger anions, such as chloride and bromide. Both chloride and bromide coordinate to this system with high binding constants and there is also a trend in relative binding constants which is consistent with observations of the structures in the solid state. The urea receptors have limited flexibility and the site of the binding cavity is determined by the particular metals that are coordinated to the salen. The preference for a particular anion is determined by geometry, size and the compatibility of the anion and receptor.

Compound 4-2 is able to coordinate chloride and this complex (4-4) has been structurally characterized giving insight into the binding mode as well as the effect this has on the binding constants (Figure 4-8). Size limitations of the binding cavity force the chloride to reside above the plane of the molecule. The structure shows that all four urea nitrogens are hydrogen bonding to the chloride at distances of $\text{N}(3)\cdots\text{Cl}(1)$ 3.490 Å; $\text{N}(4)\cdots\text{Cl}(1)$ 3.255 Å; $\text{N}(5)\cdots\text{Cl}(1)$ 3.601 Å; $\text{N}(6)\cdots\text{Cl}(1)$ 3.130 Å.

The N-H groups are all slightly distorted and pointing towards the anion since chloride is too large to be positioned any closer to the receptor. Each urea arm is splayed out as far as possible in order to limit the amount of distortions that break the planarity and conjugation of the molecule. The hydrogen bond distances from N(3) and N(5) are longer than the other two nitrogens because they are directly connected to the rigid salen backbone and have limited flexibility. The hydrogen bond distances from N(4) and N(6) to the chloride are significantly shorter as the molecule is more flexible at this position and these two N-H's are able to twist and point directly at the chloride.

The solid state structure shows the chloride ion sitting above the plane of the molecule and directly adjacent to the anion is a highly disordered tetrabutylammonium cation. Packing plots show that there is only one receptor bound to each anion in the solid state and Job plots indicate a 1 : 1 complex in solution (Figure 4-9). Job plots are prepared by measuring differences in absorption or chemical shifts of a series of solutions at various concentrations of anion and receptor, and these changes are monitored by NMR and UV-Vis spectroscopy. Due to the large changes in absorption spectra, UV-Vis spectroscopy was used for the creation of Job plots for 2-2 and 2-3. For the urea based receptors however, the shifts in the N-H peaks were distinct and the changes were monitored at different concentrations leading to a Job plot indicating there is a one to one, receptor to anion binding mode.

The solid state structure of compound 4-2 with a bound bromide ion has been obtained (Compound 4-5) and there are several structural differences to the receptor upon coordination of bromide versus chloride. The larger size of bromide causes it to be positioned high above the plane of the molecule and the hydrogen bond distances between the ureas and the bromide are longer than those of 4-4 with distances of N(3)•••Br(1) 3.616 Å; N(4)•••Br(1) 3.208 Å;

N(5)•••Br(1) 3.576 Å; N(6)•••Br(1) 3.358 Å. The long receptor-bromide distances force significant distortions in the planarity of the molecule. The distortion is not only seen in the urea groups which must bend upwards to coordinate the bromide, but is also translated to the salen backbone which has an 11.8° angle between the two nitrogen, oxygen, nickel planes [N(1), O(1), Ni(1) and N(2), O(3), Ni(1)]. The structure also shows a disorder in the urea containing N(5), N(6) and O(4), with the receptor taking two slightly different angles as a means of coordinating bromide. The receptor is trying to minimize the distortion caused as it is unfavorable to break the receptors planarity and conjugation, but in order to coordinate bromide some distortions must occur.

The addition of chloride or bromide to a solution of 4-2 leads to similar titration plots as seen with fluoride with a red shift in the absorption spectra and three distinct isobestic points (Figure 4-10). From the titration data, the binding constants were determined (Figure 4-11) and there was a correlation between these constants and the hydrogen bond lengths. While 4-2 is a strong receptor for both chloride ($\log K_s = 5.27$) and bromide ($\log K_s = 4.29$), there is an order of magnitude difference in the binding constants. Chloride is able to form a more stable complex with the 4-2 than with bromide because of its smaller size and ability to be positioned close to the receptor.

While it is seen that the relative size of the anion plays an important role in the coordination process, the spatial constraints of the receptor can be modified to make adjustments to the anion coordination process. Compound 4-3 possesses a urea cleft that is larger than the one in compound 4-2 which is caused by the incorporation of Pd (II). The binding mode of chloride and bromide as seen in the solid states in compounds 4-4 and 4-5 indicate the anions is positioned considerably above the plane of the molecule. Since 4-3 situates the two urea groups

further apart, it enables the anions to be positioned closer to the receptor and would possibly have an effect on the binding constants.

To determine the anion binding properties of 4-3 NMR and UV-Vis spectra were taken. The NMR spectrum showed distinct shifts in the positions of the urea N-H's upon addition of fluoride, chloride and bromide. The UV-Vis spectra followed similar trends to that of 4-2. Upon addition of various halides there was a red shift in the absorbance with two isobestic points. The binding constants of 4-3 were determined with the UV-Vis titration data and were found to be $\log K_s = 6.09$ for fluoride, $\log K_s = 5.53$ for chloride and $\log K_s = 4.67$ for bromide. There is approximately an order of magnitude decrease in the binding efficiency of fluoride and chloride and that of chloride and bromide.

The binding constants of both 4-2 and 4-3 decrease with an increase in anion size (Table 4-1). Both receptors show similar binding constants for fluoride as it is the smallest anion tested and spatial constraints would not be as significant of a factor. The binding constants for the larger anions chloride and bromide are higher for receptor 4-3 than 4-2, consistent with the larger separation of ureas allowing the anions to be positioned closer to the receptor. The ability to adjust the size of the system by the incorporation of different metal centers into the salen macrocycle creates a tunable system as which is demonstrated by the differences in binding constant data for 4-2 and 4-3.

While the urea based salen receptors are very efficient halide binders, the addition of a third urea arm could maximize the selectivity of the system for certain anions and still maintain the high binding constants seen with 4-2 and 4-3. The addition of a third urea arm would create a three dimensional pocket that would force the anion to be positioned inside the cavity. The structure of the C_3 symmetric receptor would have all three urea groups pointing inwards

preventing anions from residing above the plane of the molecule. Using a modified literature procedure⁷⁸ various salen type C₃ symmetric ligands could be created with the tris-amine TREN [Tris(2-aminoethyl)amine] and used to coordinate various lanthanides (Figure 4-13).

The initial work focused on the addition of lutetium to the tris-urea receptor because it is a diamagnetic metal which allows the synthesis and anion binding properties to be followed by ¹H NMR spectroscopy. Lutetium is the smallest of the lanthanides and coordination of different larger metal centers could change the receptors size and binding properties, but a urea receptor incorporating any other lanthanide was not isolated. A solid state structure of 4-6 was obtained (Figure 4-14) and it shows the coordination mode of the metal center as well as the orientation of the urea groups.

The structure shows that the Lu (III) is seven coordinate, bonding to the three imine nitrogens and three phenolic oxygens as well as forming a bond with the apical nitrogen on tren N(1). The coordination of lutetium sets the geometry of the ureas and forms a cavity that was less flexible and more size selective for anions. The solid state structure shows an intramolecular hydrogen bond between the proton on N(10) and O(4) at a distance of 2.846 Å as well as hydrogen bond between N(3), N(4) and a water molecule.

Anion binding studies of 4-6 were done with various anions by both ¹H NMR and UV-Vis spectrum. There was no change in the NMR or UV-Vis spectrum with Br⁻, I⁻, NO₃⁻, ClO₄⁻ indicating no interaction with the receptor, but it was able to bind chloride. There was however a change to the absorbance spectrum upon addition of chloride and a binding constant of logK_s = 4.45 was determined in acetone. The addition of fluoride to 4-6 causes a demetalation of the complex as noted by both the UV-Vis and ¹H NMR spectral data. Demetalation of the complex

limits its ability to be used as an anion receptor and this phenomenon has been seen in previous work in the group with other systems incorporating lanthanides.

To create a system that does not demetalate upon the addition of anions, an unreactive metal center must be incorporated. Co (III) is an inert metal that should be extremely stable in an octahedral environment. The tetra-amine tren used for the formation of 4-6 was ideal for the coordination of large metals such as the lanthanides due to its size and ability to coordinate through four nitrogens. To bind the smaller Co (III) the tris-amine tame [1,1,1-tris(aminoethyl)methane] was used to coordinate first row transition metals because they prefer to be six coordinate. The ligand synthesis and metalation of the system is summarized in Figure 4-15. For the metalation reaction, Co (II) acetate is the source of the metal and upon coordination to the ligand it is oxidized to Co (III) with a dilute solution of peroxide. The procedure for metalation must be followed as the direct addition of inert Co (III) to the ligand would not be an effective means of metalation.

A solid state crystal structure was obtained for 4-8 which crystallized as a C_3 symmetric molecule (Figure 4-16). The Co (III) metal center is six coordinated and orientates the three urea groups into a cavity with all six N-H's aligned in the same direction. There is a twist throughout the entire molecule, from the imines to the ureas, as seen in the solid state structure, but the configuration of the molecule is expected to be dynamic in solution. Differences in the lutetium (4-6) and the cobalt (4-8) receptors are mainly a result of the size difference between the two metals. The average Lu – O bond is 2.168(8) Å while the average Co –O bond is 1.896(16) and the difference is translated to the urea groups and the binding cavity.

The anion binding properties of 4-8 were test with $n\text{-Bu}_4\text{N}^+$ halide salts and the addition of bromide and iodide to the receptor caused no changes in the UV-Vis or ^1H NMR spectra

indicating that the addition of a third urea arm has placed size constraints on the binding cavity and increased the selectivity of the urea system for smaller anions. Once again the coordination of anions causes a red shift in the absorbance spectrum from which binding constants were obtained. Binding constants of $\log K_s = 5.00$ for fluoride in DMSO and $\log K_s = 4.95$ in acetone were determined, while chloride had a binding constant $\log K_s = 4.02$ in acetone, but did not bind in DMSO.

Conclusions

The incorporation of urea groups onto a metal salen macrocycle has shown to be an efficient anion sensor. The urea groups have bound halides with high binding constants which are directly proportional to the hydrogen bond lengths of the receptor to the anion. The receptors formed 1 : 1 complexes with the anions as confirmed by both solid state and solution studies. By changing the metal that is coordinated at the salen binding site, the receptor's binding ability can be altered by changing the position of the urea groups. Besides structural considerations, the metal's strong MLCT transitions and color also supply the means to monitor the binding of anions by UV-Vis spectroscopy due to strong MLCT transitions and the color allow the binding constants to be determined.

For compounds 4-2 and 4-3 anion coordination occurs at the periphery of the receptor as the anion must be positioned above the plane of the molecule for an interaction to take place. Adjustments to the size of the binding cavity can relegate the effectiveness in which coordination occurs, but can not exclude the coordination of certain anions by spatial constraints. To increase the selectivity of the system for certain anions, a third urea arm was added to the receptor. Using Lu (III) as the metal template proved ineffective however, as demetalation occurred upon the addition of certain anions. Instead, it was determined that Co (III) formed stable complexes with a C_3 symmetric ligand system and proved to be a selective binder of fluoride and chloride solely.

The binding constant of 4-6 is higher than that of 4-8 for chloride which may be a result of the larger cavity that is formed as Lu (III) is larger than Co (III).

Experimental Methods

General Considerations

^1H and ^{13}C NMR spectra were recorded on a Varian Mercury 300 MHz spectrometer at 299.95 and 75.47 MHz for the proton and carbon channels. UV-Vis spectra were recorded on a Varian Cary 50 spectrometer. All solvents were ACS or HPLC grade and used as purchased. For the metalation reactions, the solvents were dried with a Meyer Solvent Purification system. Some starting materials were synthesized by other members in the group. All NMR spectra are taken in CDCl_3 unless otherwise stated. Some structures are not fully characterized and the experimental procedures reflect known data obtained to date for these compounds. Tame was synthesized by Priya Srinivasan, and 3-5 was synthesized by Melanie Veige.

Synthesis of 4-1

A 1.0 g portion (3.23 mmol) of 3-5 was dissolved in 50 mL of absolute ethanol. To this solution was added 0.184 g (1.61 mmol) of trans-1,2-diaminocyclohexane. The reaction was refluxed open to the air for 12 hours. The solution was cooled to room temperature and 50 mL water was added to the solution resulting in the precipitation of a bright orange solid. The solid was filtered and dried to afford the product in 76% yield (0.86 g). ^1H NMR: δ 9.36 (s, 2H); 8.51 (s, 2H); 8.29 (t, $J = 2.7$ Hz, 4H); 7.45 (s, 2H); 7.43 (s, 2H); 7.26 (t, $J = 8.1$ Hz, 6H); 6.95 (t, $J = 7.5$ Hz, 2H); 6.89 (d, $J = 2.4$ Hz, 2H); 3.54 (s, 2H); 2.02-1.40 (m, 8H); 1.20 (s, 9H). ^{13}C NMR δ 165.7; 152.5; 151.8; 139.8; 139.0; 128.8; 128.5; 121.7; 119.8; 118.5; 118.0; 115.1; 68.8; 33.8; 32.1; 31.1; 23.5. HRMS: Theoretical 703.3966; Measured 703.4008.

Synthesis of 4-2

A portion of 0.5 g (0.712 mmol) of 4-1 was dissolved in 75 mL of dry THF. To this solution 0.177 g (0.712 mmol) of nickel acetate was added and it was refluxed under nitrogen for 12 hours. The solution was cooled, filtered and the solvent removed. The solid was then washed with pentane and filtered producing a red solid product in a 84% yield (0.45g). Crystals suitable for X-ray diffraction were grown by a diffusion of ether into a saturated acetone solution. ^1H NMR: δ 8.22 (s, 2H); 7.84 (bs, 4H); 7.45 (m, 4H); 7.18 (s, 2H); 7.08 (t, 4H); 6.92 (m, 2H); 6.62 (s, 2H); 3.76 (m, 2H); 3.10 (m, 2H); 2.24 (m, 2H); 1.82 (m, 4H); 1.23 (s, 18H). ^{13}C NMR δ 199.28; 158.60; 138.61; 128.82; 122.81; 122.19; 120.10; 118.75; 70.15; 34.20; 31.59; 28.96; 24.51. HRMS: Theoretical [M + Na] 781.2983; Measured 781.3002. Anal. Calc. for $\text{C}_{42}\text{H}_{48}\text{N}_6\text{O}_4\text{Ni}$: C, 66.41; H, 6.37; N, 11.06. Found C, 66.13; H, 6.39; N, 11.00.

Synthesis of 4-3

A portion of 0.5 g (0.712 mmol) 4-1 was dissolved in 75 mL of dry diethyl ether. To this solution 0.0824 g (1.56 mmol) sodium methoxide was added along with 0.195 g (0.783 mmol) of palladium acetate. The solution was refluxed for 12 hours under nitrogen during which time a green precipitate formed. The solution was cooled and the precipitate was filtered. The product was redissolved in methylene chloride, filtered and then solvent was removed leaving a yellow solid in a 48% yield (0.28 g). X-ray quality crystals were grown by a chloroform/pentane diffusion. ^1H NMR. δ 9.20 (s, 2H); 8.56 (s, 2H); 8.51 (d, , $J = 2.4$ Hz, 2H); 8.12 (s, 2H); 7.46 s, 2H); 7.43 (s, 2H); 7.21 (s, 2H); 7.17 (m, 4H); 6.97 (t, $J = 7.5$ Hz, 2H); 3.55 (m, 2H); 2.75 (m, 4H); 1.82 (m, 2H); 1.49(m, 2H); 1.28 (s, 18H). ^{13}C NMR δ 157.48; 152.50; 151.34; 139.50; 136.31; 130.08; 128.56; 122.53; 121.87; 118.85; 118.48; 118.41; 72.23; 33.78; 31.30; 28.33; 24.05. HRMS: Theoretical [M + Na] 829.2676; Measured 829.2679.

Synthesis of 4-6

A portion of tren 0.157 g (1.08 mmol) was dissolved in 10 mL methanol. To this solution was added 0.390 g (1.08 mmol) lutetium triflate. The solution was then heated to 50° c and stirred open to air for 15 minutes. A 1.0 g portion (3.23 mmol) of 1-(5-*tert*-butyl-3-formyl-2-hydroxyphenyl)-3-phenylurea was then dissolved in 25 mL of methanol, added to the solution and stirred for 15 minutes. The solution was then filtered and allowed to slowly cool and evaporate. After sitting for 12 hours large x-ray quality crystals had grown. These crystals were filtered, crushed, and dried yielding a bright yellow powder in 45% yield (0.58 g). ¹H NMR: δ 8.15 (s, 3H); 8.02 (m, 3H); 7.36 (s, 6H); 7.20 (m, 6H); 7.13 (m, 6H); 6.90 (m, 3H); 6.84 (m, 3H); 3.95 (m, 3H); 3.22 (d, 3H); 2.89 (m, 6H); 1.12 (s, 27H). ¹³C NMR δ 169.5; 156.3; 154.7; 139.0; 137.7; 129.9; 129.0; 124.2; 123.1; 120.6; 119.5; 60.1; 58.3; 34.1; 31.5.). HRMS: Theoretical [M + H] 1201.4882; Measured 1201.4898.

Synthesis of 4-7

A 1.0 g portion (3.23mmol) of 3-5 was dissolved in 50 mL of absolute ethanol. To this solution was added 0.087 g (1.08 mmol) of tame. The reaction was refluxed open to the air for 12 hours. The solution was cooled to room temperature and filtered. To the filtrate was added 50 mL of water resulting in the precipitation of a bright orange solid. The solid was filtered and dried to afford the product in 80% yield (0.86 g). ¹H NMR in DMSO: δ 9.36 (s, 3H); 8.62 (s, 3H); 8.39 (s, 6H); 7.45 (d, 6H); 7.26 (t, 6H); 7.024 (d, 3H); 6.95 (t, 3H); 3.67 (s, 6H); 1.27 (s, 27H); 1.18 (s, 3H). HRMS: Theoretical [M + H] 1000.5389; Measured 1000.5444.

Synthesis of 4-8

A portion of 1.50 g (1.50 mmol) of 4-7 was dissolved in 15mL ethyl acetate. To this solution a solution of 0.75g (3.00 mmol) of cobalt(II) acetate tetrahydrate in 50mL methanol was added. A 3% solution of hydrogen peroxide (10 mL) was then added. The solution was then

brought to a boil for 5 min. The solution and suspended solid was then extracted with chloroform (3 times 100 mL each). The extracts were washed several times with water, dried with sodium sulfate and the solvent removed to afford the product in a 52% yield (0.818 g). Crystals suitable for X-ray diffraction were grown by an acetone / pentane diffusion. ^1H NMR: δ 7.91 (s, 3H); 7.74 (s, 3H); 7.56 (s, 3H); 7.27 (s, 3H); 7.23 (s, 3H); 7.05 (t, $J = \text{xx}$, 6H); 6.91 (s, 3H); 6.82 (t, 3H); 3.74 (d, 3H); 3.39 (d, 3H); 1.13 (s, 3H); 1.09 (s, 27H). ^{13}C NMR δ 167.9; 155.5; 153.0; 139.4; 135.2; 131.1; 128.3; 122.6; 121.6; 121.0; 119.9; 118.2; 63.7; 40.6; 33.5; 31.0; 20.4. HRMS: Theoretical 1056.45; Measured 1056.45. Anal. Calc. for $\text{C}_{59}\text{H}_{66}\text{N}_9\text{O}_6\text{Co}\cdot\text{H}_2\text{O}$: C, 65.96; H, 6.38; N, 11.74. Found C, 65.30; H, 6.48; N, 10.70.

Table 4-1. LogK_s values of the two salen urea complexes with fluoride, chloride and bromide in acetone.

	Compound 4-2	Compound 4-3
F ⁻	6.10	6.09
Cl ⁻	5.27	5.53
Br ⁻	4.29	4.67

Table 4-2. X-ray data from crystal structures of 4-2, 4-3, 4-4, 4-6, 4-8.

	4-2	4-3	4-4	4-6	4-8
total reflections	19062	9871	13587	16723	4240
unique reflections	9861	6718	6020	12542	4015
Θ _{max} °	28	28	28	28	28
crystal system	triclinic	monoclinic	monoclinic	monoclinic	triclinic
space group	P-1	I2/a	c2/c	P2(1)/c	P
<i>a</i> (Å)	12.3151(6)	17.6232(10)	43.56(3)	15.0435(13)	28.0319(11)
<i>b</i> (Å)	17.2793(8)	17.2988(9)	10.203(5)	25.384(2)	28.0319(11)
<i>c</i> (Å)	20.9637(9)	28.011(2)	26.868(16)	19.0081(17)	28.0319(11)
α (°)	107.0500(10)	90.00	90.00	90.00	90.0
β (°)	92.9510(10)	94.4040(10)	91.67(7)	94.287(2)	90.0
γ (°)	95.3330(10)	90.00	90.00	90.00	90.0
<i>V</i> _c (Å ³)	4231.9(3)	8514.3(9)	11938(12)	7238.2(11)	22027.1(15)
<i>Z</i>	2	4	6	6	16

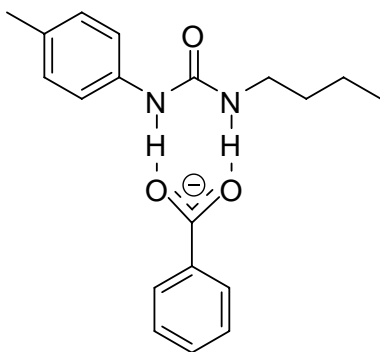


Figure 4-1. Proposed structure and binding mode of an early urea based anion receptor.⁶⁸

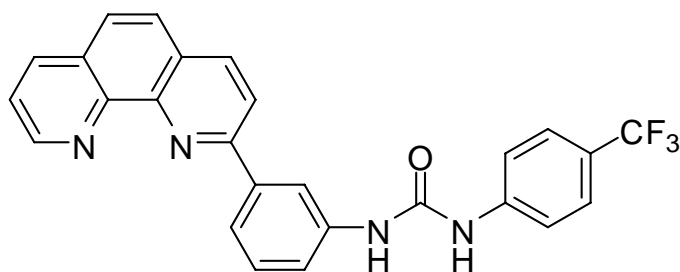


Figure 4-2. Structure of a urea subunit where the anion binding cavity is regulated by metal coordination

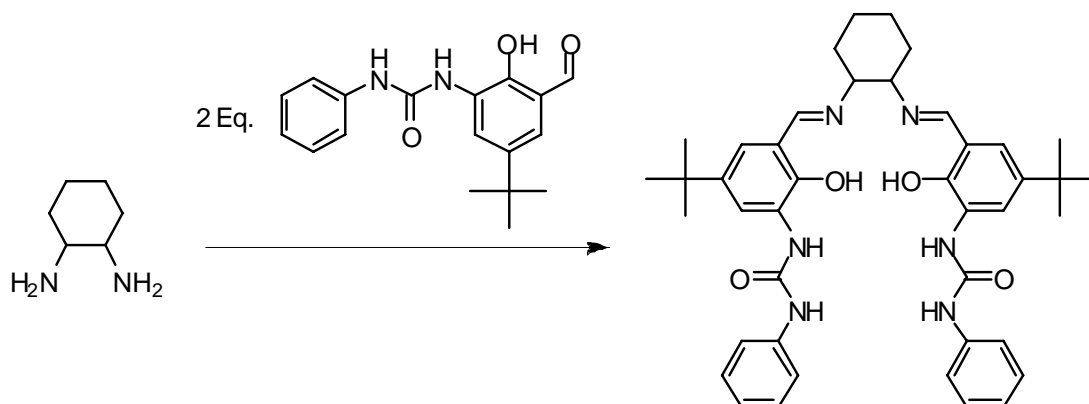


Figure 4-3. Synthetic scheme for the formation of salen urea (compound 4-1)

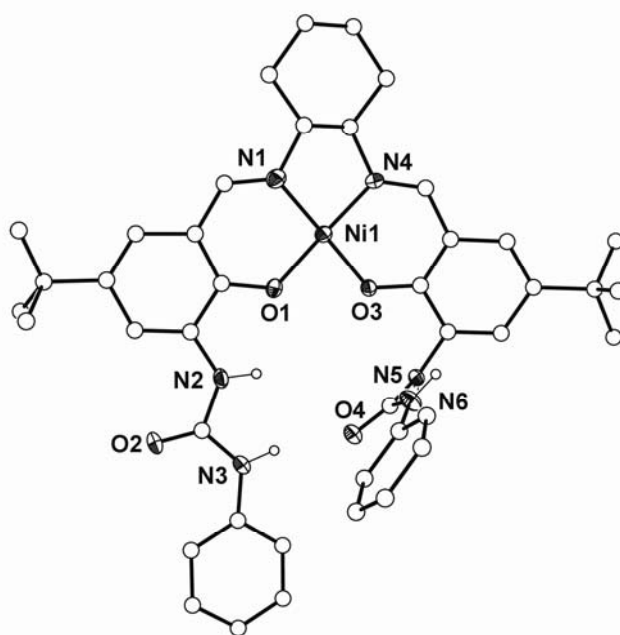


Figure 4-4. Depiction of the solid-state structure of 4-2 (30% probability ellipsoids, carbons drawn with arbitrary radii). The break in planarity of the urea group N5, O4, N6 is caused by a steric clash between the two phenyl rings as well as an intramolecular hydrogen bond between N3 and O4.

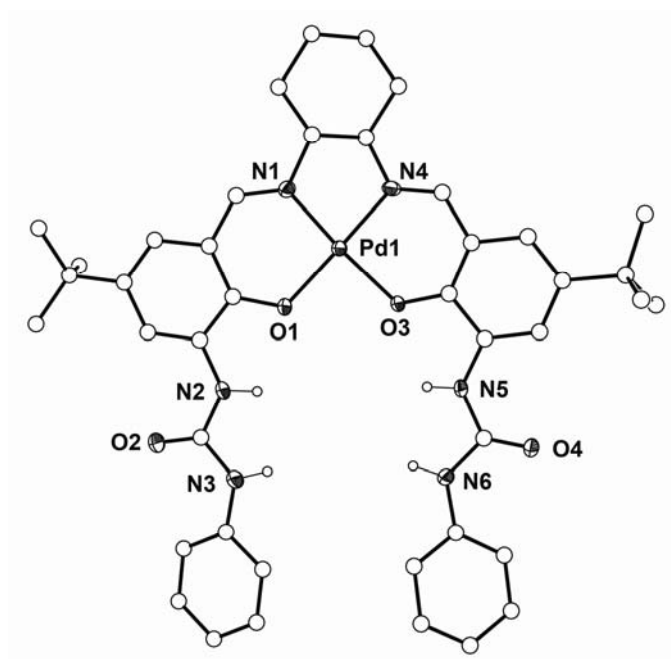


Figure 4-5. Depiction of the solid-state structure of 4-3 (30% probability ellipsoids, carbons drawn with arbitrary radii). The two urea groups are oriented to form an anion binding cavity with four N-H groups available for hydrogen bonding

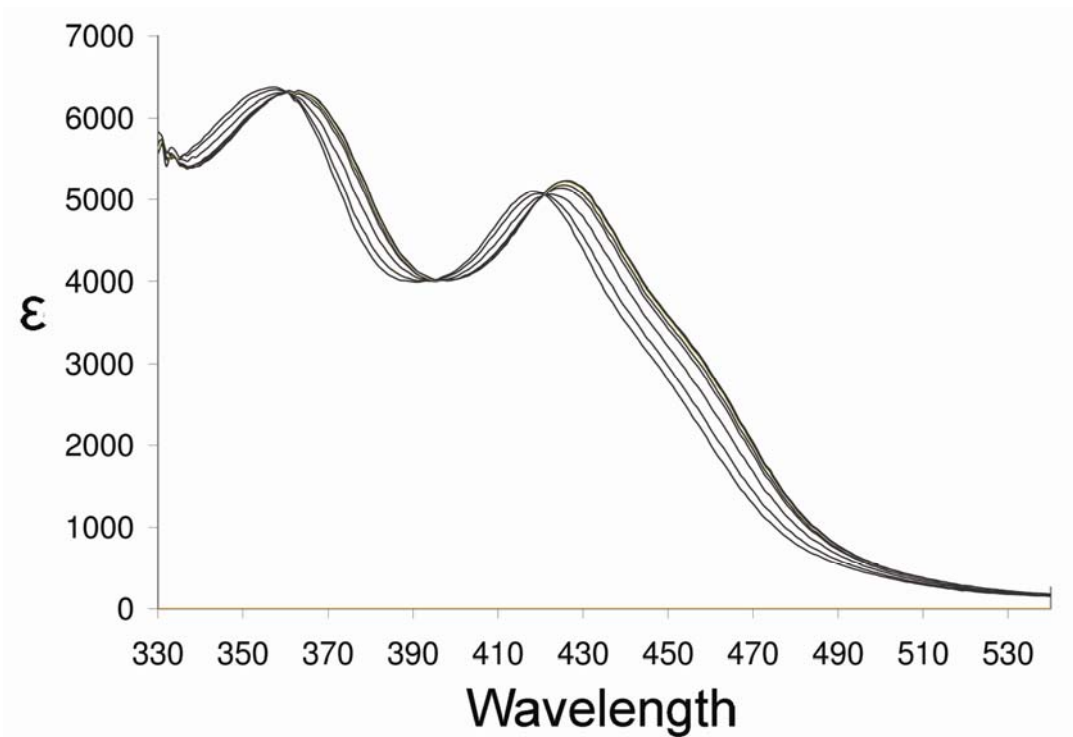


Figure 4-6. UV-Vis titration of 4-2 with tetra-butylammonium fluoride in acetone. Titration was complete after the addition of a single equivalent of fluoride.

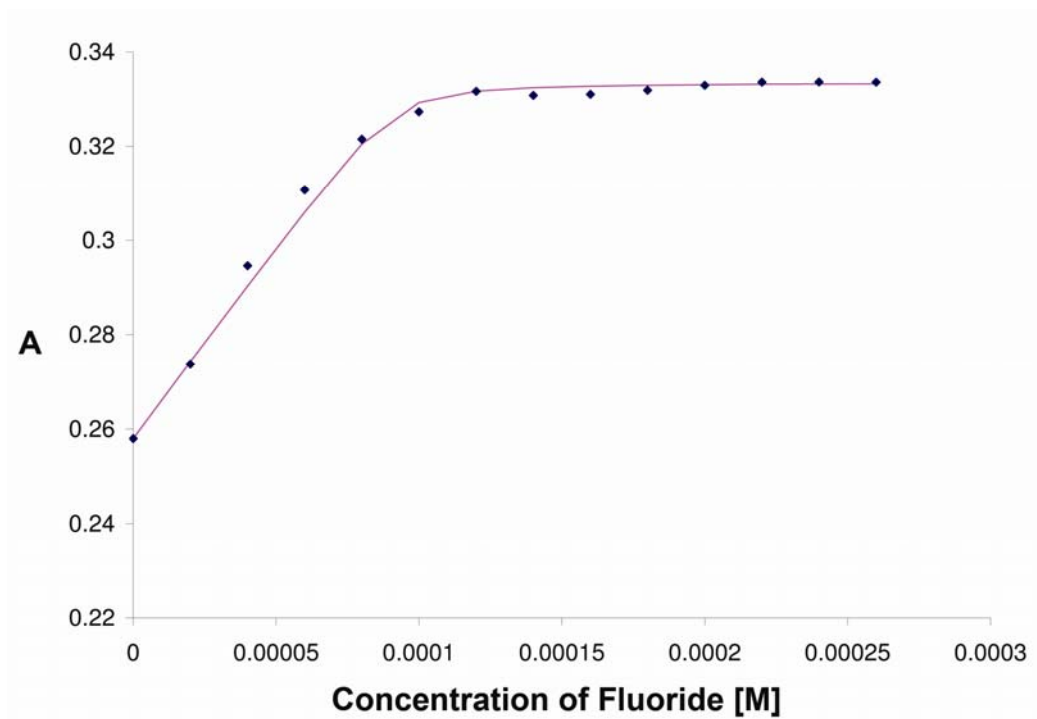


Figure 4-7. Binding constant data of 4-2 titrated with F^- at 450nm $\text{Log } K_s = 6.10$. Each point represents an experimental value and the best fit line is shown where a value of K_s is calculated to minimize the error to the system.

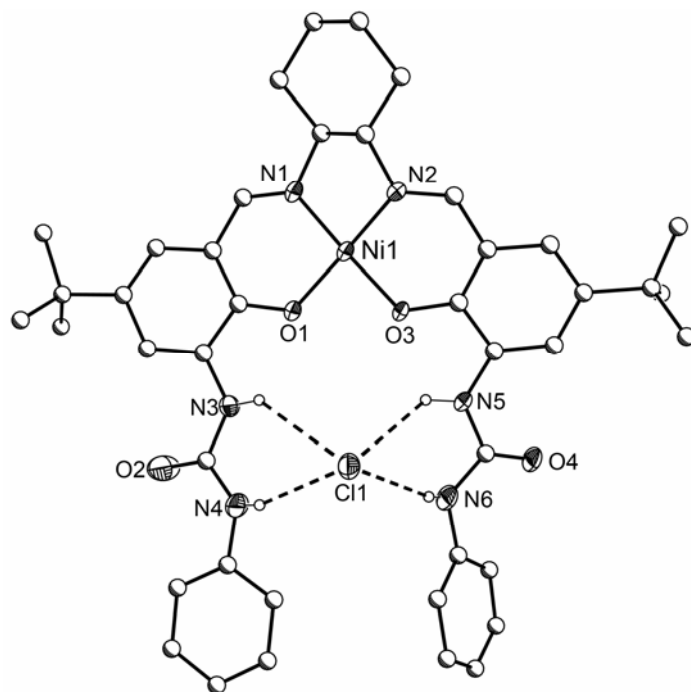


Figure 4-8. Depiction of the solid-state structure of 4-4 (30% probability ellipsoids, carbons drawn with arbitrary radii, tetrabutylammonium cation and hydrogen removed for clarity). The chloride is positioned above the plane of the molecule and the four urea N-H's are distorted in order to be aligned with the anion.

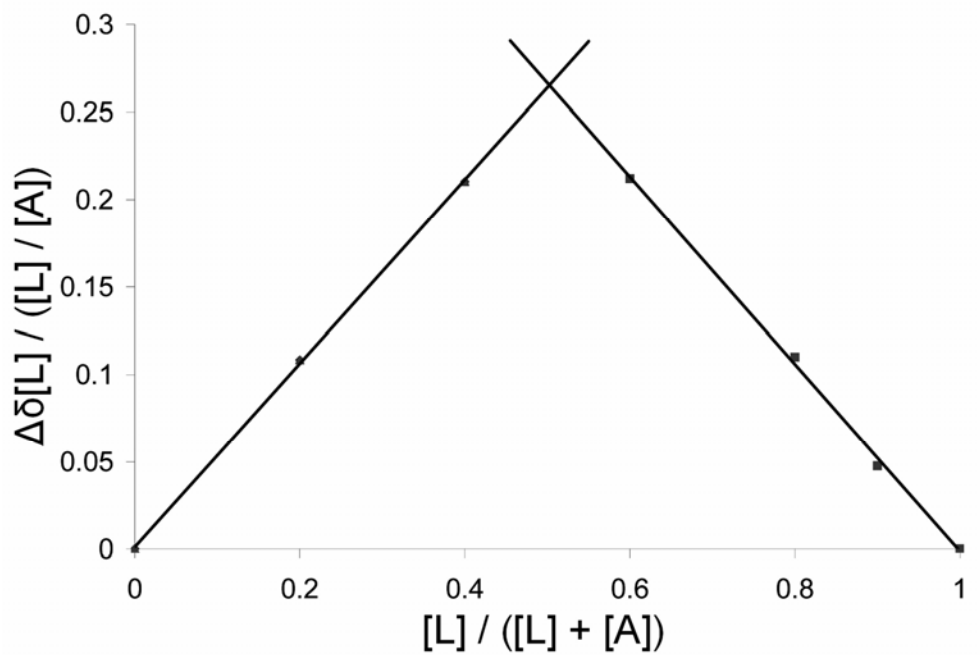


Figure 4-9. Job plot of 4-2 for chloride. An apex in the plot at 0.5 indicated that there is a 1 : 1 ratio of anion to receptor in complex 4-4. [L] = concentration of receptor; [A] = concentration of anion; δ = NMR chemical shift.

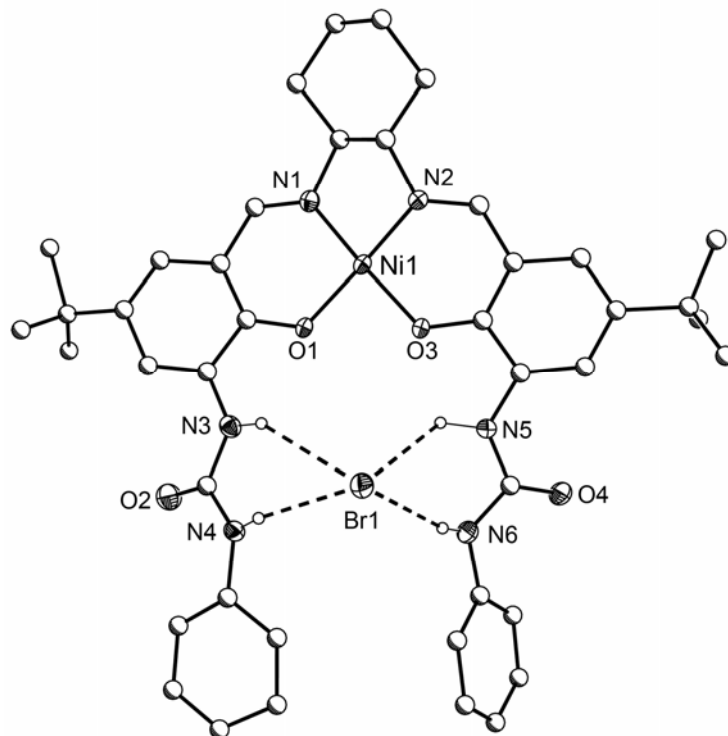


Figure 4-10. Depiction of the solid-state structure of 4-5 (30% probability ellipsoids, carbons drawn with arbitrary radii, tetrabutylammonium cation and hydrogen removed for clarity). The bromide is positioned above the plane of the molecule and the four urea N-H's are distorted in order to be aligned with the anion.

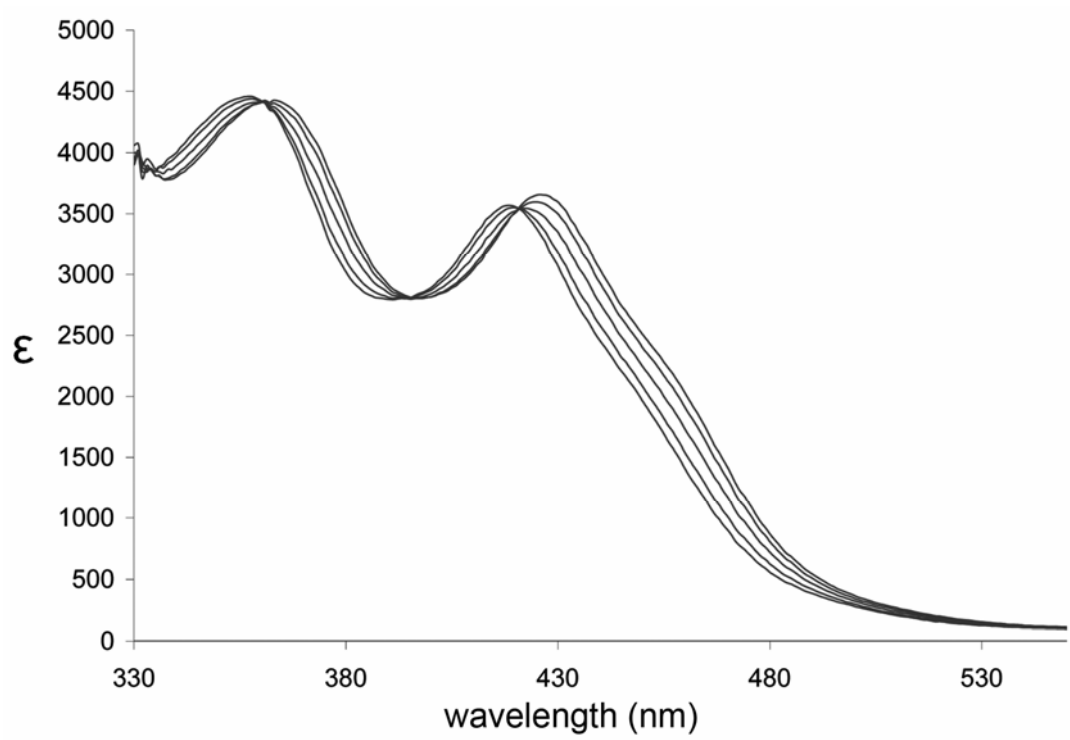


Figure 4-11. UV-Vis titration of 4-2 with tetra-butylammonium chloride in acetone. Titration was complete after the addition of a single equivalent of fluoride.

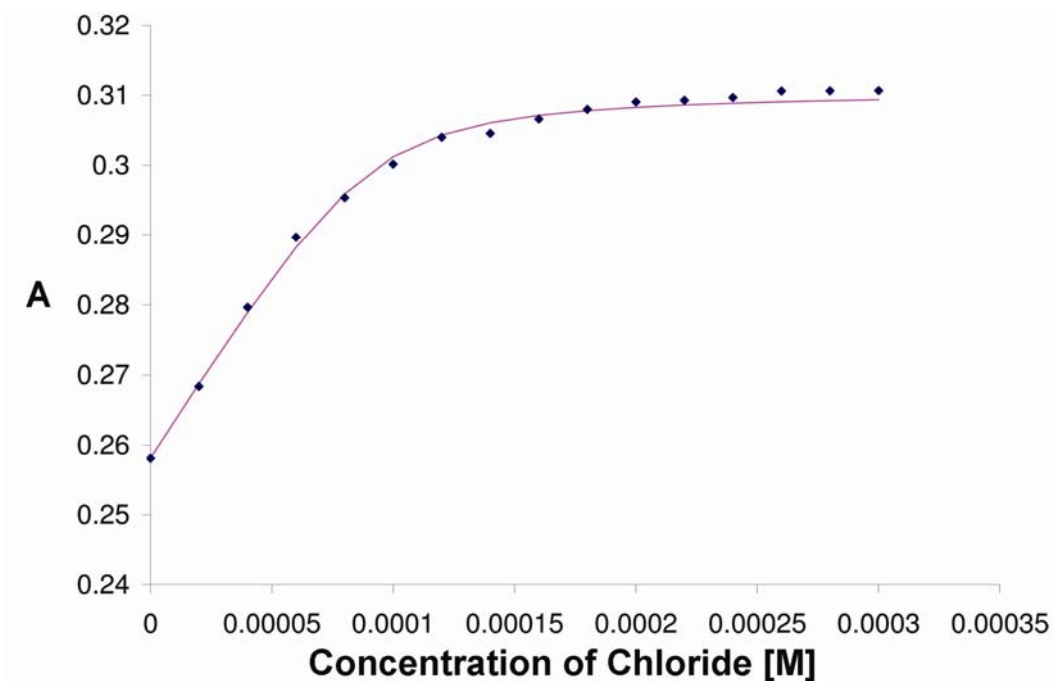


Figure 4-12. Binding constant data of 4-2 titrated with Cl^- at 450nm $\text{Log } K_s = 5.27$. Each point represents an experimental value and the best fit line is shown where a value of K_s is calculated to minimize the error to the system.

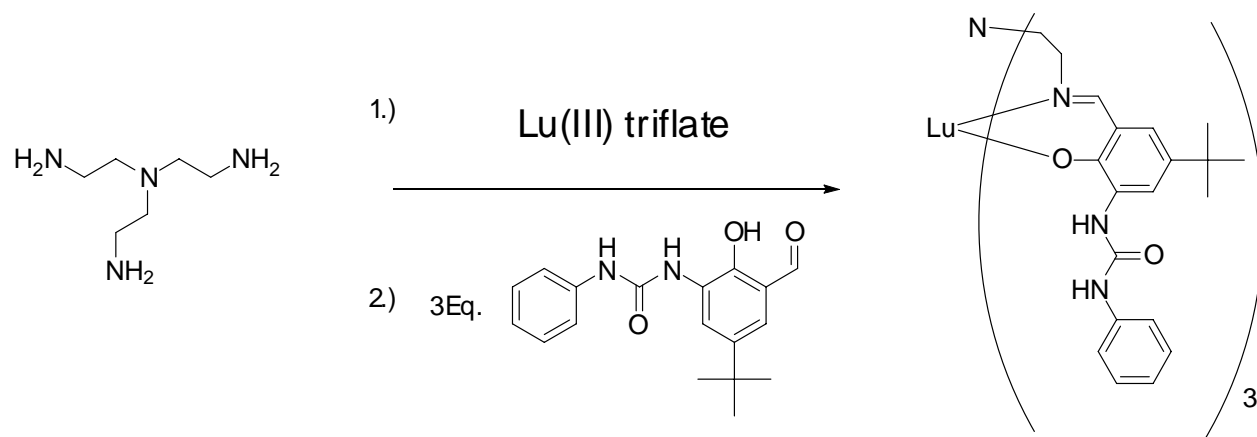


Figure 4-13. Synthetic scheme for compound 4-6. The metal Lu (III) is first reacted with tren and then the condensation reaction with the urea aldehyde to afford compound 4-6.

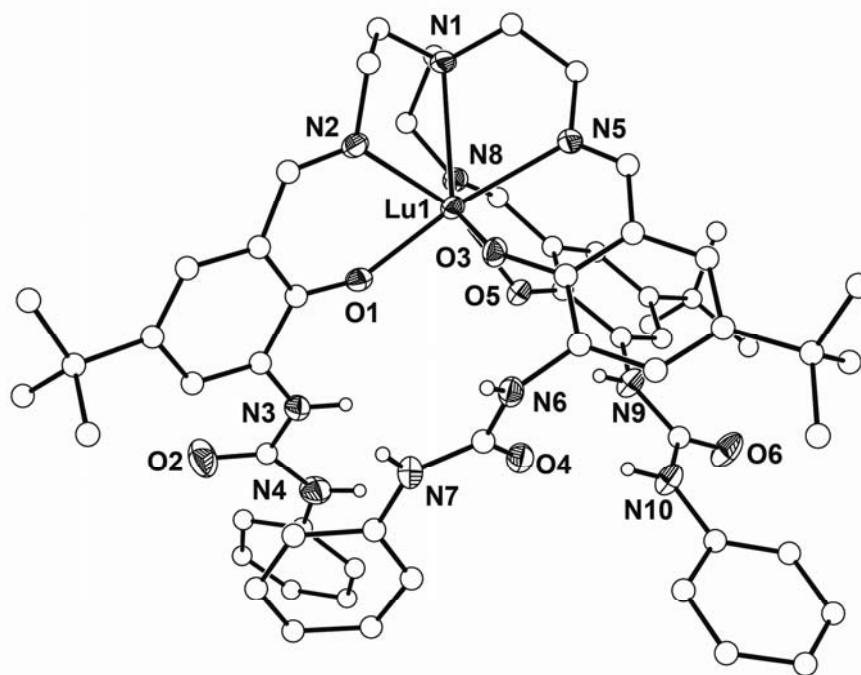


Figure 4-14. Depiction of the solid-state structure of 4-6 (30% probability ellipsoids, carbons drawn with arbitrary radii, hydrogens and water molecule removed for clarity).

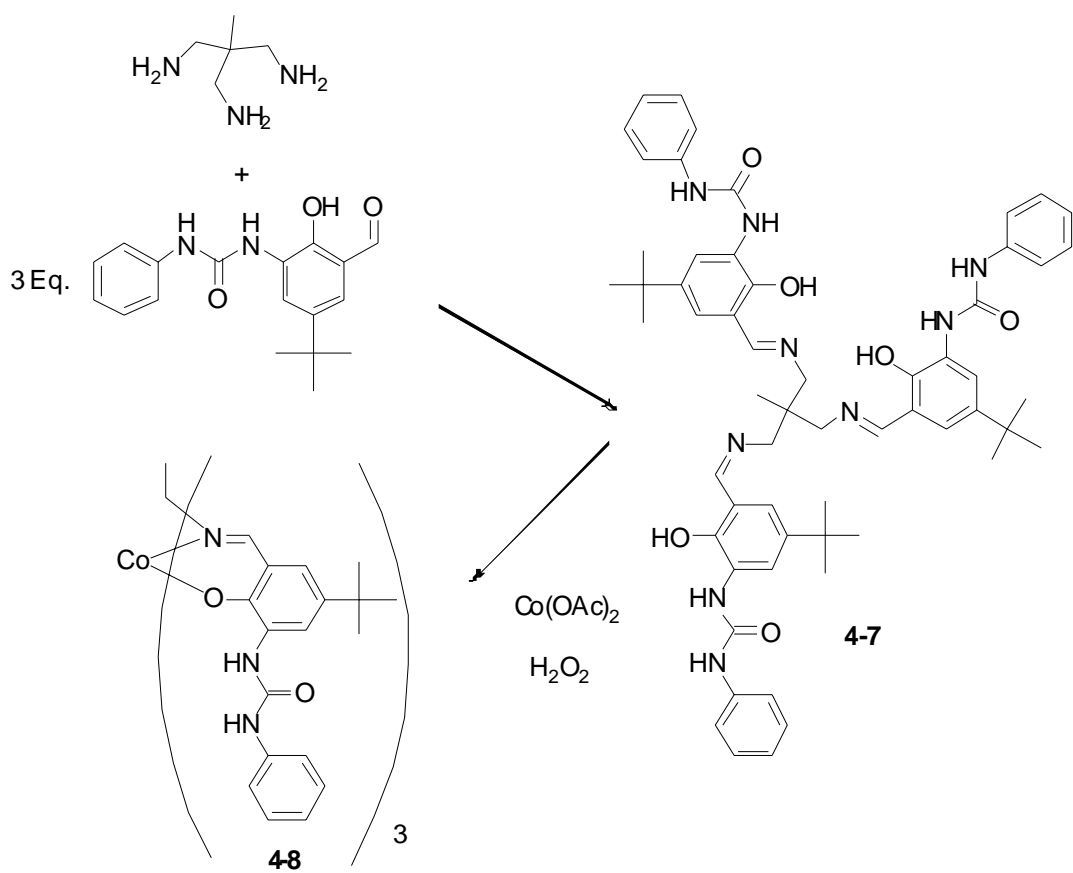


Figure 4-15. Synthesis of ligand 4-7 and C_3 symmetric anion receptor 4-8.

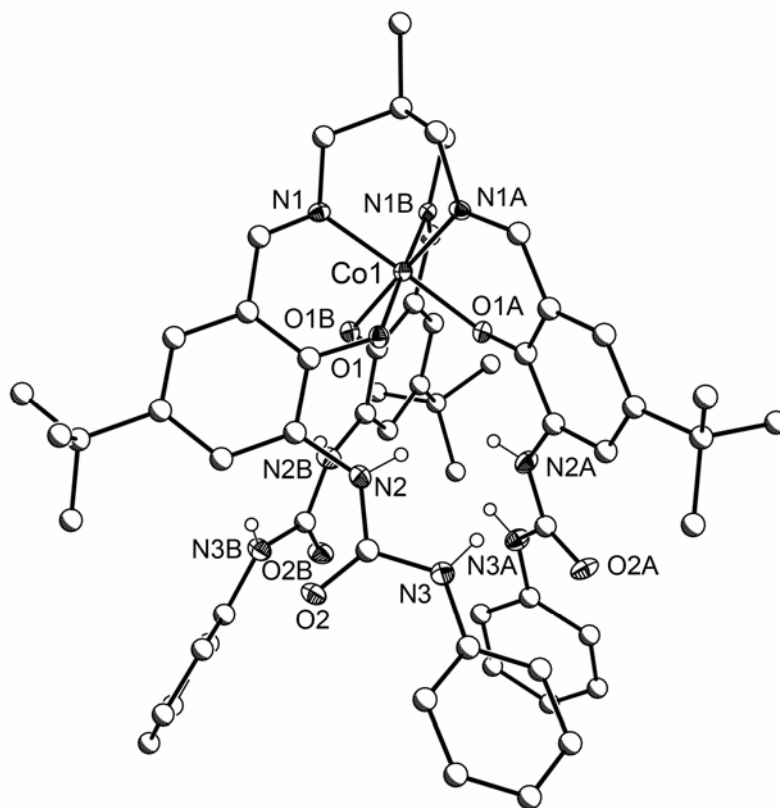


Figure 4-16. Depiction of the solid-state structure of 4-8 (30% probability ellipsoids, carbons drawn with arbitrary radii, tetrabutylammonium cation and hydrogen removed for clarity).

CHAPTER 5 DESIGNER LEWIS ACIDS; THE DEVELOPMENT OF EXREMELY BULKY AND RIGID DINUCLEAR CHIRAL CATALYSTS

Introduction

Metal salen compounds are used in a many catalytic systems as they are able to promote a variety of organic transformations.^{79, 80} Salens are formed by a condensation reaction between salicylaldehyde and a diamine and are able to coordinate many different metal centers in a wide range of oxidation states. Chiral salen catalysts are readily prepared with enantiomerically pure diamines, are adept at a number of enantioselective reactions such as alkene epoxidation,⁸¹ and the Diels Alder reaction,⁸² among numerous others.⁸³

For the design of chiral catalysts, the geometry of the salen is essential to determine the orientation of the substrate upon coordination to the binding site. Metals bound within the salen are able to transfer their chirality to the products by binding the substrate through Lewis acidic interactions. The approach of the substrate towards the catalyst and the metal center influences the conformation of the product. In the design of asymmetric catalysts, it is important to control the trajectory of the substrate.⁷⁹ The conformation of the active site is influenced by many factors including the size and oxidation state of the coordinating metal. The nature of the ligand also plays an important role as the location and steric constraints of the substituents on the salen can regulate the path of approach of the substrate.⁸⁴

Jacobsen's Catalyst

Jacobsen's catalyst is perhaps the most influential and well known metal salen compound (Figure 5-1) and it contains a Mn (III) metal center for the asymmetric epoxidation of olefins.⁸¹ Although chromium was used early to epoxidize olefins,⁸⁵ Jacobson found manganese to be a superior choice for this reaction as it proceeds through a Mn (V) – oxo species.⁸⁶ The generally accepted catalytic cycle, depicted in Figure 5-2, involves two steps. In the first, the oxidant

transfers and atom to oxidize Mn (III) to Mn (V) - oxo and this species reacts with the incoming olefin to create the epoxide. The source of oxygen for the epoxidations is typically iodosylbenzene, but other oxygen sources such as bleach or peroxide are also catalytically competent.

Many different chiral diamines such as binaphthylene⁸⁷ and diphenyl⁸⁸ are used as catalyst backbones, but 1,2-diaminocyclohexane is among the most commonly used, due to the low cost of the chiral form. A second generation Jacobsen type catalyst, with chiral diphenyl diamine and binaphthyl groups combines their chiral elements to influence the stereoselectivity of the reaction (figure 5-3).⁸⁹ Not only do the bulky chiral groups influence the approach of the substrate to the catalyst, but they cause a folding effect, altering the geometry at the metal center.

Lewis Acid Catalysts

Since chiral metal salens are able to transmit their geometry onto substrates they are often employed as Lewis acid catalysts for many organic transformations. The Friedel-Crafts reaction, the ene reaction, and Diels-Alder reaction employ ordinary Lewis acids such as AlCl₃, TiCl₄ and BF₃.⁹⁰ Although these reactions proceed very efficiently; they are neither regio nor stereoselective. Many biologically active molecules are chiral and the design of asymmetric catalysts to facilitate carbon – carbon bond formation is of particular importance to medicinal chemistry and the pharmaceutical industry because many of their products require 99% enantiomeric excess (e.e.).⁹² Modifying the ligands coordinated to the Lewis acidic metal can lead to products with higher regio and enantioselectivity.

Zn Salens in Catalysis

Chiral Zn salen compounds can catalyze stereoselective organic transformations. For example, a Lewis acidic Zn (II) can promote efficient addition of an ethyl group to aldehydes with ee's ranging from 35-70 %.⁹³ Unfortunately, the isolation of a pure metalated Zn (II) salen

is often problematic, and mixtures of metalated product and free ligand are obtained.⁷⁹ To overcome this challenge, metalation of the salen occurs *in situ* with Et₂Zn, and the resulting complex catalyzed at 10 mol. % to promote the addition of an ethyl group to benzaldehyde. The proposed reaction mechanism involves the simultaneous coordination of the aldehyde and Et₂Zn to the Lewis acidic Zn salen. The manner in which the aldehyde orients itself when coordinating to the metal center influences the stereochemistry of the product. The hydrogen atom of the aldehyde aligns itself in order to minimize its interactions with the stereo centers.

Bifunctional Zn salen catalysts that contain both a Lewis acid and a Lewis base component can promote the addition of an ethyl group to benzaldehyde with high efficiency and stereoselectivity.⁹⁴ The Lewis acidic Zn metal center coordinates and activates the aldehyde, while the aminoalkoxy groups at the periphery of the salen are able to coordinate and activate diethylzinc (Figure 5-5). Once activated, the substrates have an enhanced reactivity for the addition of diethylzinc to aldehydes with respect to other Zn salen catalyst systems.⁹³

While numerous methods promote asymmetric reactions with aldehydes, there are only a handful of examples of reactions with ketones, which are generally considered to be unreactive as substrates in asymmetric catalysis.⁹⁵ Ketones are difficult substrates due to their low reactivity as well as problems controlling their stereoselectivity.⁹⁵ A Zn salen catalyst can facilitate the stereoselective addition of terminal alkynes to a multitude of ketones with moderate yields (30-90 %) and enantiomeric excess (30-81 %) (Figure 5-6).⁹⁶ For the reaction to proceed, a zinc alkynide forms *in situ* and associates with the salen phenolates. The ketone, which is coordinated to the Lewis acidic Zn salen site, is then able to add the alkyne and a diagram of the proposed transition state is depicted in figure 5-7.

The Promotion of the Diels-Alder Reaction by a Lewis Acid

The Diels-Alder reaction, which is one of the most widely used reactions in synthetic organic chemistry can be facilitated by Lewis acid catalysts.⁹⁷ While Diels-Alder reactions can occur in the absence of a catalyst without stereoselectivity, at high temperature, the presence of a chiral Lewis acid can initiate the reaction with higher selectivity. Among the chiral Lewis acid catalysts able to promote the Diels-Alder reaction are organic iminium salts,⁹⁸ and metal salen complexes containing Co (III)⁹⁹ or Cr (III).¹⁰⁰

General Approaches of Synthetic Design

Although the work in the field of asymmetric catalysis is vast, there is always the need to create systems that are more efficient and selective. Designer Lewis acidic catalysts can promote a variety of organic transformations and particular interest has been paid to the development of catalysts that can induce regio- and stereoselective products.¹⁰¹ The nature of the ligand as well as the metal are crucial to the reactivity and selectivity of any catalyst, and modifications made to the system can influence its properties. Herein, we report the design and synthesis of an extremely bulky and rigid chiral Lewis acid catalyst.

Results and Discussion

For the design of Lewis Acidic catalysts, the salen macrocycle offers a convenient way to create a system compatible with many different metal centers to promote a variety of organic transformations. The presence of rigid and sterically bulky groups on the salen can enhance stereoselectivity by blocking the catalytic site from substrate attack. Metal salen compounds are ideal candidates for Lewis acid catalysts since they can facilitate many reactions efficiently and selectively with metals such as Ti, Cr, Al, Co, and Zn among numerous others.⁷⁹ The environment of the metal affects stereoselectivity as the chirality at the metal center can translate to the products.

Previous work with chiral metal salen compounds in the Scott lab has shown that four phenols at the periphery of a salen can be orientated into a tetrahedral environment as in compound 2-2.⁶³ In the solid state structure of 2-2, *R,R*-1,2-diaminocyclohexane is chiral, but this geometry is not translated to other parts of the ligand. The bulky phenols still have a lot of rotational freedom and their position is not influenced by the chirality of the diamine. In the solid state structure, two molecules crystallized in the asymmetric unit, each with a different orientation of the phenols, indicating that the configuration of the system would not be useful as a chiral catalyst (Figure 5-9).

Binap Ligand

In order to design a system where the chiral unit of the structure would translate its geometry to the entire molecule, it must possess a larger torsion angle than *R,R*-1,2-diaminocyclohexane. Binaphthylene is a common moiety in many catalytic systems. It is chiral and has a large angle between the two naphthyl planes (Figure 5-10). The condensation of 2,2-diamino-1,1'-binaphthylene with a portion of an aldehyde derivative of triphenoxymethane 5-1 affords compound 5-2 as depicted in Figure 5-11. Both chiral and racemic versions of ligand 5-2 were synthesized and there are noted differences in the properties of the two. The condensation reaction of the racemic compound readily forms the product (5-2), but the chiral portion does not cleanly convert to the desired product and column chromatography must be employed to isolate the ligand (5-3). Once isolated both molecules have identical NMR and absorption spectra, but have strikingly different solubilities. While 5-2 is soluble in only a handful of solvents such as THF, methylene chloride and chloroform, compound 5-3 was soluble in all organic solvents ranging from pentane to methanol.

The ability to manipulate a ligand's solubility is often important for the development of catalysts as metalation reactions of salens often require the precipitation of the complex as a

means of isolating the product. Ligands which are extremely soluble will create difficulties in the formation of the catalyst. In order to attempt to lower the solubility of the chiral system the alkyl groups on the triphenoxymethane were changed from *t*-butyl to methyl groups which would presumably diminish the compound's solubility in non-polar solvents. Both the racemic (5-4) and chiral (5-5) versions of the di-methyl derivative were made and a depiction of the synthetic scheme for the formation of 5-4 can be seen in figure 5-12.

The incorporation of the methyl groups did slightly decrease the solubility of the ligand and a solid state structure of 5-4 was obtained (Figure 5-13). The structure shows that there is a significant angle between the two naphthyl planes of 98.6° , which should force the geometry of the entire molecule upon metalation. Unlike the structure of 2-1, there is a well defined twist in the structure of the binap derivative and it is this twist that is critical to the design of our catalyst.

Racemic Zn Catalyst

All initial work in catalyst design involved the use of the racemic versions of the molecules due to the lower cost of the starting diamine. The first area of concentration included the metalation of the binap ligands with Zn (II). Zinc salens are useful as Lewis acid catalysts, and have many useful properties including no redox activity or air sensitivity. Zn (II) also is diamagnetic offering the ability to monitor the synthesis by ^1H NMR spectroscopy. Metalation of 5-2 and 5-4 with Zn(II) followed typical literature procedures by precipitating from an acetonitrile solution upon metal complexation¹⁰² to form the methyl and the *t*-butyl derivatives 5-6 and 5-7 respectively.

In solid state structure 5-6, the binaphthylene influences the geometry of the entire molecule (Figure 5-14). On each side of the structure, the phenols are orientated in the opposite direction of the naphthyl plane. There is a distinct twist to the molecule creating a channel in which substrates could coordinate. There is enough space around the catalytic site for a substrate to

bind as the solid state structure has two THF solvent molecules coordinated to the Zn (II) metal center, intimating the Lewis acid properties of the Zinc salen species. The majority of Zn salen molecules are five coordinate,¹⁰³ however, there are a few examples of six¹⁰⁴ and four¹⁰⁵ coordinate complexes. In the presence of a coordinating solvent such as THF, the metal center of 5-6 assumes an octahedral geometry with the two THF molecules in the axial positions and the four binding sites of the salen coordinating in the equatorial positions. The zinc – oxygen and zinc – nitrogen distances of 5-6 are typical for Zn (II) binap salen compounds.¹⁰⁶

The solid state structure of 5-6 was obtained in the coordinating solvent THF, but a structure of 5-7 was obtained from a solution of the non-coordinating solvent methylene chloride. There is a drastic difference between the two structures as the lack of a coordinating solvent completely changes the geometry of the metal (figure 5-15). The metal center of 5-7 is aligned in a tetrahedral geometry and the position of the four phenols is also quite different since they are spaced much further apart. There is a greater twist to the structure of 5-7 than there is for 5-6, but in both cases the geometry of the entire molecule is determined by the position of the binaphthalene. The zinc – oxygen and zinc – nitrogen distances of 5-7 are typical for Zn (II) binap salen compounds,¹⁰⁶ while the geometry is a distorted tetrahedral with N(1) – Zn(1) – N(2) angles of 96.6(4)°, and O(1) – Zn(1) – O(4) angles of 116.4(3)°.

While the position of the four phenols is influenced by the binaphthalene in the solid state, these bulky groups contain a large degree of rotational freedom and would be dynamic in solution. In order for an asymmetric catalyst to be effective, it must be able to force the stereochemistry of the substrate. The extremely bulky groups, as seen in this system on the periphery of the salen, could be an ideal means to do this, yet if the phenols are not rigidly locked into position it will not be effective. The four phenols are aligned in a pseudo tetrahedral

array and the incorporation of another metal at this site would lock them into position creating an extremely bulky and rigid multinuclear catalyst which would not be flexible in solution.

Ti (IV) will form complexes with four phenols arranging the phenolates into a tetrahedral geometry.¹⁰⁷ Since these complexes are d^0 , the products can be readily observed by ^1H NMR spectroscopy. Initial attempts at metalation involving TiCl_4 and triethylamine as a base for the deprotonation of the phenols were unsuccessful as a mixture of products was obtained. The addition of one equivalent of titanium isopropoxide to a solution of 5-7 however, led to a clean conversion to the desired catalyst 5-8 and a depiction of the solid state structure can be seen in figure 5-16.

The incorporation of titanium not only rigidifies the system, but creates a channel for substrate coordination to occur. The oxygen – titanium bond lengths in the range of 1.799(2) Å to 1.828(2) Å are typical for a Ti (IV) atom bound to four phenolates in a tetrahedral environment²⁰⁴ and the titanium is very near this geometry with angles ranging from 104.3(10)° to 118.8(11)°. The phenol that includes O(3) is aligned in a manner that blocks an entire side of the metal center from substrate attack and in combination with the binaphthalene group forms an ideal site for asymmetric catalysis to occur. Space filling models of 5-8 infer that the presence of the *t-butyl* groups on the phenols is important to create the proper steric constraint to force the stereoselectivity of the products (Figure 5-17). After this observance, no further effort was made with ligand 5-4. Zinc behaves as a Lewis acid and coordinates a THF solvent molecule to one side of the zinc in comparison to the structure of 5-6 which coordinates two THF molecules; however, compound 5-8 only binds one solvent molecule because of the rigidity and steric constraints placed on the system. The metal center is in a trigonal bipyramidal geometry as the angle of O(1) – Zn1 – O(4) is 128.92(13)° and the angle of O(1) – Zn(1) – N(1) is 90.25(10)°.

Chiral Zn Catalyst

The synthesis of the target catalyst has proven the plausibility of the system, but in order to be an effective asymmetric catalyst, a chiral molecule must be isolated, but the metalation of 5-3 with Zn (II) proved difficult. The synthesis of compound 5-6 involved the precipitation of the product from the reaction mixture upon metalation. Due to the high solubility of 5-3, the chiral complex never precipitated from the reaction mixture and all attempts to purify the mixture were unsuccessful. A multitude of reaction conditions and purification techniques were screened with none resulting in better than a 60 : 40 ratio of metalated compound to free ligand as determined by ^1H NMR spectroscopy. Difficulties in isolating chiral Zn salen compounds have been previously noted with a mixture between the metalated and free ligand species being the common product.⁷⁹ Most systems employ an *in situ* metalation method with alkyl zincs such as Et_2Zn ,^{93,94} but this is not a possibility for a multinuclear system as the Zn product must first be isolated.

Co Catalysts

Since the isolation of a chiral Zn catalyst proved difficult, other metals were examined. Both Co (II) and Co (III) are useful in asymmetric catalysis and have been able to promote organic reactions with high efficiency and selectivity.¹⁰⁹ Co salen compounds can enantioselectively facilitate the *Baeyer-Villiger* oxidation,¹¹⁰ as well as the Diels-Alder reaction⁹⁹ in good yields. The metalation of ligand 5-2 with Co (II) afforded the product 5-9. Although Co (II) is paramagnetic, the compound synthesis could be monitored by ^1H NMR spectroscopy. (Figure 5-18).

In order to rigidify the system, titanium was once again coordinated to the four phenols to lock in the geometry. The positions of the phenols have been influenced by the binaphthalene and the solid state structure of this complex (5-10) is isostructural to that of 5-8. The ionic radii

of Zn (II) (0.880 Å) and Co (II) (0.885 Å) are nearly identical and the similarity is directly translated to the structure (Figure 5-19). The metal – ligand bond lengths are similar to other Co (II) binaphthalene salen complexes,¹¹¹ and both the bond lengths and angles from the titanium to the phenolates are typical.¹⁰⁸ Much like the Zn (II) system, the isolation of a chiral Co (II) was problematic due to the high solubility of the complex, and it became apparent that in order to isolate a chiral metal salen catalyst, the solubility of the ligand had to be altered.

Low Solubility Chiral Ligands

As a starting point for the formation of less soluble triphenoxymethane aldehydes, the substituent in the R₃ position of the molecule was changed (Figure 5-20). Both 2,6-diformyl-4-bromophenol and 2,6-diformyl-4-nitrophenol are known,¹¹² and the incorporation of either the bromo or nitro group to the system decreased the solubility of the molecule. The synthetic scheme for the triphenoxymethane aldehyde compounds can be seen in figure 5-21 and both the bromo (5-11) and the nitro (5-12) derivatives were readily isolated.

The condensation reaction of *R,R*-(+)-2,2-diamino-1,1-binaphthylene and the aldehydes 5-11 and 5-12 afforded the chiral ligands 5-13 and 5-14 (Figure 5-22). The solubility of the ligands in polar and non-polar solvents is considerably lower than that of complexes 5-3 and 5-5, and the isolation of the chiral Lewis acid catalysts is attainable. The addition of a large excess of Co (II) to 5-13 and 5-14 in methanol led to the precipitation of the pure compounds 5-15 and 5-16 respectively. While the metalation of 5-13 with Zn (II) was unsuccessful the addition of a large excess of the metal to 5-14 fostered the clean conversion to 5-17.

In the solid state structure of 5-16, Co (II) is in an octahedral geometry with four bonds from the salen ligand and two coordinating methanol molecules (Figure 5-24). The coordination of methanol to the metal center has an effect on the solubility of the compound, as the reaction does not cleanly convert to product in other solvents. While other compounds in this chapter

have crystallized as a single enantiomer, 5-16 was the first structure of a metalated enantiopure compound with R-(+)-2,2-diamino-1,1-binaphthalene as a backbone. The four phenols of compound 5-16 are rigidified by the addition of titanium created an extremely bulky and rigid chiral, Lewis acid catalyst (5-18).

Initial Catalysis Studies

Throughout the process of catalyst development, the ability of the metal complexes to facilitate organic transformations has been monitored as a means to judge the feasibility of the system. The standard reaction used to determine catalyst activity was the addition of an ethyl group to benzaldehyde. In order for this reaction to occur, a Lewis acid catalyst must be present and there are many examples of Zn salen systems promoting this reaction in high yields (Figure 5-25).⁹³

The catalytic ability of the racemic Zn (II) (5-8) and Co (II) (5-10) complexes were tested and both were able to transform the reaction in quantitative yields (96-98 %). There was no indication of any remaining benzaldehyde in the ¹H NMR spectrum of the crude product. The reaction mixture contains both the alcohol product and the catalyst, but upon workup the catalyst can be recovered and reused in other reactions. The reactivity of 5-7 and 5-9 was also examined and not surprisingly they both were also able to promote this reaction. The absence of the titanium should have little impact on the reactivity at the Lewis acid site, but rather is important to lock in the chiral geometry of the system to increase enantioselectivity.

Conclusions

The ability to devise new asymmetric catalysts is of great importance to the field of synthetic organic chemistry. For this purpose, a class of multinuclear salen based, chiral Lewis acid catalysts have been developed. Both Zn (II) and Co (II) derivatives have been made and initial studies have indicated that they are able to promote the ethyl addition to benzaldehyde.

The reactivity of the system with countless other reactions has still yet to be explored. The chirality of the system is determined by the binap group as its large torsion angle is able to set the geometry of the entire compound. The addition of titanium to coordinate to the four phenols is able to rigidify the molecule and “lock in” the chirality.

Experimental Methods

General Considerations

^1H and ^{13}C NMR spectra were recorded on a Varian Mercury 300 MHz spectrometer at 299.95 and 75.47 MHz for the proton and carbon channels. UV-Vis spectra were recorded on a Varian Cary 50 spectrometer. Elemental analyses were performed at either the in-house facility of the Department of Chemistry at the University of Florida or by Complete Analysis Laboratories Inc., Parsippany, NJ. All solvents were ACS or HPLC grade and used as purchased. For the metalation reactions, the solvents were dried with a Meyer Solvent Purification system.

Synthesis of 5-2

A portion of 1.00 g (3.52mmol) of racemic 1,1'-Binaphthyl-2-2'-diamine was dissolved in 250 mL absolute ethanol. To this solution a portion of 3.34 g (7.04 mmol) of 5-1 was added. The reaction was refluxed open to the air for 12 hours. The solution was cooled to room temperature and water was added to the solution resulting in the precipitation of an orange solid. The solid was filtered and dried to afford the product in 90% yield (3.81 g). Crystals suitable for X-ray diffraction were grown by a THF / pentane diffusion. ^1H NMR: δ 13.20 (s, 2H); 8.49 (s, 2H); 8.12 (d, 2H, 9.3 Hz); 7.00 (d, 2H, 8.7 Hz); 7.46 (m, 2H); 7.29 (m, 6H); 7.05 (s, 2H); 6.98 (s, 2H); 6.93 (s, 2H); 6.78 (s, 2H); 6.65 (s, 2H); 6.56 (s, 2H); 5.63 (s, 2H); 5.42 (s, 2H); 5.07 (s, 2H); 2.19 (s, 6H); 2.14 (s, 6H); 2.12 (s, 6H); 1.45 (s, 18H); 1.32 (s, 18H). ^{13}C NMR δ 161.9; 155.8; 151.4; 151.2; 143.8; 137.7; 137.4; 135.1; 133.2; 132.9; 131.6; 130.7; 129.3; 128.9; 128.8;

128.7; 128.4; 128.1; 127.6; 127.5; 127.4; 127.3; 127.0; 126.9; 126.8; 126.3; 199.1; 117.0; 37.1; 35.1; 34.9; 30.1; 30.0; 21.3; 20.7. Anal. Calc. for C₈₂H₈₈O₆N₂: C, 82.37; H, 7.26; N, 2.34. Found C, 82.10; H, 2.61; N, 2.21.

Synthesis of 5-3

A portion of 1.00 g (3.52mmol) of *R*-(+)-1,1'-Binaphthyl-2-2'-diamine was dissolved in 250 mL absolute ethanol. To this solution a portions of 3.34 g (7.04 mmol) of 5-1 was added. The reaction was refluxed open to the air for 12 hours. The solution was cooled and the solvent removed under vacuum. The solid was dissolved in the minimum amount of methylene chloride and filtered through a plug of alumina. The solvent was then removed to afford the product in 75% yield (3.14 g). ¹H NMR: δ 13.20 (s, 2H); 8.49 (s, 2H); 8.12 (d, 2H, 9.3 Hz); 7.00 (d, 2H, 8.7 Hz); 7.46 (m, 2H); 7.29 (m, 6H); 7.05 (s, 2H); 6.98 (s, 2H); 6.93 (s, 2H); 6.78 (s, 2H); 6.65 (s, 2H); 6.56 (s, 2H); 5.63 (s, 2H); 5.42 (s, 2H); 5.07 (s, 2H); 2.19 (s, 6H); 2.14 (s, 6H); 2.12 (s, 6H); 1.45 (s, 18H); 1.32 (s, 18H). ¹³C NMR δ 161.9; 155.8; 151.4; 151.2; 143.8; 137.7; 137.4; 135.1; 133.2; 132.9; 131.6; 130.7; 129.3; 128.9; 128.8; 128.7; 128.4; 128.1; 127.6; 127.5; 127.4; 127.3; 127.0; 126.9; 126.8; 126.3; 199.1; 117.0; 37.1; 35.1; 34.9; 30.1; 30.0; 21.3; 20.7. HRMS: calcd for C₈₂H₈₈O₆N₂ 1197.6715; found 1197.6715 [MH⁺].

Synthesis of 5-4

A portion of 1.00 g (3.52mmol) of racemic 1,1'-Binaphthyl-2-2'-diamine was dissolved in 250 mL absolute ethanol. To this solution a portion of 2.75 g (7.04 mmol) of 3-(bis(2-hydroxy-3,5-dimethylphenyl)methyl)-2-hydroxy-5-methylbenzaldehyde was added. The reaction was refluxed open to the air for 12 hours. The solution was cooled to room temperature and water was added to the solution resulting in the precipitation of a pink solid. The solid was filtered and dried to afford the product in 87% yield (3.14 g). ¹H NMR: δ 13.22 (s, 2H); 8.44 (s, 2H); 8.07 (d,

2H, 9 Hz); 7.98 (d, 2H, 8 Hz); 7.51 (d, 2H, 9 Hz); 7.46 (t, 2H, 8 Hz); 7.25 (t, 2H, 9 Hz); 6.93 (s, 2H); 6.88 (s, 2H); 6.82 (s, 2H); 6.72 (s, 2H); 6.65 (s, 2H); 6.59 (s, 2H); 5.71 (s, 2H); 5.38 (s, 2H); 5.10 (s, 2H); 2.26 (s, 6H); 2.18 (s, 6H); 2.15 (s, 6H); 2.14 (s, 6H); 2.11 (s, 6H). ^{13}C NMR δ 162.1; 156.1; 150.4; 143.6; 134.5; 133.5; 133.3; 132.8; 131.5; 130.6; 130.5; 129.3; 129.2; 129.2; 129.1; 128.9; 128.7; 128.2; 127.4; 127.2; 126.9; 126.1; 125.6; 125.4; 119.1; 117.0. HRMS: calcd for $\text{C}_{70}\text{H}_{64}\text{O}_6\text{N}_2$ 1029.4837; found 1029.4794 [MH^+].

Synthesis of 5-5

A portion of 1.00 g (3.52mmol) of R-(+)- 1,1'-Binaphthyl-2-2'-diamine was dissolved in 250 mL absolute ethanol. To this solution a portions of 2.75 g (7.04 mmol) of 3-(bis(2-hydroxy-3,5-dimethylphenyl)methyl)-2-hydroxy-5-methylbenzaldehyde was added. The reaction was refluxed open to the air for 12 hours. The reaction was cooled and the solvent was removed under vacuum. The solid was dissolved in the minimum amount of methylene chloride and filtered through a plug of neutral alumina with a 90:10 methylene chloride:methanol mixture. The solvent was removed to afford an orange solid in 71% yield (2.57 g). ^1H NMR: δ 13.22 (s, 2H); 8.44 (s, 2H); 8.07 (d, 2H, 9 Hz); 7.98 (d, 2H, 8 Hz); 7.51 (d, 2H, 9 Hz); 7.46 (t, 2H, 8 Hz); 7.25 (t, 2H, 9 Hz); 6.93 (s, 2H); 6.88 (s, 2H); 6.82 (s, 2H); 6.72 (s, 2H); 6.65 (s, 2H); 6.59 (s, 2H); 5.71 (s, 2H); 5.38 (s, 2H); 5.10 (s, 2H); 2.26 (s, 6H); 2.18 (s, 6H); 2.15 (s, 6H); 2.14 (s, 6H); 2.11 (s, 6H). ^{13}C NMR δ 162.1; 156.1; 150.4; 143.6; 134.5; 133.5; 133.3; 132.8; 131.5; 130.6; 130.5; 129.3; 129.2; 129.2; 129.1; 128.9; 128.7; 128.2; 127.4; 127.2; 126.9; 126.1; 125.6; 125.4; 119.1; 117.0. HRMS: calcd for $\text{C}_{70}\text{H}_{64}\text{O}_6\text{N}_2$ 1029.4837; found 1029.4794 [MH^+].

Synthesis of 5-6

A portion of 0.25 g (0.24 mmol) of racemic 5-4 was dissolved in a minimum amount of methylene chloride. To this solution was added 200 mL of acetonitrile as well as a portion of 0.059 g (0.27 mmol) of Zinc acetate \cdot 2 H_2O . The solution was stirred and heated at 75° C for

four hours. A yellow precipitate forms and the solid was filtered and dried to afford the product in 82% yield (0.21 g). Crystals suitable for X-ray diffraction were grown by a THF / pentane diffusion. ^1H NMR: δ 8.33 (s, 2H); 8.06 (d, 2H, 9 Hz); 7.88 (d, 2H, 9 Hz); 7.45 (s, 2H); 7.42 (m, 2H); 7.21 (m, 4H); 6.86 (d, 2H, 12 Hz); 6.81 (s, 2H); 6.78 (s, 6H); 6.71 (s, 2H); 6.64 (bs, 2H); 6.38 (s, 2H); 6.33 (bs, 2H); 2.14 (s, 6H); 2.11 (s, 6H); 2.03 (s, 6H). Unable to obtain ^{13}C NMR due to low solubility. HRMS: calcd for $\text{C}_{70}\text{H}_{62}\text{O}_6\text{N}_2\text{Zn}$ 1091.3972; found 1091.3870 [MH^+].

Synthesis of 5-7

A portion of 2.00 g (1.67 mmol) of racemic 5-2 was dissolved in a minimum amount of methylene chloride. To this solution was added 200 mL of acetonitrile as well as a portion of 0.46 g (2.10 mmol) of Zinc acetate \cdot 2 H_2O . The solution was stirred and heated at 75° C for four hours at which time a yellow precipitate formed. The solid was filtered and dried to afford the product in 89% yield (1.87 g). ^1H NMR: δ 8.32 (s, 2H); 8.00 (d, 2H, 8.7 Hz); 7.89 (d, 2H, 8.7 Hz); 7.43 (m, 4H); 7.21 (m, 4H); 6.96 (m, 6H); 6.89 (d, 2H, 8.7 Hz); 6.82 (d, 4H, 7.8 Hz); 6.77 (s, 2H); 6.29 (s, 2H); 6.07 (s, 2H); 2.18 (s, 6H); 2.12 (s, 12H); 1.38 (s, 18H); 1.24 (s, 18H). ^{13}C NMR δ 171.3; 164.4; 152.1; 152.0; 144.7; 139.2; 137.5; 137.4; 135.0; 134.1; 133.8; 132.4; 131.4; 128.7; 128.5; 128.3; 128.1; 127.4; 127.3; 127.0; 126.6; 126.5; 126.4; 126.0; 125.7; 125.3; 121.4; 118.1; 35.1; 34.9; 30.1; 29.9; 21.3; 21.2; 20.4. HRMS: calcd for $\text{C}_{82}\text{H}_{86}\text{O}_6\text{N}_2\text{Zn}$ 1259.5730; found 1259.5850 [MH^+].

Synthesis of 5-8

A portion of 0.50g (0.39 mmol) of 5-7 was partially dissolved in 50 mL of dry methylene chloride under nitrogen. To this solution was added a portion of 0.12 g (0.44 mmol) titanium isopropoxide. The solid instantly dissolved into the solution which turned dark red. The solution was allowed to stir for 12 hours in the dry box at which time the solvent was removed in vacuum yielding pure product in 95% yield (0.49 g). Crystals suitable for X-ray diffraction

were grown by a pentane diffusion into an acetonitrile / THF solvent mixture. ^1H NMR: δ 8.21 (s, 2H); 7.95 (d, 2H, 9 Hz); 7.85 (d, 2H, 9 Hz); 7.58 (s, 2H); 7.39 (t, 2H); 7.14 (t, 2H); 7.02 (s, 2H); 7.00 (s, 2H); 6.79 (s, 2H); 6.75 (d, 2H); 6.70 (s, 4H); 5.84 (s, 2H); 2.39 (s, 6); 2.22 (s, 6H); 2.15 (s, 6H); 1.40 (s, 18H); 0.99 (s, 18H). ^{13}C NMR δ 170.2; 170.0; 160.4; 160.3; 145.4; 140.9; 137.1; 135.8; 134.8; 134.7; 134.1; 132.2; 130.9; 130.7; 130.6; 129.2; 128.3; 127.0; 126.7; 126.5; 126.3; 125.8; 125.7; 123.8; 123.7; 121.9; 117.4; 65.8; 44.1; 35.5; 34.5; 30.4; 30.0; 29.7; 25.4; 22.5; 21.2; 21.1; 20.6; 15.3; 13.9.

Synthesis of 5-9

A portion of 1.00 g (0.84 mmol) of racemic 5-2 was dissolved in 50 mL of methylene chloride. A portion of 0.266 g (1.07 mmol) of cobalt(II) acetate \cdot 4 H_2O was dissolved in the minimum amount of methanol under nitrogen. The cobalt solution was added to the ligand solution under nitrogen and stirred for two hours. A red /orange precipitate formed and was quickly filtered and dried to afford the product in 87% yield (0.92 g). ^1H NMR: paramagnetic signals δ 59.75; 53.98; 40.96; 15.69; 12.88; 9.13; 8.32; 7.77; 5.79; 3.87; 2.27; -1.67; -4.83; -10.3; -50.87. HRMS: calcd for $\text{C}_{70}\text{H}_{62}\text{O}_6\text{N}_2\text{Co}$ 1254.5891; found 1254.5818 $[\text{M}-\text{H}]^+$.

Synthesis of racemic 5-10

A portion of 1.00 g (0.79 mmol) of racemic 5-9 was partially dissolved in 50 mL of dry methylene chloride under nitrogen. To this solution was added a portion of 0.24 g (0.87 mmol) titanium isopropoxide. The solid instantly dissolved into the solution which turned dark red. The solution was allowed to stir for 12 hours in the dry box at which time the solvent was removed in vacuum yielding pure product in 92% yield (0.95 g). Crystals suitable for X-ray diffraction were grown by a pentane diffusion into an acetonitrile / THF solvent mixture. ^1H NMR: δ 64.56; 61.92; 46.92; 15.02; 11.79; 9.25; 7.55; 7.23; 7.17; 6.09; 5.28; 4.77; 4.05; 3.70; 3.48; 2.34; 1.84; 1.02; 0.87; -4.43; -4.80; -7.25; -7.84; -12.12; -48.1

Synthesis of 5-11

A portion of 1 g (4.37 mmol) of 2,5-diformyl-4-bromo-phenol was added to a portion of 1.79 g (10.9 mmol) of 2-*t*-butyl-4-methyl-phenol. To this was added the minimum amount of trifluoroacetic acid needed to fully dissolve the solids. The reaction was allowed to stir at room temperature for 12 hours at which point a white solid precipitated. Cold methanol was added to the reaction mixture and the product was filtered. The filtrate was taken and the solvent removed under vacuum to yield a solid which was washed with cold methanol affording more pure product. The product was a white solid and was afforded in 76 % yield (1.8 g). ¹H NMR: δ 11.40 (s, 1H); 9.89 (s, 1H); 7.68 (s, 1H); 7.33 (s, 1H); 7.07 (s, 2H); 6.54 (s, 2H); 5.99 (s, 1H); 2.20 (s, 6H); 1.38 (s, 18H). ¹³C NMR δ 195.7; 158.1; 151.0; 140.2; 137.8; 134.9; 133.91; 129.9; 127.8; 127.3; 126.5; 121.7; 112.0; 39.3; 34.7; 30.0; 21.3 HRMS: calcd for C₃₀H₃₅O₄Br 538.1719.; found 538.1680.

Synthesis of 5-12

A portion of 2.00 g (10.24 mmol) of 2,5-diformyl-4-nitro-phenol was added to a portion of 4.20 g (25.6 mmol) of 2-*t*-butyl-4-methyl-phenol. To this was added the minimum amount of trifluoroacetic acid needed to fully dissolve the solids. The reaction was allowed to stir at room temperature for 12 hours at which point a white solid precipitated. Cold methanol was added to the reaction mixture and the product was filtered. The filtrate was taken and the solvent removed under vacuum to yield a solid which was washed with cold methanol affording more pure product. The product was a white solid and was afforded in 44 % yield (2.3 g). ¹H NMR: δ 12.05 (s, 1H); 10.0 (s, 1H); 8.52 (d, 1H, 2.7 Hz); 8.22 (d, 1H, 2.7 Hz); 7.10 (s, 2H); 6.52 (s, 2H); 6.08 (s, 1H); 2.22 (s, 6H); 1.39 (s, 18H). ¹³C NMR δ 195.8; 163.9; 150.0; 140.9; 137.7; 133.6; 131.9; 130.1; 128.5; 128.0; 127.4; 127.3; 126.4; 119.3; 116.6; 39.5; 34.7; 30.1; 29.8; 21.3 HRMS: calcd for C₃₀H₃₅O₆N + Na 528.2357.; found 528.2359 [M+Na]⁺

Synthesis of 5-13

A portion of 0.50 g (1.75 mmol) of *R*-(+)-1,1'-Binaphthyl-2-2'-diamine was dissolved in 150 mL absolute ethanol. To this solution a portion of 1.84 g 5-11 was added. The reaction was refluxed open to the air for 12 hours. A pale orange precipitate had formed and was filtered which was pure product. The solvent of the filtrate was removed under vacuum and the remaining solid was dissolved in the minimum amount of methylene chloride and filtered through a plug of alumina. The solvent was then removed and the combination led to a combined 68% yield (1.59 g). ^1H NMR: δ 13.42 (s, 2H); 8.51 (s, 2H); 8.11 (d, 2H, 9 Hz); 7.99 (d, 2H, 9 Hz); 7.60 (d, 2H, 9 Hz); 7.49 (t, 2H, 9 Hz); 7.34 (m, 2H); 7.18 (d, 4H, 9 Hz); 7.06 (s, 2H); 7.00 (s, 2H); 6.57 (s, 2H); 6.51 (s, 2H); 5.60 (s, 2H); 5.19 (s, 2H); 4.96 (s, 2H); 2.18 (s, 6H); 2.15 (s, 6H); 1.43 (s, 18H); 1.34 (s, 18H). ^{13}C NMR δ 160.1; 157.3; 151.1; 151.0; 142.6; 137.7; 137.6; 136.7; 133.2; 133.1; 133.0; 131.5; 130.9; 129.8; 129.4; 129.3; 128.8; 127.5; 127.3; 127.1; 127.0; 126.9; 126.8; 126.7; 120.6; 116.4; 111.0; 37.3; 35.0; 34.9; 30.1; 30.0; 21.3; 21.2. HRMS: calcd for $\text{C}_{80}\text{H}_{82}\text{O}_6\text{N}_2\text{Br}_2$ 1325.4618.; found 1325.4368 [MH^+].

Synthesis of 5-14

A portion of 0.475 g (1.67 mmol) of *R*-(+)-1,1'-Binaphthyl-2-2'-diamine was dissolved in 150 mL absolute ethanol. To this solution a portion of 1.63 g (3.33 mmol) of 5-12 was added. The reaction was refluxed open to the air for 12 hours. The reaction was cooled and the solvent was removed under vacuum to afford the product in 97% yield (2.04 g). ^1H NMR: 14.65 (bs, 2H); 8.71 (s, 2H); 8.14 (m, 4H); 7.99 (m, 2H); 7.93 (d, 2.4 Hz, 2H); 7.84 (m, 2H); 7.68 (d, 9 Hz, 2H); 7.52 (m, 2H); 7.34 (m, 2H); 7.23 (m, 4H); 7.07 (s, 2H); 7.03 (s, 2H); 6.85 (m, 2H); 6.57 (s, 2H); 6.51 (s, 2H); 6.48 (s, 2H); 5.65 (s, 2H); 2.14 (s, 6H); 7.13 (s, 6H); 1.42 (s, 18H); 1.39 (s, 18H). ^{13}C NMR δ 166.1; 159.4; 151.0; 150.9; 104.3; 139.5; 137.7; 133.4; 137.7; 133.4; 133.1; 132.3; 131.4; 129.7; 129.5; 129.4; 129.2; 128.9; 128.7; 128.0; 127.5; 127.3; 127.1;

127.0; 126.9; 126.8; 126.7; 126.6; 117.2; 116.6; 115.8; 37.9; 34.9; 34.8; 30.1; 30.0; 29.8; 21.3.

HRMS: calcd for $C_{80}H_{82}O_{10}N_4$ 1259.6104 .; found 1259.6134 [M+H]⁺

Synthesis of 5-15

A portion of 0.50 g (0.40 mmol) of 5-14 was dissolved in 150 mL methanol. To this solution a large excess of Cobalt acetate 1.00 g (4.00 mmol) was added. The reaction was brought to a boil under nitrogen at which point the heat was removed and the reaction was stirred for 4 hours. A brown precipitate had formed and was quickly filtered to afford the pure product in 81% yield (0.84 g). ¹H NMR: δ 59.51; 53.39; 18.70; 16.81; 12.95; 9.13; 8.18; 7.06; 5.83; 4.61; 3.90; 2.92; 2.15; 1.90; 1.52; 1.32; 0.86; -1.18; -3.39; -5.49; -7.99; -9.61; -14.80; -53.96. HRMS: calcd for $C_{80}H_{80}O_{10}N_4Co$ 1315.5201; found 1315.5205.

Synthesis of 5-16

A portion of 1.00 g (0.75 mmol) of 5-13 was dissolved in 150 mL methanol. To this solution a large excess of Cobalt acetate 1.88 g (7.70 mmol) was added. The reaction was brought to a boil under nitrogen at which point the heat was removed and the reaction was stirred for 4 hours. A brown precipitate had formed and was quickly filtered to afford the pure product in 81% yield (0.84 g). ¹H NMR: δ 60.20; 55.46; 16.04; 12.86; 10.50; 9.06; 8.37; 7.55; 6.97; 5.79; 5.43; 4.91; 3.50; 2.07; 1.79; 1.35; 1.26; -1.01; -1.49; -2.95; -3.15; -4.51; -10.39; -51.76. HRMS: calcd for $C_{80}H_{80}O_6N_2Br_2Co$ 1382.3793; found 1382.3448 [MH⁺].

Synthesis of 5-17

A portion of 0.50 g (0.40 mmol) of 5-14 was dissolved in 150 mL methanol. To this solution a large excess of Zinc acetate 1.00 g (4.00 mmol) was added. The reaction was brought to a boil under nitrogen at which point the heat was removed and the reaction was stirred for 4 hours. A yellow precipitate had formed and was quickly filtered to afford the pure product in 54% yield (0.285 g). ¹H NMR: δ 8.44 (s, 2H); 8.07 (m, 6H); 7.97 (d, 2H, 9 Hz); 7.48 (t, 2H, 7.5

Hz); 7.32 (d, 2H, 9 Hz); 7.00 (s, 4H); 6.90 (d, 2H, 9 Hz); 6.76 (s, 2H); 6.54 (s, 2H); 6.21 (s, 2H); 5.94 (s, 2H); 5.42 (s, 2H); 2.19 (s, 6H); 2.13 (s, 6H); 1.34 (s, 18H); 1.28 (s, 18H). ^{13}C NMR δ 172.4; 170.3; 151.0; 150.9; 144.0; 138.1; 136.9; 136.7; 133.6; 132.5; 132.3; 131.5; 130.0; 129.7; 129.5; 128.7; 128.4; 127.9; 127.6; 127.4; 127.2; 126.8; 126.6; 126.5; 125.5; 121.2; 117.2; 37.8; 35.0; 34.8; 30.1; 21.3; 21.1. HRMS: calcd for $\text{C}_{80}\text{H}_{80}\text{O}_{10}\text{N}_4\text{Zn}$ 1320.5106; found 1320.5119.

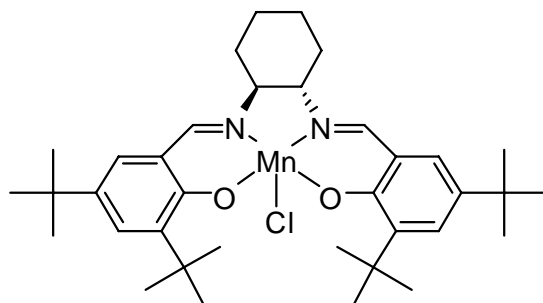


Figure 5-1. Structure of Jacobsen's catalyst used for the asymmetric epoxidation of olefins

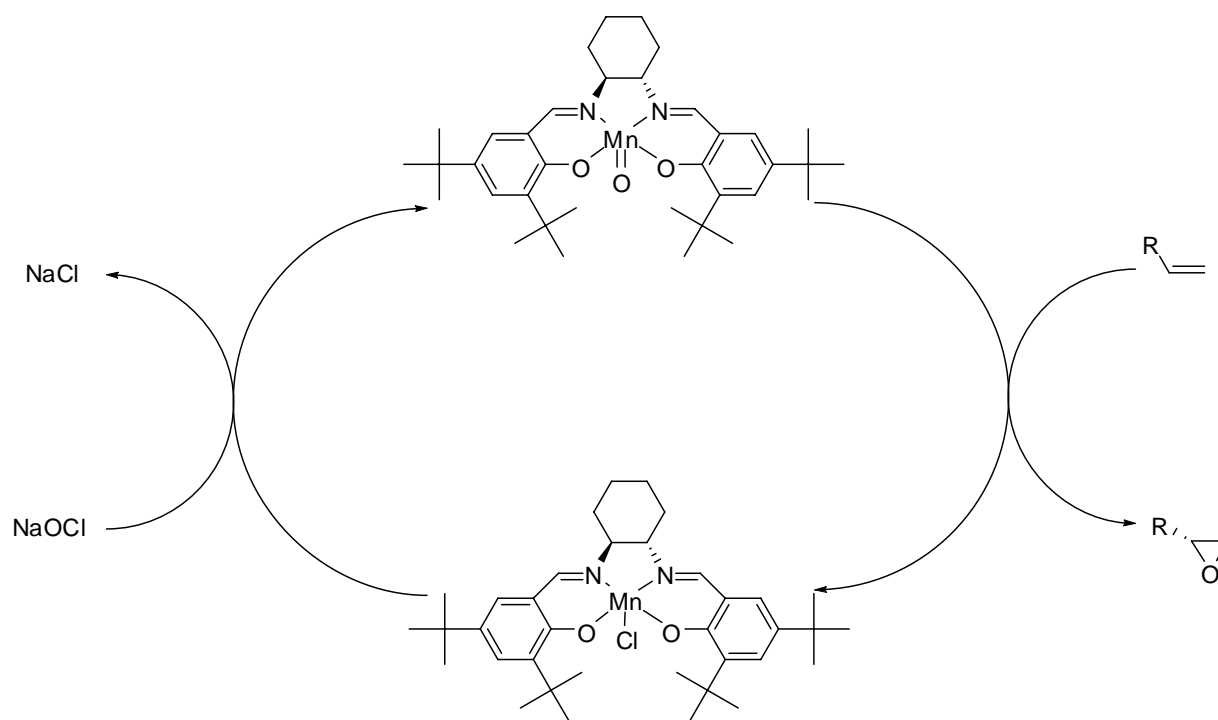


Figure 5-2. Proposed mechanism for the epoxidation of olefins with Jacobsen's catalyst.

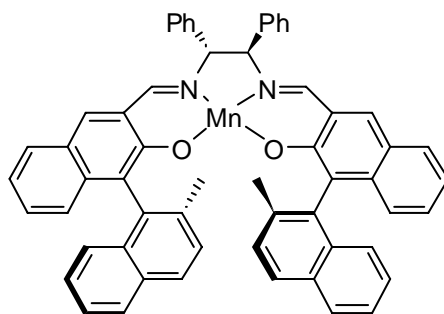


Figure 5-3. Structure of catalyst with chiral binaphthyl groups that influence the geometry of the substrate.

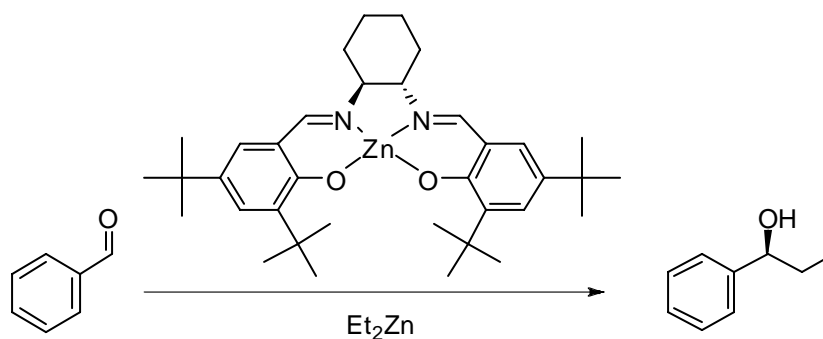


Figure 5-4. Reaction scheme for the ethyl addition to benzaldehyde. The reaction is promoted by the chiral Lewis acidic Zn-salen catalyst.

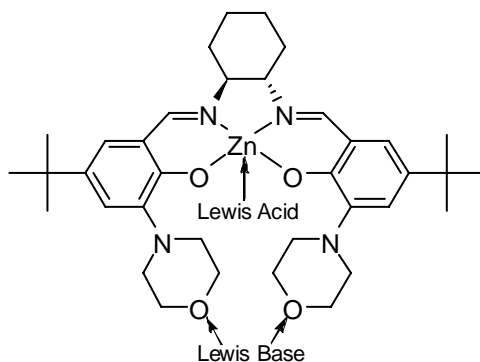


Figure 5-5. Structure of a bifunctional catalyst containing both a Lewis acid and Lewis base component.

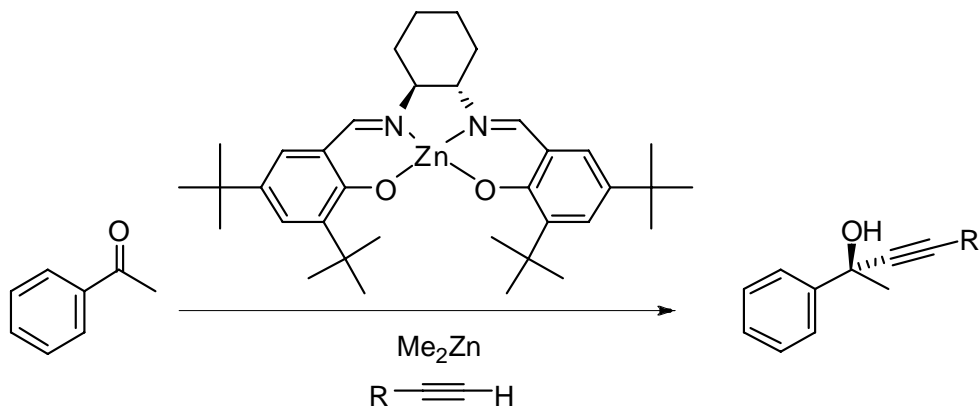


Figure 5-6. Schematic diagram of the enantioselective alkylation of ketones.

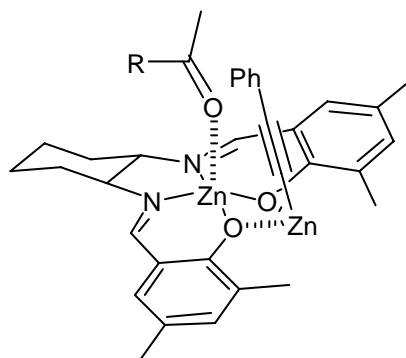


Figure 5-7. Proposed transition state for the alkylation of ketones with a zinc salen catalyst

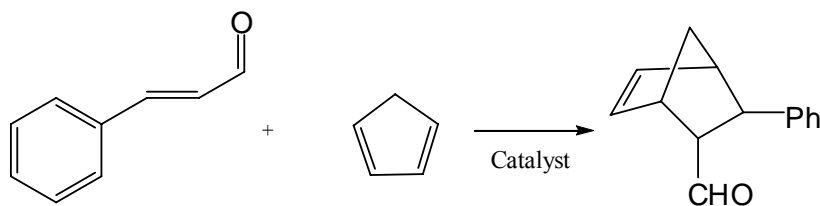


Figure 5-8. Diels-Alder reaction between cyclopentadiene and cinnamaldehyde promoted by a Lewis acid catalyst.

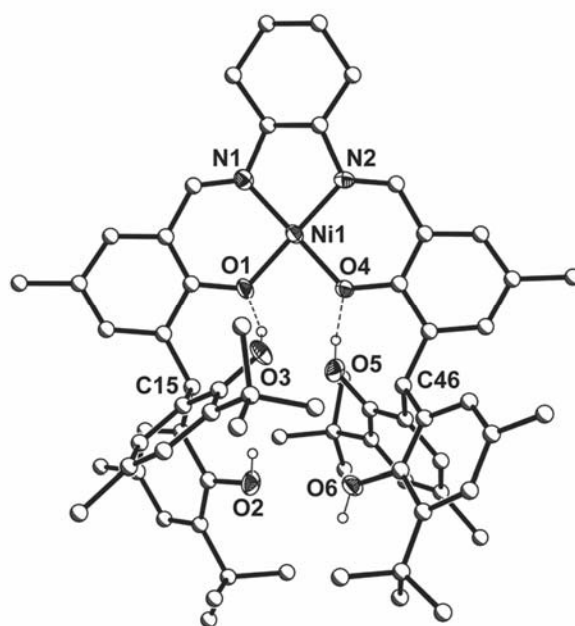


Figure 5-9. Solid state structure of compound 2-2. The chirality of the cyclohexane ring does not affect the position of the four phenols.

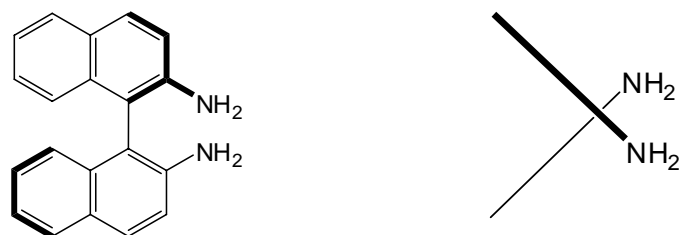


Figure 5-10. Depiction of 2,2-diamino-1,1-binaphthylene showing the large torsion angle between the two naphthyl planes.

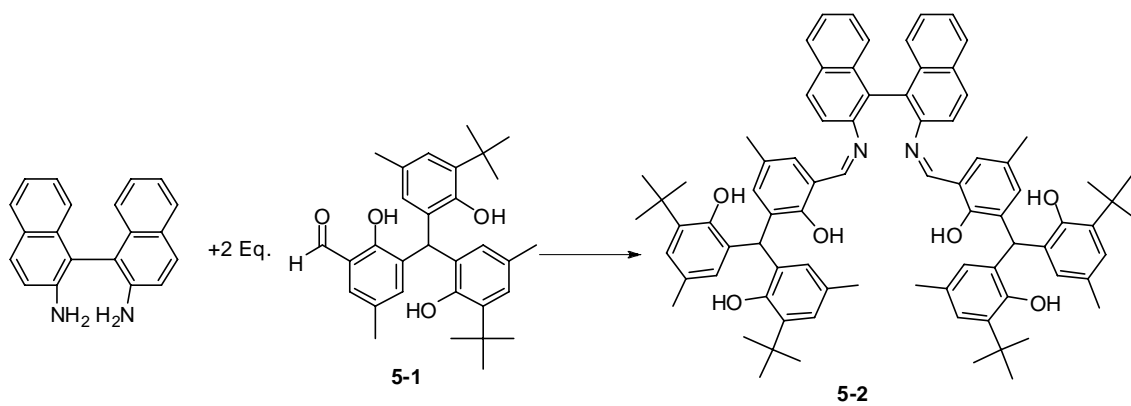


Figure 5-11. Synthetic scheme for the synthesis of 5-2.

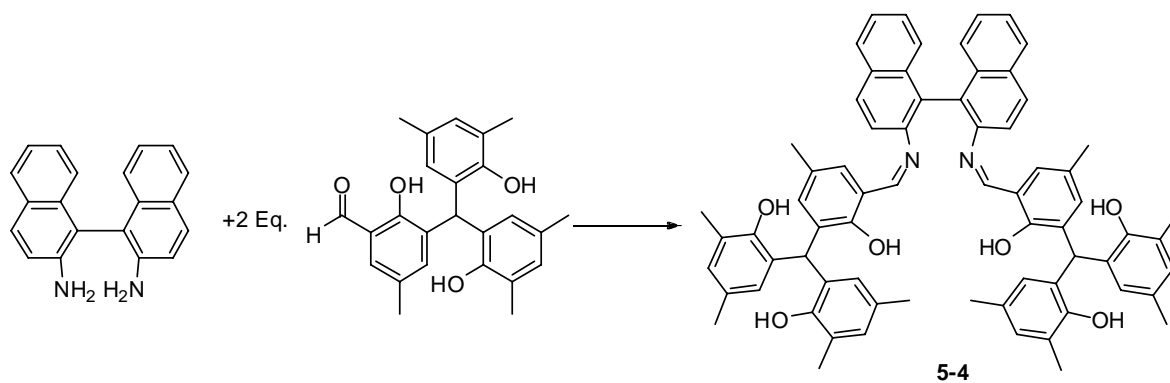


Figure 5-12. Synthetic scheme for the formation of 5-4. The *t*-butyl groups of the triphenoxymethane have been replaced by methyl groups.

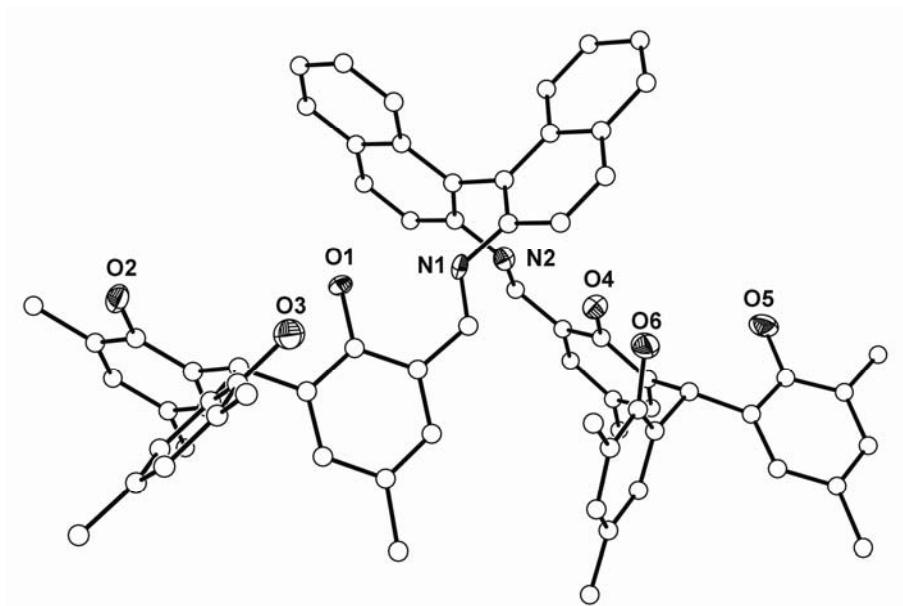


Figure 5-13. Solid state structure of compound 5-4 (30% probability ellipsoids for nitrogen and oxygen; carbons drawn with arbitrary radii)

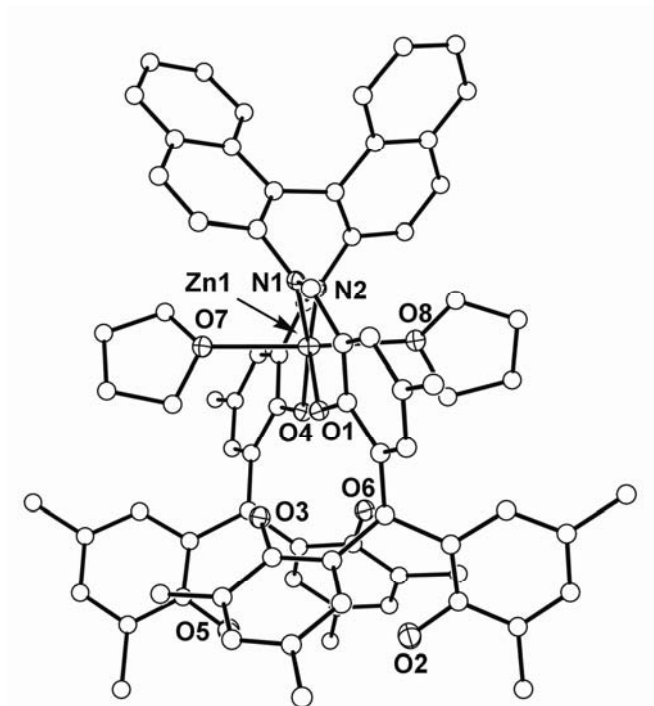


Figure 5-14. Solid state structure of 5-6 with two THF solvent molecules coordinated to the zinc. The geometry of the naphthyl rings sets the position of the four phenols. (30% probability ellipsoids for zinc, nitrogen and oxygen; carbon atoms drawn with arbitrary radii, non coordinated solvents and hydrogen atoms were removed for clarity)

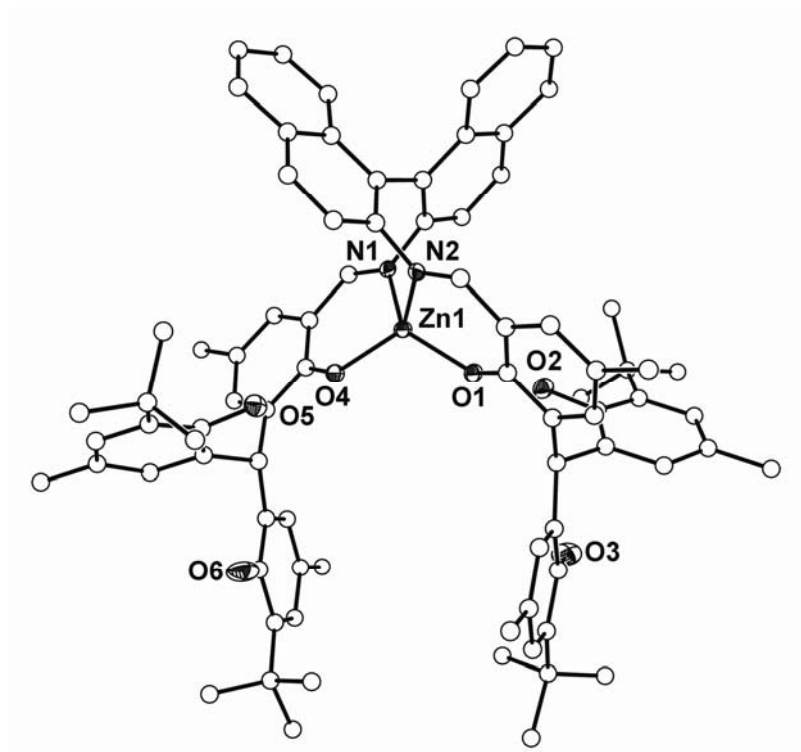


Figure 5-15. Solid state structure of compound 5-7. Without the presence of a coordinating solvent, the metal center takes a tetrahedral geometry. (30% probability ellipsoids for zinc, nitrogen and oxygen; carbons drawn with arbitrary radii, solvents and hydrogen atoms were removed for clarity)

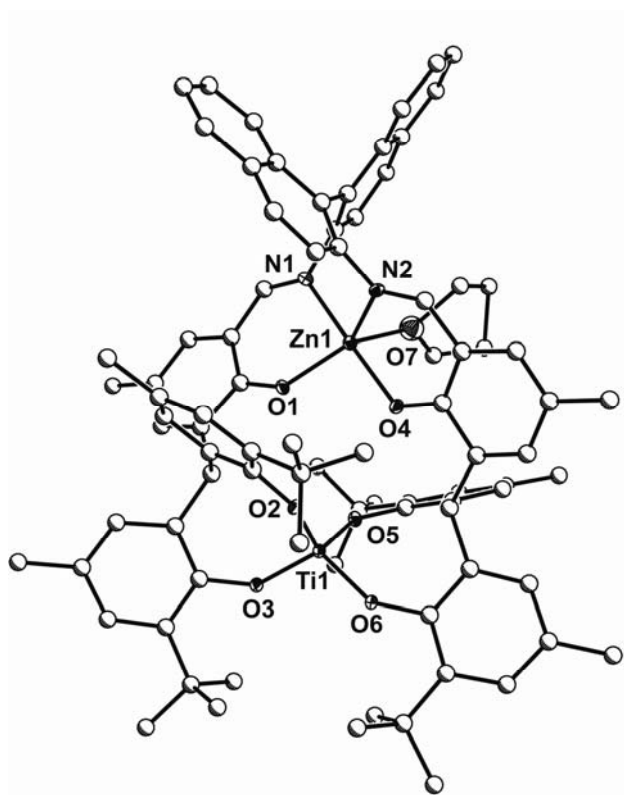


Figure 5-16. Solid state structure of the dinuclear catalyst 5-8. A Zn (II) metal is coordinated in the salen binding site and Ti (IV) is coordinated to the four phenols creating a rigid structure. (30% probability ellipsoids for zinc, titanium, nitrogen and, oxygen; carbon atoms drawn with arbitrary radii; THF and acetonitrile solvent molecules and hydrogen atoms were removed for clarity)

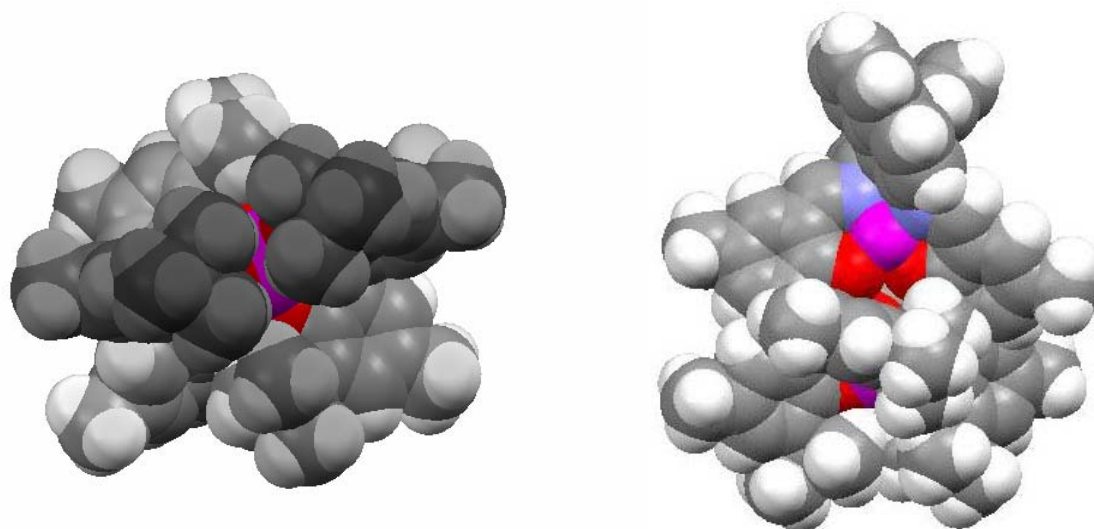


Figure 5-17. Space filling models of the solid state structure of 5-8. The catalytic site of Zn (II) is represented in purple (right), and the chiral cavity formed for possible substrate binding can clearly be seen. The titanium is deeply buried in the phenolic pocket (left)

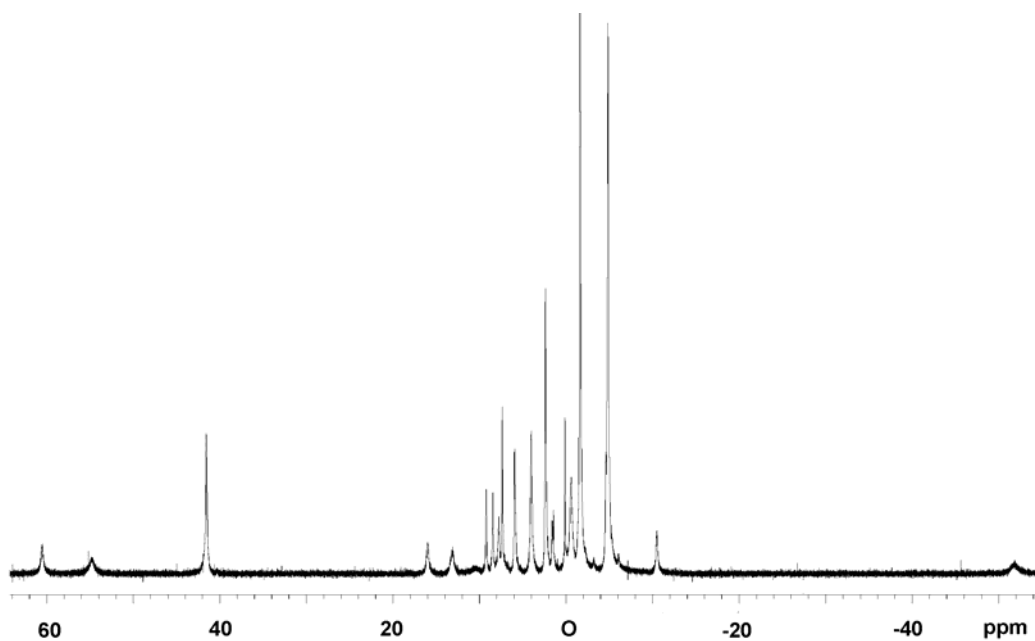


Figure 5-18. ^1H NMR spectrum of the paramagnetic compound 5-9 in CDCl_3 .

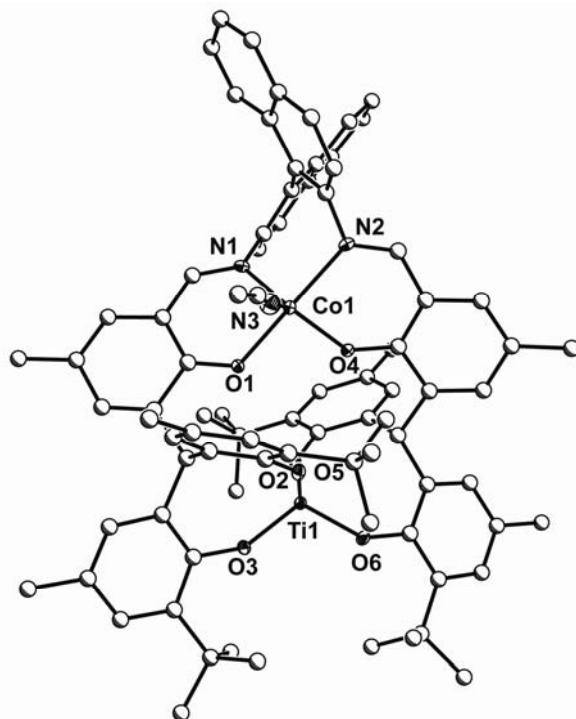


Figure 5-19. Solid state structure of the dinuclear compound 5-10

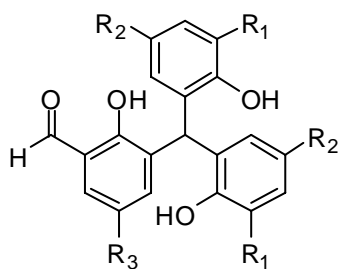


Figure 5-20. Schematic of triphenoxymethane aldehyde showing its possible positions for ligand modification.

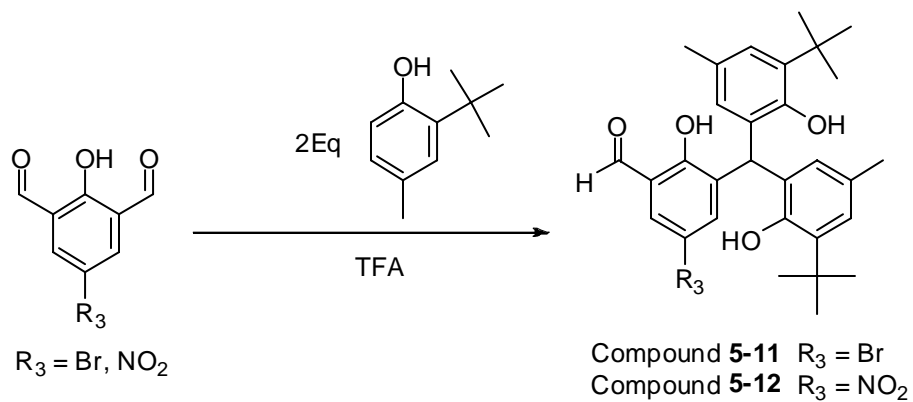


Figure 5-21. Synthetic scheme for compounds 5-11 and 5-12

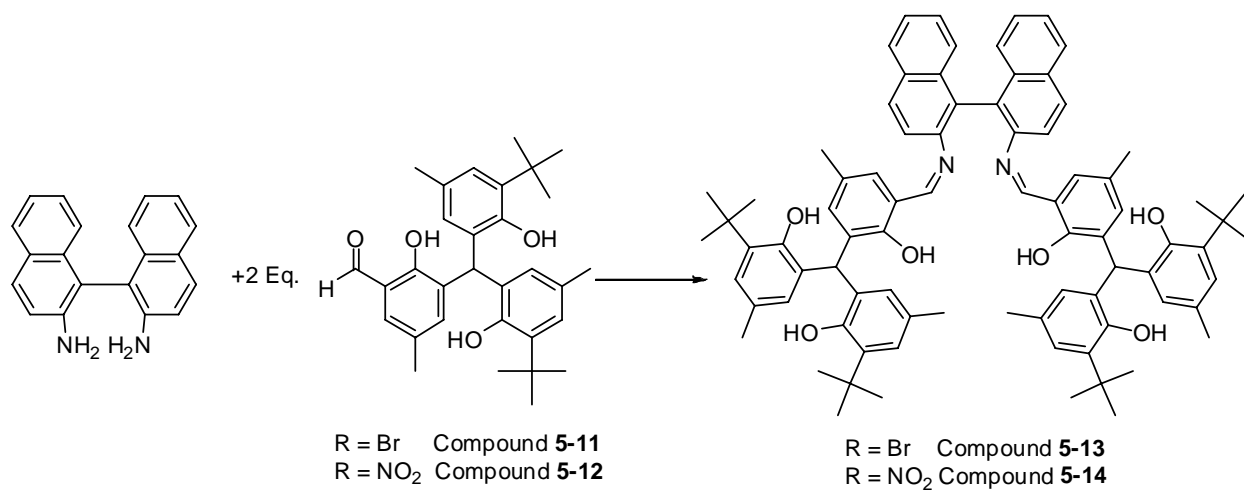


Figure 5-22. Synthetic scheme for the synthesis of 5-13 and 5-14

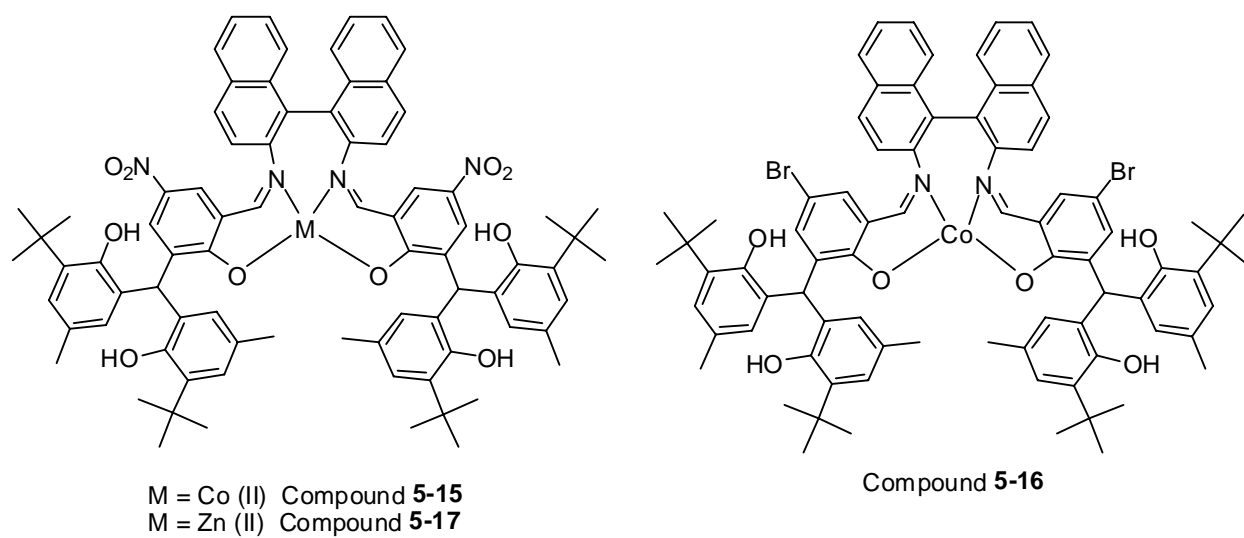


Figure 5-23. Schematic diagram of the structures of 5-15, 5-16, and 5-17.

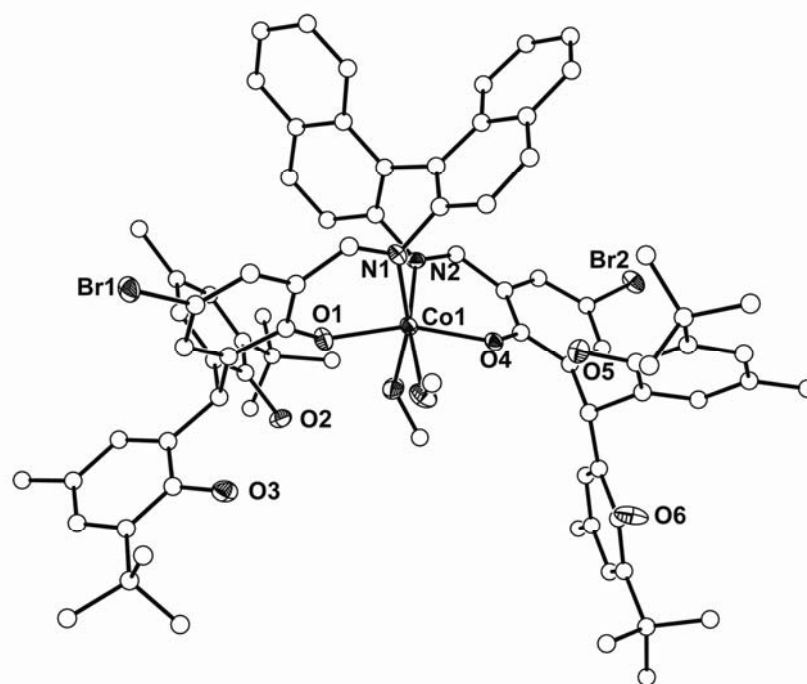


Figure 5-24. Crystal structure of 5-16; Co (II) is arranged in an octahedral geometry.

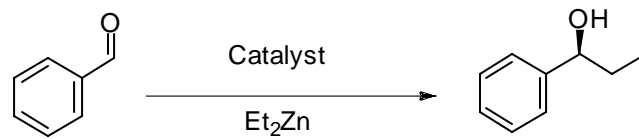


Figure 5-25. Catalytic reaction of the ethyl addition to benzaldehyde used as a standard to monitor the catalytic ability of the compounds

LIST OF REFERENCES

- 1) Bianchi, E.; Bowman-James, K.; Garcia-Espana, E., Eds. *Supramolecular Chemistry of Anions*: Wiley-VCH: New York, 1997.
- 2) Sessler, J.; Gale, P.; Cho, W. *Anion Receptor Chemistry* : RSC Publishing : Cambridge, 2006.
- 3) Alberts, B.; Bray, D.; Lewis, M.; Raff, M.; Roberts, K.; Watson, J. *Molecular Biology of the Cell*, 3rd edn, Garland Science, New York, 1994.
- 4) Anderson, M.; Gregory, R.; Thompson, P.; Souza, D.; Paul, S.; Mulligan, A.; Smith, A.; Welsh. *Science*. **1991**, 253, 202.
- 5) Simon, D.; Bindra, R.; Mansfield, T.; Nelson-Williams, C.; Mendonca, E.; Stone, R.; Schurmann, S.; Nayir, A.; Alpay, H.; Bakkaloglu, A.; Rodriguez-Soriano, J.; Morales, J.; Sanjad, S.; Taylor, C.; Pilz, D.; Brem, A.; Trachtman, H.; Griswold, W.; Richard, G.; Lifton, J. *Nat. Genet.*. **1997**, 17, 171.
- 6) Devuyst, O.; Christie, P.; Courtoy, P.; Beauwens, R.; Thakker, R. *Hum. Mol. Genet* **1999**, 8, 247.
- 7) Scott, D.; Wang, R.; Kreman, T.; Sheffield, V.; Karniski, L. *Nat. Gen.* **1999**, 21, 440.
- 8) Yoshida, A.; Taniguchi, S.; Hisotome, I.; Royaux, I.; Green, E. ; Kohn, L. ; Suzuki, K. *J. Clin. Endo. Metab.* **2002**, 87, 3356.
- 9) For Examples: (a) Schmitdchen, F.; Berger, M. *Chem. Rev* **1997**. 97, 1609. (b) Antonisse, M.; Reinhoudt, D. *Chem. Comm.* **1998**. 443. (c) Martinez-Manez, R.; Sancenon, F. *Chem. Rev.* **2003**. 103, 4419.
- 10) For example: Woods, C.; Camiolo, S.; Light, M. E.; Coles, S. J.; Hursthouse, M. B.; King, M. A.; Gale, P.A.; Essex, J. W. *J. Am. Chem. Soc.* **2002**, 124, 8644.
- 11) (a) Sessler, J. L.; Camiolo, S.; Gale, P.A. *Coord. Chem. Rev.* **2003**, 240, 17. (b) Llinares, J. M.; Powell, D.; Bowman-James, K. *Coord. Chem. Rev.* **2003**, 240, 57. (c) Bondy, C. R.; Loeb, S. J. *Coord. Chem. Rev.* **2003**, 240, 77. (d) Choi, K.; Hamilton, A. D. *Coord. Chem. Rev.* **2003**, 240, 101. (e) Lamber, T. N.; Smith B. D.; *Coord. Chem. Rev.* **2003**, 240, 129. (f) Davis, A. P.; Joos, J.-B. *Coord. Chem. Rev.* **2003**, 240, 143.
- 12) Lehn, J. *Supramolecular Chemistry*; VCH Weinheim, 1995.
- 13) Lohr, H.; Vogtle, F. *Acc. Chem. Res.* **1985** 18, 65.
- 14) Czarnik, M. *Acc. Chem. Res.* **1994**. 27, 302.
- 15) Bowman-James, K. *Acc. Chem. Res.* **2005**, 38, 671.

- 16) For example: (a) Melaimi, M.; Gabbai, F. P. *J. Am. Chem. Soc.* **2005**, 127, 9680. (b) Cottone, A.; Scott, M.J. *Organometallics* **2000**, 19, 5254. (c) Katz, H. *J. Org. Chem.* **1985**, 50, 5027. (d) Katz, H. *J. Am. Chem. Soc.* **1986**, 108, 7640. (e) Tamao, K.; Hayashi, T.; Ito, Y. *J. Organomet. Chem.* **1996**, 506, 85. (f) Williams, V.; Piers, W.; Clegg, W.; Elsegood, M.; Collins, S.; Marder, T. *J. Am. Chem. Soc.* **1999**, 121, 3244. (g) Solé, S.; Gabbai, F.P.; *Chem Commun.* **2004**, 11, 1284. (h) Chaniotakis, N.; Jurkschat, K.; Müller, D.; Perdikaki, K.; Reeske, G. *Eur. J. Inorg. Chem.* **2004**, 11, 2283.
- 17) For example: (a) Anzenbacher, P.; Jursikova, K.; Sessler, J. *J. Am. Chem. Soc.* **2000**, 122, 9350. (b) Woods, C.; Salvatore, C.; Light, M. E.; Coles, S. J.; Hursthouse, M. B.; King, M. A.; Gale, P.A. Essex, J. W. *J. Am. Chem. Soc.* **2002**, 124, 8644. (c) Kang, S. O.; VanderVelde, D.; Powell, D.; Bowman-James, K. *J. Am. Chem. Soc.* **2004**, 126, 12272.
- 18) Moyer, B.; Bonnesen, P. in *Supramolecular Chemistry of Anions*, ed. A. Bianchi, K. Bowman-James, K. Garica-Espana and E. Garcia-Espana. Wiley-VCH, New York, 1997, pp.1-44.
- 19) Jeffrey, G. *An Introduction o Hydrogen Bonding*; Oxford Universities Press: New York, 1997.
- 20) Desiraju, G. *Acc. Chem. Res.* **2002**. 35, 565.
- 21) Pauling, L. *The Nature of the Chemical Bond*. Cornel University Press: Ithica, New York, 1939.
- 22) Kubik, S.; Reyheller, C.; Stuwe, S.; *J. Incl. Phenom. Macroc. Chem.* **2005**, 52, 137.
- 23) Park, C.; Simmins, H. *J. Am. Chem. Soc.* **1968**. 90, 2431.
- 24) Graf, E.; Lehn, J. *J. Am. Chem. Soc.* **1976**. 98, 6403.
- 25) Lehn, J.; Sonveaux, E.; Willard, A. *J. Am. Chem. Soc.* **1978**. 100, 4914.
- 26) Dietrich, B.; Lehn, J.; Guilhem, J.; Pascard, C. *Tetrahedron Lett.* **1989**. 30, 4125.
- 27) Reilly, S.; Khalsa, D.; Ford, D.; Brainard, J.; Hay, B.; Smith, P. *Inorg. Chem.* **1995**. 34, 569.
- 28) Schmidtchen, F. *Angew. Chem. Int. Ed. Engl.* **1977**. 16, 720.
- 29) Worm, K.; Schmidtchen, F.; Schier, A.; Schafer, A.; Hesse, M. *Angew. Chem. Int. Ed.* **1994**. 33, 327.
- 30) Bauer, V.; Clive, D.; Dolphin, D.; Paine, J.; Harris, F.; King, M.; Loder, S.; Wang, W.; Woodward, R. *J. Am. Chem. Soc.* **1983**. 105, 6429.
- 31) Sessler, J.; Cyr, M.; Lynch, V.; McGhee, E.; Ibers, J. *J. Am. Chem. Soc.* **1990**. 112, 2810.

- 32) Sessler, J.; Cyr, M.; Furuta, H.; Kral, V.; Mody, T.; Morishima, T.; Shionoya, M.; Weghorn, S. *Pure Appl. Chem.* **1993**. 65, 393.
- 33) Dietrich, B. *Pure Appl. Chem.* **1993**. 7, 1257.
- 34) Schmidtchen, F.; *Tetrahedron Lett.* **1989**. 30, 4493.
- 35) Valiyaveetil, S.; Engbersen, F.; Verboom, W.; Reinhoudt, D. *Angew. Chem. Intl. Ed.* **1993**. 32, 900.
- 36) Gale, P. *Coord. Chem Rev.* **2003**. 240, 191.
- 37) Kang, S.; Llinares, J.; Powell, D.; VanderVelde, D.; Bowman-James, K. *J. Am. Chem. Soc.* **2003**. 125, 10152.
- 38) Katz, H. in *Inclusion Compounds*. Atwood, J.; Davies, J.; MacNicol, D. Oxford University Press Publishers, Oxford, **1991**. Vol 4, Chapter 9, pp. 391-405.
- 39) Rudkevich, D.; Verboom, W.; Reinhoudt, D. *J. Org. Chem.* **1994**. 59, 3683.
- 40) D. M. Rudkevich, W. Verboom, Z. Brzozka, M. J. Palys, W. P. R. V. Stauthamer, G.J. van Hummel, S. M. Fraken, S. Harkema, J. F. J. Engbersen and D. N. Reinhoudt, *J. Am. Chem. Soc.* 1994. 116, 4341.
- 41) (a) White, D.; Laing, N.; Miller, H.; Parsons, S.; Coles, S.; Tasker, P. *Chem. Commun.* **1999**. 2077. (b) Miller, H.; Laing, N.; Parsons, S.; Parkin, A.; Tasker, P. *J. Chem. Soc. Dalton Trans.* **2000**. 3773.
- 42) (a) Vermersch, P.; Lemon, D.; Tesmer, G.; Quioco, F. *Biochemistry.* **1991**. 30, 6861. (b) Vyas, N.; Vyas, M.; Quioco, F. *Science.* **1988**. 242, 1290. (c) Spurlino, J.; Lu, G.; Quioco, F. *J. Biol. Chem.* **1991**. 266, 5202.
- 43) Smith, D. *Org. Biol. Chem.* **2003**. 1, 3874.
- 44) Zhou, G.; Cheng, Y.; Wang, L.; Jing, X.; Wang, F. *Macromolecules.* **2005**. 38, 2148.
- 45) Dinger, M.; Scott, M. J. *Eur. J. Org. Chem.* **2000**, 2467. Dinger, M.; Scott, M. J. *Chem. Commun.* **1999**, 2525.
- 46) For example: (a) Turner, D. R.; Spencer, E. C.; Howard, J. A. K.; Tocher, D. A.; Steed, J. W. *Chem. Commun.* **2004**, 1352. (b) Bondy, C. R.; Gale, P. A.; Loeb, S. J. *J. Am. Chem. Soc.* **2004**, 126, 5030. (c) Beer, P. D.; Hayes, E. J. *Coord. Chem. Rev.* **2003**, 240, 167.
- 47) (a) Dutzler, R.; Campbell, E. B.; MacKinnon, R. *Science* 2003, 300, 108. (b) Dutzler, R.; Campbell, E.; Cadene, M.; Chait, B.; MacKinnon, R. *Nature*, 2002, 415, 287.

- 48) (a) Kolbe, M.; Besir, H.; Essen, L. O.; Oesterhelt, D. *Science* 2000, 288, 1390. (b) Facciotti, M. T.; Cheung, V. S.; Lunde, C. S.; Rouhani, S.; Baliga, N. S.; Glaeser, R. M. *Biochemistry* 2004, 43, 4934.
- 49) For a review of sulphate and phosphate binding sites see: Copley, R. R.; Barton, G. J.; *J. Mol. Biol.* 1994, 242, 321.
- 50) Channa, A.; Steed, J. W.; *J. Chem. Soc. Dalton Trans.* 2005, 2455. Ghosh, S.; Choudhury, A. R.; Row, T. N. G.; Maitra, U. *Org. Lett.* 2005, 7, 1441. Zhou, G.; Cheng, Y.; Wang, L.; Jing, X.; Wang, F. *Macromolecules*, 2005, 38, 2148. Smith, D.; *Org. Biomol. Chem.* 2003, 1, 3874. Lee, K. H.; Lee, H. Y.; Lee, D. H.; Hong, J. I. *Tetrahedron Lett.* 2001, 42, 5447.
- 51) Kondo, S. I.; Suzuki, T.; Toyama, T.; Yano, Y. *Bull. Chem. Soc. Jpn.* 2005, 78, 1348. Hiratani, K.; Sakamoto, N.; Kameta, N.; Karikomina, M.; Nagawa, Y. *Chem. Commun.* 2004, 1474. Miyaji, H.; Sessler, J. L.; *Angew. Chem. Int. Ed.* 2001, 40, 154. Jeong, K. S.; Hahn, K. M.; Cho, Y. L. *Tetrahedron Lett.* 1998, 39, 3779. Davis, A. P.; Gilmer, J. F.; Perry, J. J. *Angew. Chem., Int. Ed. Engl.* 1996, 35, 1312. Beer, P. D.; Dent, S. W.; Wear, T. J. *J. Chem. Soc. Dalton Trans.* 1996, 2341.
- 52) Antonisse, M. M. G.; Reinhoudt, D. N. *Chem Commun.* 1998, 443. Plieger, P. G.; Tasker, P. A.; Galbraith, S. G. *J. Chem. Soc. Dalton Trans.* 2004, 313.
- 53) Cottone, A.; Morales, D.; Lecuivre, J.; Scott, M. J. *Organometallics.* 2002, 21, 418.
- 54) de Castro, B.; Ferreira, R.; Freire, C.; Garcia, H.; Palomares, E. J.; Sabater, M. J. *New. J. Chem.* 2002, 26, 405.
- 55) Shimazaki, Y.; Tani, F.; Fukui, K.; Naruta, Y.; Yamauchi, O. *J. Am. Chem. Soc.* 2003, 125, 10512.
- 56) Kang, S.; Llinares, J.; Powell, D.; VanderVelde, D.; Bowman-James, K. *J. Am. Chem. Soc.* 2003, 125, 10152.
- 57) Shionoya, M.; Furuta, H.; Lynch, V.; Harriman, A.; Sessler, J. *J. Am. Chem. Soc.* 1992, 114, 5714.
- 58) Kang, S. O.; VanderVelde, D.; Powell, D.; Bowman-James, K. *J. Am. Chem. Soc.* 2004, 126, 12272.
- 59) Bourson, J.; Pouget, J.; Valeur, B.; *J. Phys. Chem.* 1993, 97 4552.
- 60) With help from Chase Rainwater on computer program
- 61) Lai, C.; Mak, W.; Chan, E.; Sau, Y.; Zhang, Q.; Lo, S.; Williams, I.; Leung, W. *Inorg. Chem.* 2003, 42, 5863.
- 62) Zhou, X.; Huang, J.; Yu, X.; Zhou, Z.; Che, C. *J. Chem. Soc. Dalton Trans.* 2000, 7, 1075.

- 63) Libra, E.; Scott, M. *Chem Commun.* 2006. 1485.
- 64) Campbell, E.; Nguyen, S. *Tett. Lett.* 2001. 42, 1221.
- 65) Synthesis developed by Melanie Veige
- 66) Etter, M.; Urbanczyk-Lipkowska, Z.; Zia-Ebrahimi, M.; Pununto, T. *J. Am. Chem. Soc.* **1990**. 112, 8415.
- 67) Gale, P. *Coor. Chem. Rev.* **2003**. 240, 191.
- 68) Kelly, T.; Kim, M. *J. Am. Chem. Soc.* **1994**. 116, 7072.
- 69) Snellink-Ruel, B.; Antonisse, M.; Engberson, J.; Timmerman, P.; Reinhoudt, D. *Eur. J. Org. Chem.* **2000**. 165.
- 70) (a) Turner, D.; Paterson, M.; Steed, J. *J. Org. Chem.* **2006**. 71(4), 1598. (b) Oh, J.; Cho, E.; Ryu, B.; Lee, Y.; Nam, K. *Bull. Korean Chem. Soc.* **2003**. 24, 10.
- 71) Bondy, C.; Gale, P.; Loeb, S. *J. Am. Chem. Soc.* **2004**, 126, 5030.
- 72) Bordwell, F. *Acc. Chem. Res.* 1988, 21, 456.
- 73) Nishizawa S.; Buhlmann P.; Iwao M.; Umezawa Y. *Tetr. Lett.* **1995**, 36, 6483.
- 74) Gomez, D.; Fabbrizzi, L.; Licchelli, M.; Monzani, E. *Org. Biomol. Chem.* 2005, 3, 1495.
- 75) Boiocchi, M.; Del Boca, L.; Esteban-Gomez, D.; Fabbrizzi, L.; Licchelli, M.; Monzani, E. *Chem. Eur. J.* **2005**, 11, 3097.
- 76) Amendola, V.; Boiocchi, M.; Colasson, B.; Fabbrizzi, L. *Inorg. Chem.* 2006, 45(16), 6138.
- 77) Shimazaki, Y.; Tani, F.; Fukui, K.; Naruta, Y.; Yamauchi, O. *J. Am. Chem. Soc.* **2003**, 125, 10512.
- 78) Mizukami, S.; Houjou, H.; Kanosato, M.; Hiratani, M. *Eur. J. Chem.* **2003**. 9(7), 1521.
- 79) Cozzi, P. *Chem Soc. Rev.* **2004**, 33, 410.
- 80) Baleizao, C.; Garcia, H. *Chem. Rev.* **2006**, 106, 3987.
- 81) Jacobson, E.; Zhang, W.; Muci, A.; Ecker, A.; Deng, J. *J. Am. Chem. Soc.* **1991**, 113, 7063.
- 82) Schaus, S.; Branalt, J.; Jacobson, E. *J. Org. Chem.* **1998**, 63, 403.

- 83) (a) Saito, B.; Katsuki, T. *Tetrahedron Lett.* **2001**, 42, 3873. (b) Li, Z.; Conser, K. R.; Jacobsen, E. N. *J. Am. Chem. Soc.* **1993**, 115, 5326. (c) Martinez, L. E.; Leighton, J. L.; Carsten, D. H.; Jacobsen, E. N. *J. Am. Chem. Soc.* **1995**, 117, 5897.
- 84) Katsuki, T. *Synlett.* **2003**, 281.
- 85) Samsel, E.; Srinivasan, K. Kochi, J. *J. Am. Chem. Soc.* **1985**, 107, 7606.
- 86) Srinivasan, K.; Michaud, P.; Kochi, J. *J. Am. Chem. Soc.* **1986**, 108, 2309.
- 87) For example: Collin, J.; Daran, J.; Schulza, E.; Trifonov, A. *Chem. Commun.* **2003**, 3048.
- 88) For examples: Zhang, W.; Loeban, J.; Wilson, S.; Jacobson, E. *J. Am. Chem. Soc.* **1990**, 112(7), 2801.
- 89) Fukuda, T.; Irie, R.; Katsuki, T. *Synlett.* **1995**, 197.
- 90) Yamamoto, H.; Susumu, S. *Pure & Appl. Chem.* **1999**, 71(2) 239.
- 91) Corey, E.; Huzman-Perez, A. *Angew. Chem. Int. Ed.* **1998**, 37, 388.
- 92) Dias, L. *Current Org. Chem.* **2000**, 4, 305.
- 93.) Cozzi, P. ; Papa, A. ; Umani-Ronchi, A. *Tett. Lett.* **1996**, 37(26), 4613.
- 94) DiMauro, E. ; Kozlowski, M. *Org. Lett.* **2001**, 3(19), 3053.
- 95) (a) Garcia, C. ; LaRochelle, L.; Walsh, P. *J. Am. Chem. Soc.* **2002**, 124, 10970. (b) DiMauro, E.; Kozlowski, M. *J. Am. Chem. Soc.* **2002**, 124, 12668.
- 96) Cozzi, P. *Angew. Chem. Int. Ed.* **2003**, 42, 2895.
- 97) Corey, E. *Angew. Chem. Int. Ed.* **2002**, 41, 1650.
- 98) Ahrendt, K.; Borths, C.; MacMillan, D. *J. Am. Chem. Soc.* **2000**, 122, 4243.
- 99) Chapman, J.; Day, C.; Welker, M. *Organometallics.* **2000**, 19(9), 1615.
- 100) Takenaka, N.; Huang, Y.; Rawal, V. *Tetrahedron.* **2002**, 58, 8299.
- 101) Yamamoto, H.; Futatsugi, K. *Angew. Che. Intl. Ed.* **2005**, 44, 1924.
- 102) Chang, K.; Huang, C.; Liu, Y.; Hu, Y.; Chou, P.; Lin, Y. *Dalton Trans.* **2004**, 1731.
- 103) (a) Morris, G.; Zhou, H.; Stern, C.; Nguyen, S. *Inorg. Chem.* **2001**, 40, 3222. (b) Korupoju, S.; Mangayarkarasi, N.; Ameerunisha, S.; Valente, E.; Zacharias, P. *Dalton Trans.* **2000**, 2845. (c) Szlyk, E.; Wojtczak, A.; Surdykowski, A.; Gozdzikiewicz, M. *Inorg Chem Acta*, **2005**, 358, 467.

- 104) (a) Gao, J.; Reibenspies, J. H.; Zingaro, R. A.; Woolley, F. R.; Martell, A. E.; Clearfield, A. *Inorg. Chem.* **2005**, 44(2), 232. (b) Huang, W.; Gou, S.; Hu, D.; Chantrapromma, S.; Fun, H.-K.; Meng, Q. *Inorg. Chem.* **2001**, 40(7), 1712.
- 105) Chen, G.; Zhai, B.; Sun, M.; Qi, W.; *Acta Crystallogr. E.* **2005**, 61, m1869.
- 106) Wiznycia, A.; Desper, J.; Levy, C.; *Chem. Commun.* **2005**, 37,4693.
- 107) Bunge, J.; Boyle, T.; Pratt, H.; Alam, T.; Rodriguex, M. *Inorg. Chem.* **2004**, 6035.
- 108) (a) Bunge, S. D.; Boyle, T. J.; Pratt, H. D., III; Alam, T. M.; Rodriguez, M. A. *Inorg. Chem.* **2004** 43(19); 6035. (b) Chisolm, M.; Huang, J.; Huffman, T.; Streib, W.; Tiedtke, D. *Polyhedron*, **1997**, 16, 2941.
- 109) (a) Gambarotta, S.; Arena, F.; Floriani, C.; Zanazzi, P. *J. Am. Chem. Soc.* **2000**, 122, 8946. (b) Schaus, S.; Brandes, B.; Larrow, J.; Tokunaga, M.; Hansen, K.; Gould, A.; Furrow, M.; Jacobsen, E. *J. Am. Chem. Soc.* **2002**, 124, 1307.
- 110) Uchida, T.; Katuski, T.; Ito, K.; Akashi, S.; Kuroda, T. *Helvetica Chimica Acta.* **2002**, 85, 3078.
- 111) Shen, Y.-M.; Duan, W.-L.; Shi, M. *J. Org. Chem.* **2003** 68(4), 1559.
- 112) Lindoy, L.; Meehan, G.; Svenstrup, N. *Synthesis.* **1998**, 7, 1029.

BIOGRAPHICAL SKETCH

Eric Libra was born in Erie, Pennsylvania in 1980. His love for science began at an early age and an interest in chemistry began while at General McLane High school, where he graduated as valedictorian in 1998. He earned a B.S. in chemistry from Boston College in 2002 where he worked in Professor William Armstrong's research group, which was his first exposure to inorganic chemistry. Eric began his graduate studies at the University of Florida in 2003 where he joined Professor Michael Scott's group. Upon completion of his Ph.D, Eric will join Adesis Inc. in New Castle, Delaware as a synthetic chemist.